THE ROLE OF MONOCYTES AND MACROPHAGES IN THE PATHOGENESIS OF AUTOIMMUNE MYOCARDITIS AND DILATED CARDIOMYOPATHY

by
Xuezhou (Snow) Hou

A dissertation submitted to Johns Hopkins University in conformity with the requirements for the degree of Doctor of Philosophy

Baltimore, Maryland
January, 2019

Abstract

Approximately 30% of myocarditis patients progress to develop dilated cardiomyopathy, which is a major cause of sudden death in children and young adults. Ly6C^{hi} inflammatory monocytes are thought to play a detrimental role in a mouse model of experimental autoimmune myocarditis (EAM). Their recruitment in large numbers to the heart has been linked to cardiac fibrosis and ventricular dysfunction. However, the mechanism underlying the pathogenic role of Ly6C^{hi} monocytes has been overlooked, and the protective role of Ly6C^{lo} monocytes was largely presumed based on extrapolation from other disease models. We therefore studied the fates and functions of these two types of monocytes to better understand their roles in the injured myocardium. We demonstrated *in vitro* that cardiac fibroblasts mediate monocyte-to-macrophage differentiation through direct contact with Ly6C^{hi} and Ly6C^{lo} monocytes. IL-17A is significantly elevated during acute myocarditis. It signals through cardiac fibroblasts to abolish Ly6C^{lo} monocyte-to-macrophage differentiation as well as to hamper phagocytic function in Ly6C^{hi} monocyte-derived macrophages. Phagocytosis of apoptotic/necrotic myocardial cells by macrophages plays a crucial role in minimizing myocardial damage and subsequent dysfunction. Strikingly, cardiac IL-17A in heart failure patients is inversely correlated with phagocytic receptor expression in the myeloid compartment. This highlights the clinical relevance of our finding and can lead to the development of diagnostic biomarkers or novel treatment approaches. IL-17A signaling wanes during inflammation resolution, allowing Ly6C^{lo} monocyte-to-macrophage differentiation to resume. These macrophages display antigen presentation properties which coincide with cardiac protection in IL-17Ra$^{-/-}$ mice *in vivo*. In conclusion, we described how the inflammatory environment modulates

the phenotype and functions of infiltrating monocytes with potential implications for other autoimmune and inflammatory diseases.

Advisor: Daniela Čiháková, M.D., Ph.D.

Thesis readers: Alan Scott, Ph.D., Fengyi Wan, Ph.D., Abdel Rahim Hamad, Ph.D.

Alternate readers: Diane E. Griffin, M.D., Winnie Wan-yee Tang, Ph.D.

Preface

Growing up, I listened to my parents' stories about the 1966 Culture Revolution in China. Along with 17 million urban youths, my parents were forced out of school to work on rural farms, which deprived them of opportunities to receive proper educations for almost a decade. As a result, my parents have aspired to provide me with the best education. This thesis is dedicated to my parents and family, for without their endless love, support and encouragement it would have been difficult for me to succeed in this arduous journey toward a Ph.D. I am extremely thankful for the encouragement and trust that my parents bestowed upon me to study abroad in the United States.

During my senior year in high school I was invited by Pam and John Brebner to study at Brauer College in Australia. I was awed by the volume of knowledge available, the encouragement to innovate and the freedom to explore. I also came to realize that educational disparity is not just temporal, but spatial. After high school I was determined to come to the United States to pursue higher degrees of education with the intention of making a positive impact in science. I feel immensely fortunate to have met Pam and John Brebner, for without them I wouldn't have made the decision to come to the States.

I am tremendously grateful for the friendship and mentorship that Doug Noble has offered me throughout the past decade. He has tirelessly helped me edit all of my drafts and assays during college, and he has connected me with many friends and family as I have moved around the country for work and school. I cannot forget the hundred-dollar bill he put in my hand when I got my first job. "To help you travel." He said.

I am incredibly fortunate to have met Frederick C. Tucker, the love of my life, who has been a constant source of support and encouragement through not just graduate school

but also life. Together with his mother Susan R. Tucker, M.D., his father Frederick C. Tucker Jr, M.D. and his siblings, they made me feel like I have a home here where I belong. I really appreciate Dr. Frederick C. Tucker's dedication and opinions during the writing of my thesis.

I also want to thank Uncle Steve Lo, Aunt Catherine Sun, Aunt Tang Li, Sybille Stadtmueller, Jeff Bender, Sylvia Craig, Steve Albright, Patrice McPeak and Eric Anderson for their love and friendships.

I am immensely grateful for the mentorship of my sponsor and advisor Daniela Čiháková and my co-sponsor Noel Rose. The completion of my thesis was only possible thanks to their guidance, support and dedication to mold me into a better scientist. Daniela Čiháková has granted me enormous trust and freedom to implement my own experiments and allow me to establish many multi-disciplinary collaborations. Both Daniela Čiháková and Noel Rose allowed me many opportunities to attend national conferences, and present my work to receive necessary feedbacks to advance my research.

I want to express my gratitude to my colleagues and fellow students who were essential to our supportive and collaborative lab environment. My heartfelt appreciations go to Jobert Barin, who offered me tremendous help and knowledge getting started on the myeloid project, Monica V. Talor, who took care of me when I injured my knee and tirelessly assisted me with almost all of my experiments and Hee Sun Choi and Nicola L. Diny, who generously offered me help and guidance. My thanks also go to Lei Wu, SuFey Ong, AeRyon Kim, Guobao Chen, William Bracamonte-Baran, Taejoon Won, Julie Schaub, Uasim Harkus, David Hughes and Megan Wood for all their friendships and support.

I want to thank our collaborators Isabelle Coppens, David Joel Hackam, Jungeun Sung, Karin Klingel, Giovanni E. Davogustto and Heinrich Taegtmeyer for kindly sharing their resources, expertise and clinical samples. I am thankful that my thesis committee members Alan Scott, Diane E. Griffin and Fengyi Wan have been very inquisitive and supportive over the past few years.

I also extend my gratitude to the Johns Hopkins core facility staff members Xiaoling Zhang from the Ross Flow Cytometry Core; Jessica Gucwa from the SKCCC Flow Cytometry Core; Leonard Marque and Firozeh Dastani from the Animal Resources; Karen Fox-Talbot from the Oncology Tissue Services; Haiping Hao and C Conover Talbot Jr. from the Deep Sequencing and Microarray Core Facility and MMI departmental administrative staff Gail O'Connor and Thomas Hitzelberger for all their patience and help.

This work was made possible by grant funding from the National Institutes of Health/National Heart, Lung, and Blood Institute grants R01HL118183, R01HL136586, American Heart Association AWRP Winter 2017 Grant-in-Aid (17GRNT33700274) and Matthew Poyner MVP Memorial Myocarditis Research Fund to Daniela Čiháková. Myocarditis Foundation Postdoctoral Fellowship (90072351) to Guobao Chen, American Heart Association Postdoctoral Fellowship (16POST31330012) to William Bracamonte-Baran and Predoctoral Fellowship (16PRE31170040) to Hee Sun Choi and Nicola L Diny. AARDA awards to William Bracamonte-Baran. Gilead Research Scholar grant and AARDA award to Jobert G. Barin, and Deutsche Forschungsgemeinschaft grant KL595/2-3 to Karin Klingel.

I am fortunate to have received the Johns Hopkins Autoimmune Disease Research Center O'Leary-Wilson Fellowship and the Johns Hopkins Bloomberg School of Public

Health Richard J and Margaret Conn Himelfarb Student Support fund for additional funding support.

Table of Contents

List of Tables

List of Figures

Chapter 1

Introduction

A. Myocarditis definition, diagnosis and etiology

Myocarditis is responsible for a significant number of chronic and acute heart failure cases involving children and young adults [1]. Although the majority of affected patients recover, myocarditis contributes to the global cardiovascular disease burden mainly through the development of dilated cardiomyopathy and ultimately to sudden heart failure [2]. It is often challenging to diagnose myocarditis due to the its broad range of clinical presentations and heterogenous disease manifestation [3-5]. Currently the diagnostic gold standard of myocarditis is endomyocardial biopsy (EMB) and is based on histological, immunological and immunohistochemical criteria [5]. Established in 1986, the *Dallas criteria* provides a histopathological definition for myocarditis that require the presence of inflammatory infiltrates in the myocardium accompanied by cardiomyocyte deterioration and necrosis not characteristic of an ischemic event [6, 7]. In 2013 the European Society of Cardiology Working Group on Myocardial and Pericardial Diseases published a statement emphasizing the importance of histological and immunohistochemical characterization to provide evidence for myocardial inflammation. The immunohistochemical criteria describing abnormal cardiac immune cell infiltrates was stated as *"≥ 14 leucocytes/mm^2 including up to 4 monocytes/mm^2 with the presence of CD3 positive T-lymphocytes ≥ 7 cells/mm^2"* [8-10]. Therefore, EMB made it possible to

help distinguish unique subtypes of myocarditis with variable prognoses. It also allows for identification of the presence of viral genomes using molecular techniques such as reverse transcriptase-PCR with significant prognostic and therapeutic consequences [8, 9, 11-16]. However, the limitations for EMB are its low sensitivity, high sampling error and potential for complications. The fact that it is an invasive procedure makes it less desirable for routine use and follow up [17]. Moreover, clinical presentations for myocarditis range widely from moderate chest pain with transient palpitations detectable by ECG to sudden cardiac death [3, 18-20]. As a result, other diagnostic methods such as cardiovascular magnetic resonance imaging (CMR) are increasingly being utilized in the initial diagnostic workup of suspected myocarditis patients (Table 1) [15, 21-23].

Table 1. Current myocarditis and cardiomyopathy diagnostic methods

Diagnostic method	Specificity and sensitivity for myocarditis
Electrocardiogram	Can be considered as part of the initial testing. However, myocarditis patients can show normal or nonspecific abnormalities or patterns similar to that of acute isolated pericarditis acute myocardial infarction.
ELISA	Elevated serum cardiac troponin levels are tested as an indicator for myocardial necrosis; elevated serum B-type natriuretic peptide (BNP) and N-terminal pro b-type natriuretic pepti (NT-proBNP) levels reflect diminished cardiac capacity. However, findings can be non-specific.
Chest radiograph	Of limited sensitivity, but used to view cardiac enlargement in the absence of pulmonary congestion.
Cardiac catheterization	Optional test for evaluation of coronary status.
2D or 3D Echocardiography	Key method used to detect abnormal ventricular function even at the subclinical stage. Car detect abnormal ejection fraction and changes in ventricular geometry. Doppler echocardiography can be useful to assess blood flow, avoiding invasive measurements su as cardiac catheterization. This method has replaced Radionuclide ventriculography.
Cardiovascular magnetic resonance (CMR)	CMR can be used as a powerful predictor of adverse cardiovascular outcomes. Specifically can distinguish myocarditis from ischemic cardiomyopathy, and allows the visualization of myocyte necrosis, fibrosis, changes in ventricular size and geometry. A combined imaging method termed “Lake Louise criteria†”. This method has largely replaced Gallium scanning which detects severe myocardial infiltration.
F-18 fluorodeoxyglucose (FDG) positron emission tomography (PET)	Relatively new imaging technology. Limited reports have shown high sensitivity and specifi when used in conjunction with CMR. Not routinely used, with the exception of suspected cardiac sarcoidosis.

This table is based on [24-39]. †Lake Louise criteria (proposed diagnostic CMR criteria) for myocarditis diagnosis means that in clinically suspected myocarditis cases at least two of the three following criteria need to be satisfied: 1) Myocardial signal intensity increases in T2-weighted images regionally or globally; 2) Myocardial early gadolinium enhancement ratio is increased globally between myocardium and skeletal muscle in T1-weighted images; 3) At least one non-ischemic focal lesion in inverse-recovery late gadolinium-enhancement T1-weighted images [40].

Unfortunately, no single test can reliably confirm the diagnosis of many cases, which makes myocarditis diagnosis a challenging task and ultimately contributes to the underestimation of global myocarditis prevalence [3-5].

Myocarditis can be caused by both infectious and non-infectious agents (Table 2). However, evidence suggests that viral infections such as coxsackie B3, parvovirus B19 and adenoviruses are the most common causes of myocarditis in developed nations [3-5, 7, 12, 14, 41-45]. Regardless of myocarditis etiology, clinical presentation of the acute phase can range from mild and transient to fulminant.

Table 2. Etiology of myocarditis and inflammatory dilated cardiomyopathy

Genetic	
GENES AND SYNDROMES	> 60 known genes including most prevalent TTN, LMNA, MYH7, and the rarest TTNT2, Duchenne muscular dystrophy, Barth syndrome.
Microorganisms	
BACTERIA	*Staphylococcus, Clostridium, Diphtheria, Chlamydia psittaci, Streptococcus, Pneumococcus, Meningococcus, Gonococcus, Salmonella, Corynebacterium diphtheriae, Haemophilus influenzae, Mycobacterium tuberculosis, Mycoplasma pneumoniae, Brucella Spirochaetal, Borrelia, Leptospira, Coxiella burnetiid, Rickettsia rickettsia, Syphilis*
RNA VIRUSES	*Coxsackie, Echoviruses, Poliomyelitis, Influenza, Respiratory syncytial virus, Mumps, Measles virus, Rubella virus, Hepatitis C virus, Dengue virus, Yellow fever virus, HIV-1, Chikungunya virus, Junin virus, Lassa fever virus, Rabies virus*
DNA VIRUSES	*Adenoviruses, Parvovirus B19, Cytomegalovirus, Epstein-Barr virus, Varicella-zoster virus, Herpes simplex virus, Variola virus, Vaccinia virus*
FUNGI	*Aspergillus, Actinomyces, Blastomyces, Candida, Coccidioides, Cryptococcus, Histoplasma, Mucormycoses, Nocardia, Sporothrix*
PROTOZOANS	*Trypanosoma brucei gambiense, Trypanosoma brucei rhodesiense, Trypanosoma cruzi, Toxoplasma gondii, Taenia solium, Entamoeba histolytica, Leishmania, Strongyloides, Ancylostoma duodenale, Necator ame*ricanus,
HELMINTHS	*Echinococcus granulosus, Trichinella spiralis*
Toxins	
DRUGS	Phenothiazines, Amphetamines, Anthracyclines, Cyclophosphamide, Cocaine, Cyclophosphamide, 5-Fluorouracil, Lithium, Catecholamines, Hemetine, Interleukin, Trastuzumab, Clozapine, Tricyclic antidepressants, Dobutamine, Epinephrine, Dopamine, Norepinephrine, Phenylpropanolamine, Ferrous sulfate, Immune checkpoint inhibitors, Cholorquine, Zidovudine
VENOMS	Insect stings, Snake bites
ENDOCRINES	Hypo- or hyper-thyroidism, Diabetes mellitus, Cushing's syndrome, Phaeochromocytoma, Growth hormones imbalance, Preganacy
OTHERS	Alcohol, Carbon monoxide, Phosphorus, Arsenic, Sodium azide, Heavy metal
Hypersensitivity	
DRUGS	Penicillin, Cefaclor, Colchicine, Furosemide, Isoniazid, Lidocaine, Tetracycline, Sulfonamides, Phenytoin, Phenylbutazone, Methyldopa, Thiazide diuretics, Amitriptyline, Tetanus toxoid
Physical assault	
PROCEDURES	Radiation, Electric shock, Heart transplantation rejection
Systemic	
AUTOIMMUNE	Celiac disease, Hypereosinophilia, Systemic lupus erythematosus, Rheumatoid arthritis, Churg-Strauss syndrome, Kawasaki's disease, Inflammatory bowel disease, Scleroderma, Polymyositis, Myasthenia gravis, Insulin-dependent diabetes mellitus, Thyrotoxicosis, Sarcoidosis, Wegener's granulomatosis, Rheumatic heart disease, Dermatomyositis

This table is based on [18, 46-55].

B. Selected forms of myocarditis

EMB also permits immunopathological examination of the infiltrating leukocyte profile in the myocardium, which helps to further classify myocarditis into several forms.

1. Lymphocytic myocarditis is the most common form of myocarditis, primarily defined by diffuse focal aggregates of cardiac T lymphocyte infiltrates, typically as a result of a viral respiratory tract infection. The severity of myocardial fibrosis is used to define the progression of lymphocytic myocarditis from acute to chronic phase [18]. Clinical presentation of lymphocytic myocarditis can vary widely from flu-like symptoms to fulminant left ventricular failure. Since a significant number of patients can also be asymptomatic, disease prevalence in the general population can be underestimated [52, 56]. Approximately 50% of the patients were reported to survive without cardiac transplantation at five years from symptom onset [57]. Immunosuppressive drugs can significantly alleviate the worsening of ejection fraction in affected individuals if circulating autoantibodies against cardiac antigens are detected, whereas immunosuppressive treatments are ineffective in patients with detectable viral genomes in the heart [58, 59]. A murine CVB3-induced myocarditis model was developed to draw a parallel between human lymphocytic myocarditis (see experiment vial myocarditis model below) [60, 61].

2. Eosinophilic myocarditis is a relatively rare form of myocarditis characterized by eosinophilic infiltrates in the myocardium and is often associated with peripheral eosinophilia [62]. Although the underlying etiology for eosinophilic myocarditis remains largely unknown, case reports have shown correlation of eosinophilic myocarditis patients with drug hypersensitivity and parasitic infections, and most commonly with the idiopathic hypereosinophilic syndrome [63-65]. Necrotizing eosinophilic myocarditis is the most

severe form, frequently presenting with acute onset, rapid progression and severe necrosis [56]. Immunosuppressive treatment doesn't significantly improve long term prognosis, and disease outcomes are dire for the majority of patients [18, 56, 66]. A murine model has been developed to better understand the pathogenesis of eosinophilic myocarditis in humans [67].

3. Giant cell myocarditis is the rarest but most fulminant form of myocarditis with poor prognosis. It is characterized by the presence of multinucleated giant cells among numerous other cardiac infiltrates [56]. Histologically the predominant infiltrates consist of $CD68^+$ macrophage lineage with the presence of T lymphocyte and frequently with eosinophils [68]. In contrast to the heterogeneous clinical features of lymphocytic myocarditis, giant cell myocarditis manifestation typically results in fulminant left ventricular systolic dysfunction and heart failure, with some patients developing ventricular arrhythmias and heart block [69]. The rapidly progressive nature of giant cell myocarditis results in poor survival with only about 11% of patients surviving over 4 years without a need of cardiac transplantation. Treatment with the appropriate immunosuppressive combination therapies can improve prognosis and increase survival rates, yet options are highly limited [69, 70]. Giant cell myocarditis is thought to be autoimmune in nature as 17 – 19% of patients typically suffer from other non-cardiac related autoimmune diseases [68, 69, 71]. A murine model termed experimental autoimmune myocarditis (EAM) closely resembles the phenotype of this disease [56].

4. Sarcoidosis, or idiopathic granulomatous myocarditis, is a heterogeneous disease of unknown etiology characterized by non-caseating granulomas in various organs, including the heart. The clinical presentation of sarcoidosis ranges from nonspecific

symptoms to sudden death caused by atrioventricular block and congestive heart failure despite having a relatively indolent clinical course [72, 73]. Sarcoidosis is associated with even higher rates of ventricular arrhythmias and heart block when compared to giant cell myocarditis [74]. Heart transplantation is often the treatment of last resort for end stage disease management. However, recurrence of sarcoidosis cannot be prevented with this approach [75].

Regardless of etiology, acute myocarditis in susceptible populations can progress to subacute and chronic phase, and ultimately proceed to dilated cardiomyopathy (DCM). Myocarditis is responsible for approximately 9 – 16% of newly diagnosed DCM cases [76-78]. DCM is the most common cardiomyopathy worldwide, and the major cause of heart failure in patients under the age of 40 [79]. According to the WHO/ISFC criteria, patients with DCM develop dilatation and systolic dysfunction (abnormality of contraction) of the left or both ventricles in the absence of abnormal loading conditions or coronary artery disease. DCM can be further categorized into several subtypes including idiopathic, familial/genetic, pathogen, autoimmune and environmental toxin [3, 5, 18, 42]. Although DCM is associated with fulminant congestive heart failure, patients may or may not experience overt heart failure. Both etiology and diagnosis of DCM largely overlaps with that of myocarditis (Table 1 and Table 2). Unfortunately, a clear mechanism of progression from myocarditis to dilated cardiomyopathy has not been elucidated.

C. Experimental autoimmune myocarditis - murine model

To improve current treatment regimens and to understand the mechanism of how myocarditis progress to heart failure, it was important to create a mouse model of

autoimmune myocarditis. The two main murine models of myocarditis are coxsackievirus B3 (CVB3) myocarditis and experimental autoimmune myocarditis (EAM).

In humans, CVB is one of the most frequent cause of myocarditis in males. The murine CVB3 myocarditis model has a wide spectrum of disease severity, successfully recapitulating human viral myocarditis [80]. The presence of heart specific autoantibodies and myocyte-reactive T cells indicates the autoimmune nature of the disease [81, 82]. The initial hypothesis was that virus-mediated myocyte damage enables cardiac myosin to be exposed, which becomes readily accessible to the immune system. This hypothesis had led to the development of the EAM model, where genetically predisposed mice (typically BALB/c or A/J mice) are immunized with mouse cardiac myosin or peptides derived from heavy chain α emulsified in complete Freund's adjuvant (CFA) supplemented with heat-killed *Mycobacterium tuberculosis* [80, 83] (Figure 1). On day 0, mice receive peptide emulsion subcutaneously together with an intraperitoneal injection of 500 ng of pertussis toxin. On day 7, mice receive a booster shot of peptide emulsion without pertussis [83]. It has been indicated that pertussis toxin can promote T cell proliferation and cytokine production as well as break T cell tolerance in an EAE model, though the precise mechanism underlying the role of pertussis toxin in EAM induction is not well understood [84]. In addition, substituting CFA for either incomplete Freund's incomplete adjuvant or alum as the adjuvant on either day will not induce EAM, highlighting that a breakdown of immune tolerance is central for EAM induction [85].

We used exclusively BALB/c male mice in our studies. They tend to develop myocarditis of moderate severity and progress to DCM. The induction phase of myocarditis is established by day 10, during which an adaptive immune response to cardiac myosin

develops. The acute phase of myocarditis begins between day 10-12, when immune cells start to infiltrate the myocardium. During this time autoantibodies emerge in the serum and autoreactive T cells can be detected in the heart. On day 21 post-immunization, the intensity of the immune infiltrate reaches its peak. The cell number starts to decline thereafter, marking the beginning of myocarditis resolution phase. Occasionally chronic inflammation does not subside even after day 60 post-immunization. As cardiac immune cell infiltrates diminish, there is an increase in cardiac fibrosis and a decrease of ventricular functions that can be observed via histology and detected by echocardiography, respectively [56].

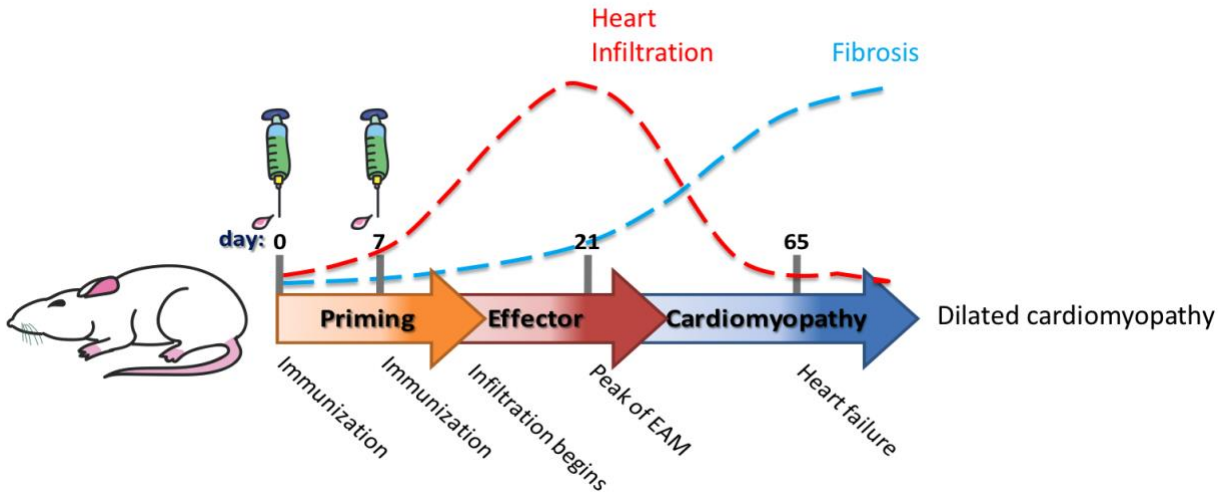

Figure 1. Model of experimental autoimmune myocarditis in BALB/c mice experimental viral myocarditis

D. Experimental viral myocarditis murine model

CVB3 is an enterovirus that belongs to the *Picornaviridae* family [60]. CVB3 is implicated as one of the primary pathogens responsible for acute and fulminant viral myocarditis in

humans [86]. One of the most commonly used myocarditis mouse models is via CVB3 infection to recapitulate viral myocarditis in humans [60]. Heart-passaged CVB3 virus (Nancy strain) are inoculated intraperitoneally into susceptible strains of mice. Acute myocarditis develops from day 7 to day 14 post-infection and progresses to DCM around day 35 post-infection [60]. A male gender bias in this model also replicates the human disease [87]. A recent study showed that sex hormones such as estrogen play a beneficial role in myocarditis progression [88].

Chapter 2:

Monocytes and macrophages

Monocytes and macrophages are highly conserved populations found in all vertebrates and play crucial roles in tissue homeostasis and protective immunity. Additionally, their roles in pathological processes such as myocarditis make them attractive therapeutic targets. However, the minimization of their pathogenic roles and maximization of their reparative functions during tissue injury requires an in-depth understanding of their origins, functions and interactions with the tissue microenvironments.

A. Origins of tissue-resident macrophages

Elie Metchnikoff was credited in 1882 for his seminal work describing phagocytosis, a process of phagocytes engulfing pathogens [89]. Macrophages are professional phagocytes that exist in all organs of the body as well as across diverse species. With the readily available techniques such as genetic fate mapping and lineage tracing our knowledge of macrophage role during disease and homeostasis has rapidly evolved over the past decade. We have gained an appreciation for the versatile roles and trophic/regulatory functions of macrophage in organogenesis, tissue homeostasis, immune surveillance, and post-injury tissue restoration [90]. During fetal organogenesis,

macrophages orchestrate long-distance communication between pigment cells in zebra fish skin to establish striped patterns [91]. They participate in synaptogenesis, synaptic pruning, neurogenesis and assembly of murine brain circuits [92-104]. In murine testes they contribute to testis morphogenesis, spermatogenesis, and production of male hormone during puberty [105-107]. They are indispensable in adult salamander limb regeneration [108].

Before the term “mononuclear phagocyte system” (MPS) was coined in 1969 to describe the functions and morphology of monocytes, macrophages, dendritic cells, and their precursors from the bone marrow an older term, “reticuloendothelial system”, or RES, was used to describe these phagocytes and their antecedents. RES was based on the observation that sinus-lining intravascular phagocytes frequently form reticular networks. However, we now know that macrophages and endothelial cells are separate entities [109, 110]. Macrophage phagocytosis is a process important for debris clearance and tissue remodeling. For instance, synaptic pruning by microglia eliminates defective and immature neuronal synapses during brain development [111]. While macrophage phenotypes are determined by tissue origin, an anti-inflammatory signature of high CD206 and low IL-1β expression can be unanimously elicited by phagocytic activity [112]. Additionally, macrophages are major cytokine producers that participate in innate and adaptive immune responses [113, 114].

A growing body of literature has shown that adult murine tissue resident macrophages are mostly embryonically-derived, contradicting the long-held belief that macrophages are derived from circulating monocytes released from the bone marrow and spleen [115-119]. Surprisingly, discoveries made decades ago already acknowledged that yolk sac and fetal

liver of early embryos contained macrophage precursors [120, 121]. We now understand that during embryogenesis macrophages colonize developing organs in several overlapping waves [115-117] (Figure 2).

The first wave of macrophage tissue colonization occurs at embryonic day 7 (E7), before the establishment of embryonic circulation [120, 122, 123]. $Csf1r^{+}c\text{-}Kit^{+}CD45^{low}AA4.1^{+}$ Erythro-myeloid progenitors (EMPs) are released from yolk sac blood islands and capillary endothelia [124]. EMPs readily acquire macrophage transcriptional signatures and differentiate into pre-macrophages (pMacs) prior to seeding the tissue as resident macrophages (MØ) [116, 125, 126].

From E8.5, a second wave commence as yolk sac hemogenic endothelia release another set of EMPs. The development of these EMPs relies on a master transcriptional regulator called c-Myb, whereas the EMPs from the first wave were c-Myb-independent [117, 127-129]. At this stage of the embryonic development, the newly formed vasculature allows yolk sac macrophages to enter both brain and liver, as well as permit the EMPs derived from the second wave to seed the liver [122, 125, 130, 131]. EMPs expand rapidly in the fetal liver where they also differentiation into monocytic intermediates or pMacs at E11.5 [117, 125, 131]. Both monocytic intermediates and pMacs then exit the fetal liver and seed all embryonic tissues with the exception of the brain [132]. These yolk sac-derived and fetal liver-derived tissue-resident macrophages persist into adulthood. Their renewal relies mostly on proliferation and minimally depends on replenishment by blood monocyte-derived macrophages [116, 118]. Skin and gut macrophages are exceptions in that they entirely depend on monocyte-derived macrophage replenishment to sustain the local macrophage pool [133, 134]. Lastly, the third wave of macrophage tissue

colonization occurs at E10.5, when hematopoietic stem cells (HSCs) derived from hemogenic endothelium in the dorsal aorta enter the fetal liver [115, 135, 136]. Upon entry, HSCs expand and differentiate into monocytic intermediates which then colonize the tissue to become resident macrophages [115, 137, 138]. HSCs also seed the bone marrow and spleen during embryogenesis to produce a constant supply of circulating monocytes postnatally to replenish macrophage pool in specialized organs under steady state or inflammation [119, 139]. A type of early pro-B cell that expresses both myeloid and lymphoid markers has recently been discovered as a progenitor for both tissue resident or monocyte-derived macrophages during both inflammation and homeostasis [140].

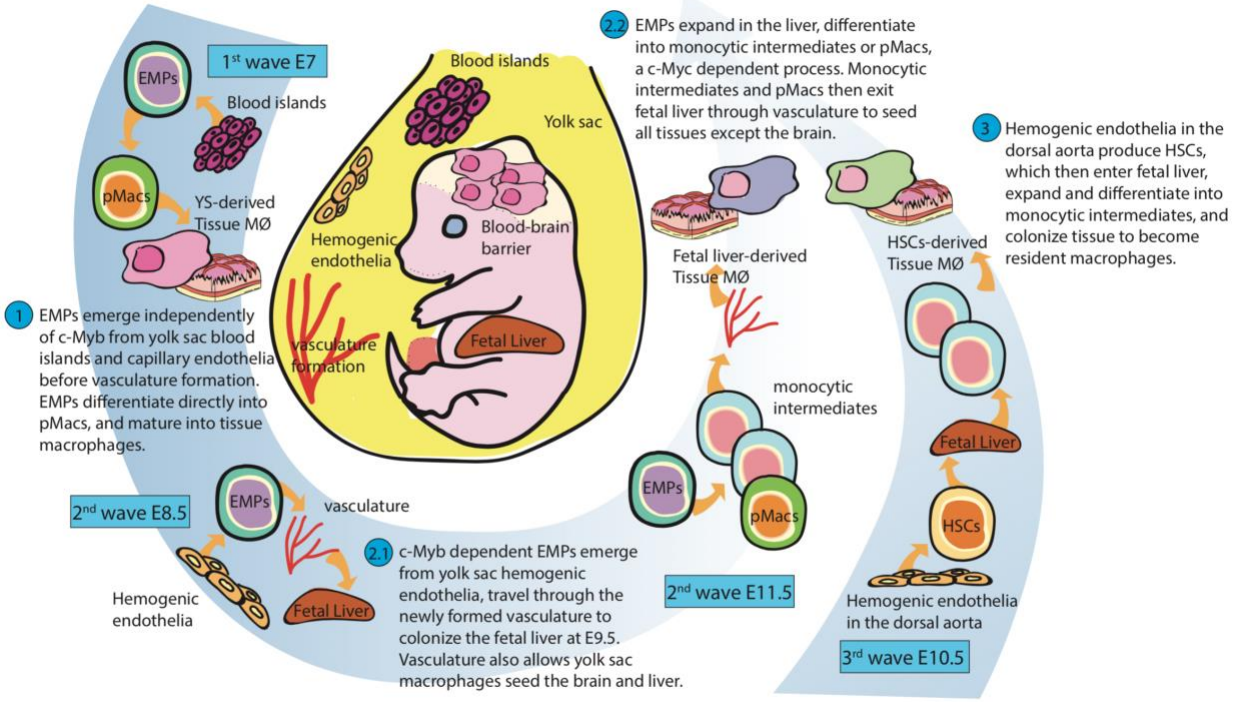

Figure 2. Macrophages colonize developing organs in several overlapping waves during embryogenesis.

Figure drawn by X. Hou.

B. Heterogeneity of tissue macrophages

A robust steady-state condition is required to ensure proper tissue function and maintain homeostasis of an organism. However, organ homeostasis varies considerably owning to differences in tissue metabolic and mechanical activities, physical barriers, the levels of exposure to commensals and nutrients, as well as maturation status. Most of the macrophages that populate tissues during organogenesis persist into adulthood as resident, self-maintaining populations in steady state [118, 141]. Tissue-resident macrophages hone their phenotypes in response to local microenvironmental signals and turnover in a tissue-specific manner (Figure 3). Central nervous system, epidermis and lung macrophages are exclusively yolk-sac and/or fetal liver derived. They have robust self-renewal potential and persist into adulthood under steady-state [142, 143]. These relatively ontogenically homogeneous populations can even cope with experimental depletion [144]. A small portion of liver Kupffer cells are derived from BM monocytes immediately after birth. They self-renew in adulthood without further contributions from monocytes [117, 145-147]. This is similar to arterial macrophages [148]. Cardiac resident macrophages consist of yolk-sac and fetal liver derived macrophages before birth [119, 149]. Embryonically derived $CCR2^-$ macrophages are positioned near coronary vasculature, whereas fetal monocyte-derived macrophages tend to cluster near endocardial trabeculae [150]. This uneven distribution suggests their role in cardiac development. These yolk-sac-derived and fetal liver-derived macrophages are gradually replaced by monocyte-derived macrophages with age [149]. It has been demonstrated that at birth, almost all cardiac macrophages are $CCR2^-MHCII^-$ (major histocompatibility complex class II). This relatively homogenous population diversifies into 4 subpopulations

with the increase of both CCR2 and MHCII expression [149]. Intestinal macrophages have a relatively short half-life (4 – 6 weeks). Both yolk sac-derived and fetal liver-derived macrophages begin to wane after birth in the lamina propria, and they require constant replenishment from BM-derived monocytes. This drastic replacement of embryo-derived macrophages by monocyte-derived cells coincides with commensal bacteria colonization and is highly depended on CCL2/CCR2 axis [139]. Similar to intestinal macrophage maintenance, dermal macrophages also rely on monocyte replenishment. They are thought to be highly phagocytic but are less sufficient in eliciting T cell activation [133]. The above evidence highlights the role of the tissue microenvironment in controlling macrophage origin and fate, as well as in determining monocyte recruitment and differentiation during steady-state. This remains an active area of research. Macrophages are highly adaptive. Their close association with the local habitat allows them to evolve and develop tissue-specific features defined by particular transcription factors and epigenetic marks [151-153]. Not surprisingly, when tissue macrophages are isolated to culture they rapidly lose tissue-specific phenotypes [152]. An example of how transcription factor influences tissue macrophage phenotype is Spi-C. Spi-C is crucial for maintenance of both splenic red-pulp macrophages and liver-resident Kupffer cells. These cells are positioned to engulf aging $CD47^{-}$ erythrocytes, which induce Spi-C to assist in heme-metabolizing processes [154]. Another example could be GATA-6 expression in peritoneal macrophages of embryonic origin [155-157]. These cells are characterized as large $F4/80^{hi}MHCII^{lo}$ [158]. However, both retinoic acid and omental tissue-derived signals are needed for GATA-6 expression [156].

Macrophage functions vary widely depending on changes that occurring in its residing tissue niche including metabolites [152, 153, 159], intracellular metabolism [160], and genetic and intrinsic epigenetic factors [113, 161-163]. One of the most exciting advances in the field is the understanding of the epigenetic changes that characterize different population of tissue-resident macrophages. Although all immune cells share the identical genome, chromatin modification enables them to acquire distinct roles [164-168]. Particularly, comparison of the promoter and enhancer regions reveals that few macrophages are identical across different tissue microenvironments [153]. This demonstrates that local microenvironments imprint macrophages and creates heterogeneity within this population. Reciprocally, tissue macrophage expresses a variety of sensors located on the surface and inside the vacuoles and cytosol to provide contact and control to its residing environment. Since macrophages are prominent participants in disease pathologies, including heart failure, rheumatoid arthritis, multiple sclerosis and cancer, the study of chromatin landscape can identify targets for genetic manipulations of macrophage that could serve as a potential treatment strategy.

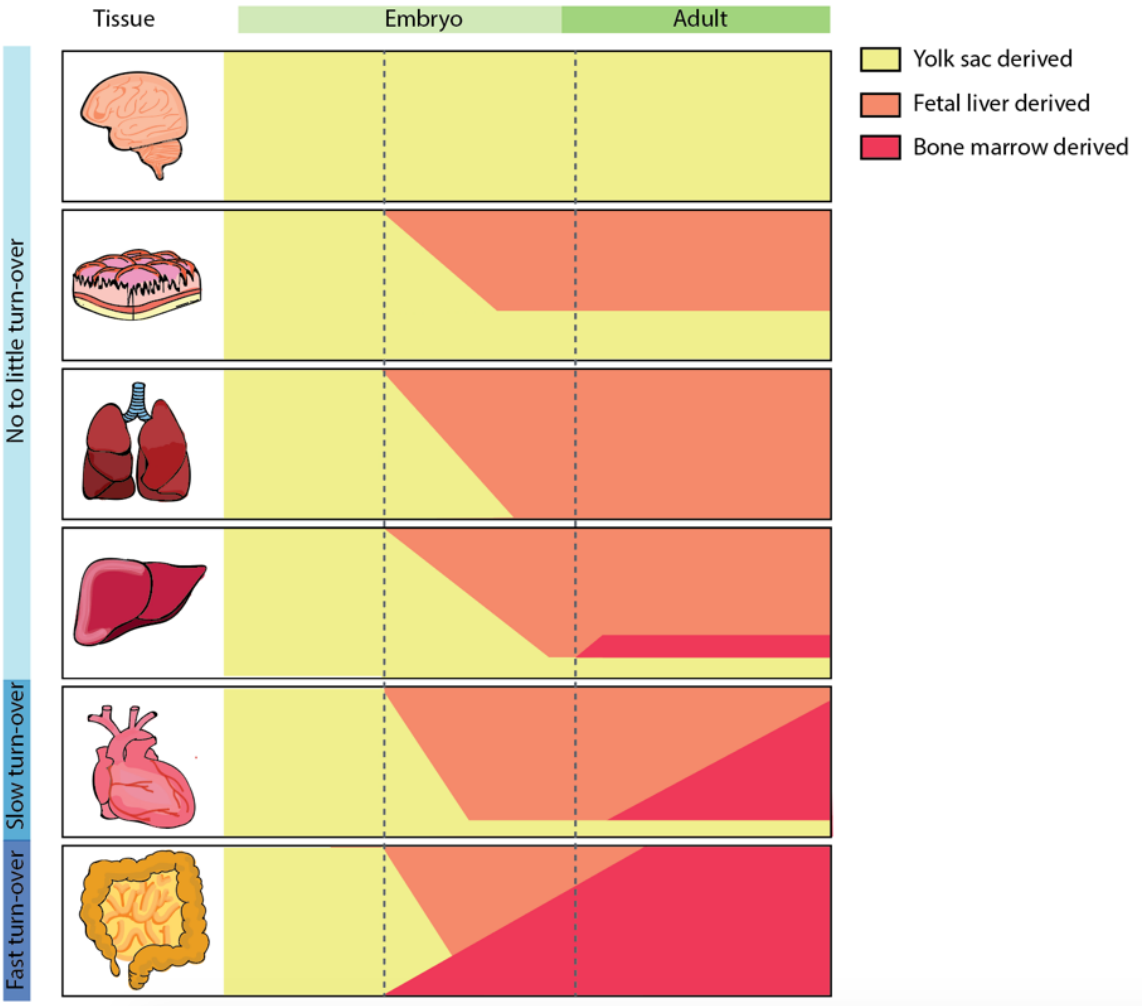

Figure 3. Steady state macrophage origins in multiple adult tissues.

Figure drawn by X. Hou.

C. Monocytes

Monocytes comprise approximately 4% and 10% of all circulating leukocytes in mice and in humans, respectively. There are two main monocyte subsets in mice, the "classical" Ly6C^{hi}CCR2^{+}CD62L^{+}CX3CR1^{-} inflammatory monocytes and the "alternative/non-classical" Ly6C^{lo}CCR2^{-}CX3CR1^{+} patrolling monocytes [169, 170]. The former is known to extravasate into tissue after an insult and release pro-inflammatory cytokines such as interleukin-1β, tumor necrosis factor-α, and reactive oxygen species. Ly6C^{hi} monocytes also have a high tendency to differentiate and replace the diminishing tissue macrophage pool [169-173]. Ly6C^{lo} monocytes are known to patrol the lumen of the vessels, scavenging for dead cells, oxidized lipids and pathogens [174]. Their differentiation into reparative macrophages has been reported in skeletal muscles and in soft tissue [175-177]. In terms of phenotypes, function and gene expression profiles, human CD14^{hi}CD16^{-} and CD14^{+}CD16^{+} monocytes account for about 90% of all circulating monocytes and resemble proinflammatory Ly6C^{hi}CCR2^{+} monocytes in mice. Human CD14^{-}CD16^{hi} monocytes account for about 10% of the peripheral monocyte population and resemble patrolling Ly6C^{lo}CCR2^{-} monocytes in mice [178-183].

D. Monocyte development

The homeostatic production of monocytes requires defined developmental stages and commitment in the bone marrow (Figure 2, Table 3). Monocytes are heterogenous populations that originate from HSCs, and can also arise from fetal liver during embryogenesis (Figure 2). It has been demonstrated that the spleen harbors monocytic

precursors that can also contribute to monocytopoiesis during inflammation, a process termed “extramedullary hematopoiesis” [184]. HSCs, which represent about 0.05% of the adult mouse bone marrow population, are cells that possess multipotency and can self-renew [185-189]. It has been shown that HSCs can give rise to long-term HSC (LT-HSC), short-term HSC (ST-HSC) and Multi-Potent Progenitors (MPP) (Figure 4). The latter two can no longer self-renew [190]. Lineage-restricted differentiation happens when MPP are produced. These MPPs then give rise to both common myeloid progenitors (CMP) and common lymphoid progenitors (CLP), which are both oligopotent progenitors (possessing relatively finite differentiation capacity) [191-194]. CMPs subsequently give rise to granulocyte and macrophage progenitors (GMP) and megakaryocyte/erythrocyte progenitors (MEP) [195, 196]. GMPs can further give rise to macrophage and DC precursors (MDP) [197], which are dedicated clonotypic precursors to common monocyte progenitor (cMoP) and common dendritic cells precursors (CDP) [198]. Common monocyte progenitors strictly generate monocytes, but not plasmacytoid DCs or cDCs [198]. Isolated cMoP can differentially give rise to both $Ly6C^{hi}$ and $Ly6C^{lo}$ monocytes [198]. On a molecular level, monocyte development is precisely controlled by lineage-defining transcription factors during each stage of development [199] (Figure 4). PU.1 or *Sfpi1* (also known as Spleen focus forming virus proviral integration oncogene) is critical in early steps of monocyte development, especially during the stage of CMP, GMP and MDP differentiations [200-202]. PU.1 knockout mice have an embryonic lethal phenotype or they die shortly after birth [203]. PU.1 binds to GATA-1 and inhibit CMP differentiation into MEP [204].

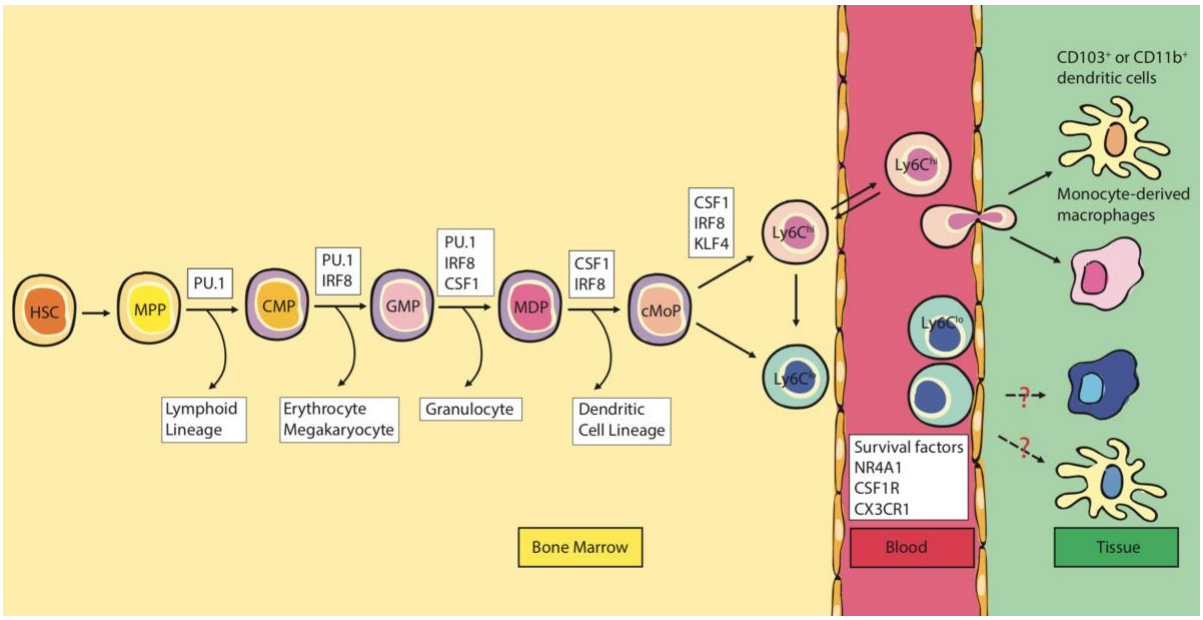

Figure 4. Monocyte development from the bone marrow.

Figure drawn by X. Hou.

Another family of transcription factors known as C/EBP belongs to the basic leucine zipper family that recognizes and binds to DNA motif (5'-T(T/G)NNGNAA(T/G)-3') [205, 206]. While *Cebpb* is important for the development and maintenance of monocytes, *Cebpa* is important for monopoiesis [207-210]. Interestingly, *Cebpa* expression allows T and B lymphocytes to transdifferentiate into macrophages [211, 212]. IRF8 (interferon consensus sequence-binding protein) is another critical transcription factor required for monocyte development in the bone marrow. It is specifically induced in CMP and GMP [213]. IRF8 interacts with PU.1 to form heterodimers to regulate functions of both monocytes and macrophages [214]. IRF8 promotes monocyte differentiation and persists in differentiated monocytes and macrophages, whereas IRF8 subsides in granulocyte and inhibits their production [215]. IRF8 downstream directly regulates KLF4 (Kruppel-like factor 4), a key transcription factor for myelopoeisis [216]. KLF4 is indispensable for $Ly6C^{hi}$ monocyte development [217]. NR4A1 (Nuclear Receptor Subfamily 4, Group A, Member 1) is a master transcription factor required for $Ly6C^{lo}$ monocyte development, survival, and myelopoiesis [176, 218, 219].

Finally, there are also a few negative regulators of monocyte production. The lack of either GATA-2, Fli-1 (Friend leukemia integration 1) or RUNX1 (RUNT-related transcription factor 1) leads to upregulation of monocyte production and release [220-226]. Other factors also play a role in monocyte development. Colony-stimulating factor 1 (M-CSF) is indispensable for monocytes survival and development in mice. Animals deficient in M-CSF or M-CSF receptors (CD115 or M-CSFR) such as op/op mice suffer from severe monocytopenia [227-229]. M-CSF is also involved in tissue-resident macrophage

proliferation and survival by apoptosis reduction [155, 230, 231]. CX3CR1 is also important to promoting long term survival in monocytes [232].

During steady state, monocytes are released from the BM with a regular circadian rhythm associated with regulatory genes such as *Bmal1*, *Nrld1* and *Dbp*. Blood monocytes' diurnal rhythm peaks at Zeitgeber times (ZT) 4 and reaches nadir at ZT 16 [233]. The fluctuation of blood monocytes is also important in determining mortality and morbidity after myocardial infarction (MI), which will be discussed at a later chapter [234].

Table 3. Markers defining myeloid progenitor populations

Myeloid progenitors	Markers in mice	Markers in human
HSC	$Lin^-cKit^+Sca1^+Flk2^-CD34^-Slamf1^+$	$Lin^-CD38^-CD90^+CD45RA^-CD34^+$
MPP	$Lin^-cKit^+Sca1^+Flk2^-CD34^-Slamf1^+$ $Lin^-cKit^+Sca1^+Flk2^-CD34^-Slamf1^-$ $Lin^-cKit^+Sca1^+Flk2^+CD34^-Slamf1^-$	$Lin^-CD38^-CD90^-CD45RA^-CD34^+$
CMP	$Lin^-cKit^+Sca1^{lo/-}IL7Ra^-CD34^+FcgR^{lo}$	$Lin^-CD38^+IL3Ra^{lo}CD45RA^-CD34^+CD123^{lo}$ $CD10^-Flt3^+$
CLP	$Lin^-Flk2t^+IL7Ra^+CD27^+$	$Lin^-CD38^+CD10^+CD34^+CD45RA^+CD45^+$
GMP	$Lin^-cKit^+IL7Ra^-Sca1^-CD34^+FcgR^+$	$Lin^-CD38^+IL3Ra^+CD45RA^+CD34^+CD123^{lo}$ $CD10^-CLEC12A^{hi}CD64^{int}Flt3^+$
MEP	$Lin^-cKit^+Sca1^-CD34^-FcgR^-$	$Lin^-CD38^+IL3Ra^-CD45RA^-CD34^+$
MDP	$Lin^-cKit^+IL7Ra^-Sca1^-Flt3^+CD115^+FcgR^-$	$Lin^-CD38^+CD115^+CD45RA^+CD34^+CD123^{int}$
CDP	$Lin^-cKit^{int}Sca1^-Flt3^+CD115^+CD11b^-$	$Lin^-CD38^+CD115^-CD45RA^+CD34^+CD123^{hi}$
cMoP	$Lin^-cKit^+IL7Ra^-Sca1^-CD115^+FcgR^-$	$Lin^-CD38^+CD115^-CD45RA^+CD34^+CD123^{lo}$ $CD10^-CLEC12A^{hi}CD64^{hi}Flt3^+$

This table is based on [235-239].

Chapter 3:

Monocytes and macrophages in cardiovascular disease

A. Monocytes and macrophages in Heart Failure (HF)

An estimated 26 million people are affected by HF worldwide and its prevalence is projected to continue to increase [240]. HF adversely affects quality of life and reduces the overall lifespan [241]. The pathological signs of HF are progressive impairment of cardiac function with many patients developing atrial fibrillation [242]. Globally, rheumatic heart disease remains a major cause for HF. Cardiac inflammation from rheumatic disease results in scarring of the heart valves, primarily the mitral valve, with consequent valvular malfunction and HF [243]. In developed nations myocardial infarction (MI) is the leading cause of HF [244]. MI is typically the result of atherosclerotic plaque rupture and coronary occlusion [242]. Murine models have helped to demonstrate that both monocytes and monocyte-derived macrophages play a pivotal role in the pathogenesis of MI. It is thought that monocyte subsets are designated to perform distinct but complex roles that may be beneficial or detrimental [245-247]. Although studies are limited in human subjects, it has been shown that there is a post-infarction increase in the total number of blood monocytes and this correlates with an increased left ventricular end-diastolic volume and a decreased ejection fraction [248].

Under steady state, resident cardiac macrophages in healthy adult mice represent less than 10% of the total non-cardiomyocyte population [249]. However, cardiac ischemia

from MI drives hematopoiesis that mobilizes immune cells, including pro-inflammatory monocytes, to enter the infarct zone and differentiate into macrophages [171, 250]. When diurnal monocyte fluctuation is disrupted, myocardial remodeling and function worsen in post-infarct mice [234]. The observation of diurnal variation extends to human subjects with MI who manifest increased ST-segment elevations that correlate with peaking of their infarct size at 1:00 in the morning [251]. Furthermore, it is thought that sequential recruitment of Ly6C^{hi} and Ly6C^{lo} monocytes to the infarct zone regulates the inflammatory and reparative response post-infarct, respectively [245]. However, the exact function of Ly6C^{lo} monocytes is unknown. It has been shown that the orphan nuclear receptor NR4A1 controls BM differentiation and survival of the Ly6C^{lo} monocytes, since Ly6C^{lo} monocytes are absent from Nr4a1$^{-/-}$ mice [218]. Nr4a1 was proposed to be an important factor required for Ly6C^{hi} monocytes to differentiate into reparative macrophages [171].

B cells in post-infarct myocardium are thought to also play a role in monocyte recruitment. They are thought to predominantly produce CCL7, a ligand for CCR2. B cell depletion, therefore, results in reduced monocyte trafficking and improved ventricular function [252]. Neutrophils, on the other hand, produce gelatinase-associated lipocalin to promote a reparative phenotype in macrophages which is beneficial in infarct healing [253]. Monocyte and macrophage activation potentiates the cardiac inflammatory response by exerting a wide range of functions. They are thought to promote myofibroblast accumulation, collagen and extracellular matrix deposition, phagocytosis and angiogenesis, all of which promote myocardium remodeling post infarct [254].

CCR2^{+} macrophages, in particular, have the capacity to produce large amounts of pro-inflammatory cytokines [119]. CCR2 blockade or deficiency reduces inflammation and

cardiac fibrosis without changing hypertrophy outcomes in a model of pressure overload [255]. Ischemic injury results in rapid accumulation of dying myocytes [256]. Paradoxically, phagocytosis of dead cell and matrix debris triggers an anti-inflammatory profile in macrophage subsets [257]. As a result, macrophage depletion during infarct healing jeopardizes proper repair and increases mortality [258, 259]. Therefore, monocytes and macrophages are also indispensable in tissue remodeling post-infarct [250, 260, 261]. It was demonstrated that a significant macrophage expansion occurs between 4 to 8 weeks post MI in the remote non-infarcted myocardium [262, 263]. Fate mapping studies showed that this macrophage expansion results from both CCL2 (C-C chemokine receptor type 2) dependent monocyte recruitment and local macrophage proliferation [262]. The inhibition of monocyte infiltration at late time-points in non-infarct areas significantly reduced adverse remodeling, indicating that monocyte-derived macrophages in the non-infarct myocardium play a role in aggravating post-infarct heart failure [262]. It has been proposed that higher diastolic pressure in the left ventricle creates a cytokine environment that drives similar macrophage expansion in humans as well [262].

Heart failure with preserved ejection fraction (HFpEF) accounts for approximately half of the patients suffering from HF [264]. HFpEF has been increasing in prevalence due to increasing extracardiac comorbidities such as hypertension, diabetes and obesity [265, 266]. Although the high mortality and morbidity for HFpEF make it a significant clinical problem, there is no treatment currently available [265, 267]. Despite significant cardiomyocyte death, HFpEF has a relatively normal systolic contraction. The pathophysiology of HFpEF includes diastolic impairment and chronotropic incompetence [268]. Chronotropic incompetence is the inability of the heart to increase its rate to

compensate for strenuous activities [269]. A recent study showed that mice receiving salty drinking water, unilateral nephrectomy, and chronic exposure to aldosterone (SAUNA) developed hypertension and HFpEF similar to human patients [270]. An expansion of the macrophage population was found in both mice and humans when compared to healthy controls. These murine MHCII^{hi} macrophages produce IL-10 as an autocrine factor. Macrophage specific depletion of IL-10 ameliorates fibrosis and diastolic function [270]. IL-10 producing macrophages are also active during the reparative phase post-MI to promote scar formation through myofibroblast activation and proliferation [271].

Because exacerbated monocytosis in the damaged heart impairs the post-infarct healing process, there are several proposed methods to curb monocyte recruitment. First would be the reduction of HSC egress from the BM. It was shown that β3-adrenoreceptor blockade in ApoE$^{-/-}$ mice post-infarct reduced monocytosis [272]. Second would be the reduction of extramedullary monocytosis from the spleen. Disruption of angiotensin II-angiotensin 1 receptor signaling can potentially inhibit monocytes' release from spleen [273, 274]. Lastly, would be the reduction of monocyte recruitment to the infarct. CCR2 knockdown decreased proinflammatory monocytes trafficking that improved proper infarct healing [275, 276]. And the treatment of *Irf5* siRNA nanoparticle delivery to the heart has been proposed to reduce myelotropic chemokine production and overall inflammation in mice post-infarct [277, 278].

Notably, it has been recently proposed that macrophage immunometabolism could be a promising HF therapeutic target. Changes in metabolic states dictate macrophage pro- and anti-inflammatory functions [279-281]. Engulfed apoptotic cells generate metabolites that downstream promote a reparative phenotype in macrophages [281].

B. Monocytes and macrophages in Atherosclerosis

Atherosclerosis is one of the leading causes of death in Western society and is associated with a number of risk factors such as obesity, insulin resistance, smoking and physical inactivity [282, 283]. Atherosclerosis is a chronic arterial inflammatory disease, triggered by apolipoprotein-B-containing lipoproteins (apoB-LPs) retained inside the subendothelial space called the intima [284]. ApoB-LPs consist of a neutral lipid core, composed predominantly of cholesteryl fatty acyl esters and triglycerides, enclosed by a monolayer phospholipids and proteins. There are two types of apoB-LPs: hepatic and intestinal. Hepatic apoB-LPs are circulating low-density lipoprotein (LD) and the intestinal apoB-LPs are remnant lipoproteins; both are highly atherogenic [283]. Retention of apoB-LPs predominantly occurs at arterial branch points and bifurcations that leads to disturbed laminar flow [285, 286]. Although normally this retention is benign due to preservation of the arterial lumen, a vulnerable plaque containing a necrotic core can lead to major problems. A local occlusive luminal thrombosis can form in patients with ruptured or eroded large arterial atherosclerotic plaques, which are likely to result in acute MI, stroke or sudden cardiac death [287, 288] (Figure 5). The extent of apoB LP retention is determined by multiple factors, including peripheral apoB LP concentration, age and genetic background of the individual [289]. Additional risk factors such as hypertension, diabetes, obesity, rheumatoid arthritis and psoriasis can also accelerate atherosclerosis progression [287].

While a good deal of the information that we have on the pathogenesis of atherosclerotic lesions has been derived from murine models, it is important to note that the

atherosclerotic mouse models only partially recapitulate human disease. There are currently two widely used murine models: high fat, Western diet fed *Ldlr*$^{-/-}$ mice and chow fed or Western diet fed *Apoe*$^{-/-}$ mice [290]. Although neither model sufficiently replicates human plaque rupture and acute luminal thrombosis, the preponderance of evidence provided by mouse models indicated that monocyte and macrophages play a decisive role in atherosclerosis development in both humans and mice [291].

The number of circulating inflammatory monocytes ($CD14^+$ in human and $Ly6C^{hi}$ in mice) is positively correlated with atherosclerosis [292, 293]. It has been shown that these circulating inflammatory monocytes are tethered to activated endothelial cells and migrate to the intima and differentiate into inflammatory macrophages [294, 295]. However, one study has shown that $Ly6C^{hi}$ monocytes can also contribute to anti-inflammation macrophages during plaque regression [296]. It is unclear whether $Ly6C^{lo}$ monocytes are capable in becoming macrophages [297]. Nevertheless, when blood monocyte recruitment to the plaque is inhibited, lesion formation is markedly decreased [298]. Tacke and colleagues have shown that maximal suppression of atherogenesis can only be achieved by blockade of both $Ly6C^{hi}$ and $Ly6C^{lo}$ monocytes trafficking to the atherosclerotic plaques [299].

It has been reported that monocyte-derived macrophages together with local proliferating resident macrophages are the most predominant populations within the plaque [300, 301]. Macrophages contribute to plaque growth and apoB-LP retention by either engulfing oxidized low-density lipoprotein particles (oxLDL) to become foam cells, or secreting proteoglycans that bind to apoB-LP [286]. Notably, the two most important changes mediated by pro-inflammatory monocytes/macrophages are plaque necrosis and

weakening of the protective fibrous cap, which ultimately leads to lesion rupture (Figure 5). It has been demonstrated that a combination of macrophage apoptosis and defective macrophage efferocytosis functions contribute to plaque necrosis in advanced atherosclerosis [302, 303]. Several mechanisms that lead to inefficient efferocytosis were proposed including oxidative stress as a result of defective cholesterol efflux or proteolytic cleavage of MerTK efferocytosis receptor [304, 305]. Moreover, macrophage-derived matrix metalloproteinases (MMPs) have been shown to contribute to fibrous cap thinning, particularly MMP2, MMP9, MMP13 and MMP14 [306-308]. A separate pathway has been described that macrophages can trigger the apoptosis pathway of the smooth muscle cells through Fas and Fas ligand interactions as well as TNFα and nitric oxide production, which also increase plaque vulnerability [309]. Conversely, anti-inflammatory macrophages are crucial in stabilizing plaque by engulfing debris to prevent plaque necrosis and producing collagen to strengthen the fibrous cap [289, 310]. Both pro- and anti-inflammatory macrophages are present in human atherosclerotic lesions [311]. In addition, increased sympathetic nervous system activity was found to worsen atherogenesis post-infarct by promoting hematopoietic stem and progenitor cells (HSPCs) to egress from the BM [272]. These HSPCs seed the spleen and contribute to the increase in blood Ly6C^{hi} monocytes number through extramedullary hematopoiesis [184].

Monocyte-derived macrophages produce significant levels of IL-1β in the failing heart. Antibody or targeted gene therapies used to prevent monocyte entry into atherosclerosis lesions ameliorate disease progression in mice [283, 295]. In clinical settings, neutralizing immune cell functions using anti-IL-1β has resulted in improving atherosclerosis outcomes despite some adverse effects in the Canakinumab (a human anti-IL-1β

monoclonal antibody) anti-inflammatory thrombosis outcomes study (CANTOS) [312]. The study concluded that anti-IL-1β not only reduces monocyte entry into lesions but also promotes macrophage egress from lesions without altering apoB-LP levels in blood [313, 314].

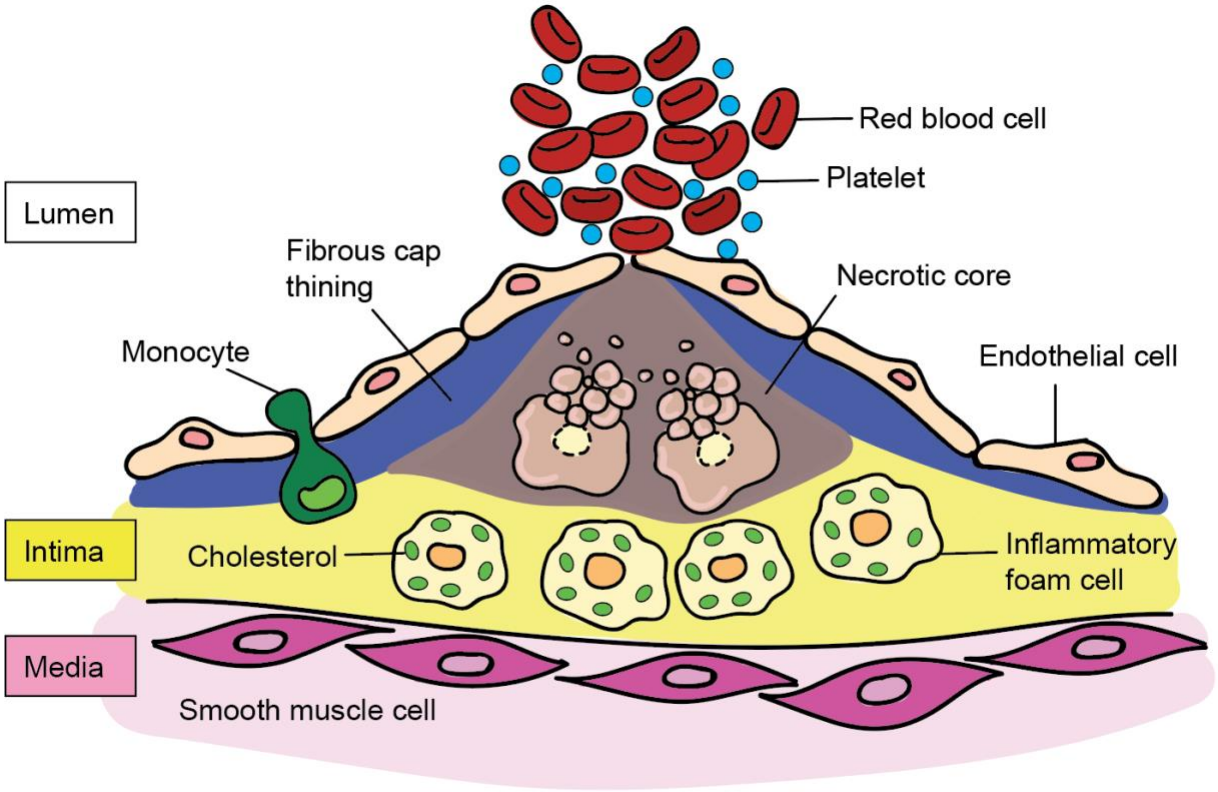

Figure 5. Manifestations of atherosclerosis arise when fibrous cap thins and plaques undergo rupture.

Figure drawn by X. Hou.

Chapter 4:

Monocytes and macrophages in autoimmune disease

Autoimmunity reflects dysregulation of host tolerance. Dysfunction in central tolerance predisposes autoimmunity and faulty peripheral tolerance unleashes autoimmune disease pathology. Otherwise speaking, a defective immune system that cannot discriminate self from non-self is the basis for autoimmune diseases [315]. In order to maintain tolerance, self-reactive lymphocytes must be eliminated, sequestered, or silenced in a timely manner. The presence of autoantibodies is an important serological feature of autoimmune diseases and signals the breakdown of immune tolerance. Central tolerance, peripheral anergy, and secretion of regulatory cytokines/chemokines by T regulatory and key innate cells are essential components needed to maintain immune tolerance [316]. Autoimmune diseases encompass nearly 100 types of disorders and affect about 5% of the population in the Western hemisphere [315, 316]. Despite recent advances in the diagnosis and the treatment of the symptoms of autoimmune diseases, both mortality and morbidity in affected populations remain high. Monocytes and macrophages have been implicated in the pathogenesis of several autoimmune diseases including myocarditis, DCM, systemic lupus erythematosus (SLE), multiple sclerosis (MS), inflammatory bowel disease (IBD) and rheumatoid arthritis (RA).

Macrophages function as phagocytes that recognize and sequester foreign agents and apoptotic debris [317]. They are also capable in secreting cytokines and chemokines as

paracrine factors that modulate activities of other cells [317]. Macrophages can act as potent antigen presenting cells that instigate adaptive immune responses [317]. Additionally, macrophages are known to promote angiogenesis and fibrosis during tissue injury [318]. Macrophage subsets are highly diverse with regard to their ontogenies, phenotypes and functions (see above). It has therefore been challenging to decipher their role during autoimmune pathogenesis. However, current advances in lineage tracing and fate mapping allow us to distinguish monocyte-derived from embryo-derived macrophages in different tissues and organs.

A. Monocytes and macrophages in multiple sclerosis (MS)

Multiple sclerosis (MS) is a neurodegenerative autoimmune disorder affecting approximately 2.5 million young adults worldwide [319, 320]. It is characterized by axonal and neuronal loss as a result of chronic inflammation and demyelination in the central nervous system (CNS). Macrophages and resident microglia comprise the predominant pathogenic leukocytes present in the CNS during disease development, followed by $CD4^+$ T cells, likely as a result of breakdown of the blood-brain barrier [321-324]. Like many other autoimmune diseases, MS is the result of a combination of genetic predisposition and environmental influences. Genome-wide association studies (GWASs) have identified more than 230 genetic variants that increase disease susceptibility for MS [325-327]. A significant expansion of peripheral blood nonclassical $CD16^+CD14^-$ monocytes was observed in patients with MS compared to healthy controls [328]. This observation coincides with similar nonclassical monocyte expansion in psoriasis, rheumatoid arthritis and other autoimmune disorders [329, 330]. Experimental autoimmune encephalomyelitis

(EAE) is one of the most well characterized animal models of MS disease [331]. EAE can be induced by either immunization with myelin peptide emulsified in CFA or adoptive transfer of encephlitogenic T cells [332, 333]. The former model requires pertussis toxin injection to induce EAE in susceptible strains of mice [333]. Although EAE is associated with encephalitogenic lymphocyte mediated demyelination, monocyte infiltration into the CNS is correlated with EAE initiation and the progression of paralysis [334-337]. It has been shown that monocyte-derived macrophages mediate myelin destruction, whereas microglia-derived macrophages are required for debris clearance [338]. Recently it has been shown that the receptor for tumor necrosis factor, TNFR2, plays a dichotomous role in the regulation of EAE pathophysiology. Specifically, TNFR2 promotes microglia activation and proliferation, which in turn provides anti-inflammatory signals to suppress neuroinflammation, whereas TNFR2 signaling in monocytes and monocyte-derived macrophages is detrimental, driving immune activation and EAE initiation [339].

B. Monocytes and macrophages in rheumatoid arthritis (RA)

Rheumatoid arthritis (RA) is a chronic autoimmune joint disease. Inflammatory pathology is localized in the synovium of multiple joints. Cartilage and bone damage results when RA is left untreated [340]. Macrophages are known to play a crucial role in the pathogenesis of rheumatoid arthritis (RA) by augmenting and orchestrating a pro-inflammatory environment. An increased number of synovial macrophages correlates with the cartilage and bone destruction that results in joint erosion [341]. Depletion of Synovial macrophages has offered tremendous therapeutic benefit in animal models of RA [341, 342]. An early hallmark of active rheumatic disease is an

increase number of HLA-DR$^+$ macrophages in both the lining and sub-lining synovial membranes [341]. Synovial lining consists of tissue-resident macrophages and fibroblasts, whereas the synovial sub-lining (beneath synovial lining and facing synovial fluid) consists of infiltrating monocyte-derived macrophages, fibroblasts, scattered blood vessels and fat cells [341, 343]. An early hypothesis stated that macrophages initiate RA through antigen presentation to infiltrating T cells, similar to disease mechanism proposed for Graves' disease and type 1 diabetes mellitus [344]. The development of anti-TNF treatment for RA and other diseases represents a major clinical effort to downregulate HLA expression and inhibit excessive TNF production by macrophages [345, 346]. So far the origin of resident synovial macrophages is not well understood. Phenotypic differences between synovial lining macrophages and cartilage junction macrophages were reported in patients with RA [347]. However, there is no obvious evidence indicating macrophage polarization in the inflamed joints, although higher TNF and IL-1 and lower IL-10 suggest enhanced M1 activities in patients with RA [348].

The K/B x N serum-transfer mouse model of sterile inflammatory arthritis is used to mimic the effector phase of human RA [349]. This model allowed researches to conclude that Ly6C^{lo} monocytes are able to differentiate into MHCII$^+$ macrophages during effector stage after recruitment to drive disease pathology [350]. This is distinctly different from MHCII$^-$ tissue-resident synovial macrophages, which were thought to limit arthritis development [350].

An antigen-induced arthritis (AIA) model has been developed to recapitulate both the induction and effector phase of human RA [349]. CFA induces systemic inflammation,

which promotes predominantly Ly6C^{hi} monocytes to infiltrate the knee and differentiation into macrophages [351].

The model that most closely resembles human RA is collagen-induced arthritis (CIA). The breakdown of immune tolerance, release of autoantibodies, and excessive pro-inflammatory cytokine release are all indispensable components in this model [349]. Multiple studies have concluded that Ly6C^{hi} monocyte are pathogenic in this model [352-354]. CD14^{+}CD16^{+} intermediate human blood monocytes were more elevated in RA patients than in healthy controls [355]. These monocytes are thought to possess a potent ability to secrete inflammatory cytokines [356]. Therefore, we must be extremely cautious when proposing macrophage targeted treatment for RA patients since as yet there is no consensus regarding which exact populations are important in RA pathology. In addition to many proposed cytokine inhibitory treatments, nanoparticle delivery of *Irf5* siRNA has been proposed [277]. IRF5 is a transcription factor important for monocyte differentiation into MHCII^{+} macrophages, as well as GM-CSF and CXCL1 release [351, 357].

C. Monocytes and macrophages in inflammatory bowel disease (IBD)

Inflammatory bowel diseases (IBDs) are chronic relapsing disorders of the gastrointestinal (GI) track due to environmental perturbation and genetic predisposition. More specifically, it is due to the failure of the immune system in the GI track to maintain its balance between keeping harmful pathogens at bay while retaining tolerance to the commensal microbiota [358]. There are two main forms of IBDs, Crohn's disease (CD) and ulcerative colitis (UC) [359].

Monocyte-derived Ly6C^{lo}CX3CR1^{hi}MHCII^{hi} intestinal resident macrophages make up the largest tissue-associated macrophage population in the body. They are essential in protecting the host against opportunistic pathogens as well as maintaining GI homeostasis [358, 360, 361]. In mice, the half-life for intestinal resident macrophages is approximately 3 to 5 weeks [362]. Therefore, Ly6C^{hi}CX3CR1^{lo}MHCII^{lo} monocytes are thought to be the precursors that continuously replenish the intestinal macrophage pool after birth [358]. The majority of intestinal macrophages are strategically positioned in the lamina propria beneath of the epithelium surface as sentinels [360]. Because these intestinal tissue macrophages express high levels of MHCII, they are thought to play a role in Foxp3^{+} T regulatory cell maintenance in the lamina propria [363]. Similarly, these macrophages support generation of commensal-specific Th17 cells, which are key immune cells that support barrier integrity [364, 365]. Apart from performing phagocytic housekeeping functions, intestinal resident macrophages also produce prostaglandin E_2 to support epithelial integrity [366-368]. Furthermore, they are known to support peristalsis by interacting with enteric neurons [369]. The intestinal mucosa induces intestinal macrophages to constitutively produce anti-inflammatory cytokines such as IL-10 which act as an autocrine factor that dampens macrophages' pro-inflammatory responses and excessive activation [368, 370-375]. Chronic inflammation such as IBD has a profound impact on tissue macrophage compartments. There are two subsets of macrophages in the inflamed gastrointestinal track that exhibit vastly different functions, CX3CR1^{hi} resident and CX3CR1^{int} inflammation-elicited intestinal macrophages [134, 370]. CX3CR1^{int} macrophages exhibit a pro-inflammatory signature and are thought to be pathogenic in the colitis mouse model [134, 376]. The current hypothesis is that the

local microenvironment, which is critical for instructing Ly6C^{hi} monocytes to become anti-inflammatory CX3CR1^{hi} macrophages, is instead arresting the monocyte differentiation pathway [134, 370]. As a result, during the resolution of inflammation, CX3CR1^{int} macrophages are removed from the microenvironment, possibly due to apoptosis or through differentiation into resident macrophages [134, 366, 377]. The present knowledge about intestinal macrophages is predominantly generated through murine models; studies in human subjects are sparse. While CD results from impaired bacterial clearance by macrophages, UC results from heightened response against bacteria [378, 379]. Overall, intestinal CD14^{hi} mononuclear phagocytes are markedly increased in IBD patients [380, 381]. These pro-inflammatory CD14^{hi} cells produce high levels of IL-6, IL-23, TNF-α and IL-1β but not IL-10 [382, 383]. Although the overall macrophage numbers are similar between CD and UC patients, it is thought that the composition and function of intestinal macrophages differ greatly [384]. For example, CD patients develop more fibrosis in the GI track than UC patients [385-387]. Tissue fibrosis has been shown to be closely associated with macrophage-mediated excessive wound healing. MMP-2 produced by macrophages to breakdown extracellular matrix has been shown to increase in CD patients' mucosa relative to healthy controls [388, 389]. Taken together, the involvement of macrophage subsets in the pathogenesis of UC and CD needs to be further elucidated to establish clinical relevance.

D. Monocytes and macrophages in systemic lupus erythematosus (SLE)

In patients with Systemic lupus erythematosus (SLE), the continuous production of a wide array of autoantibodies ensures chronic inflammation and tissue damage in multiple organs [390]. It is increasingly recognized that aberrations of monocytes and macrophages are the basis of the pathogenesis of SLE in both mice and humans [391, 392]. Uptake of apoptotic and necrotic debris by macrophages through phagocytic processes is essential in maintaining homeostasis. Ineffective phagocytosis enables exposure of autoantigens that triggers autoimmune responses [391]. It has been documented that patients with SLE have defective macrophages that are incapable of apoptotic cell clearance compared to the control patients [393, 394]. More recent studies have demonstrated that sera from SLE patients possess apoptosis-inducing-properties and SLE patients' lymph nodes have increased accumulation of apoptotic cells and decreased presence of phagocytic macrophages [395, 396]. Phagocytic defect is then compounded by chronic inflammation, which further drives SLE pathology [397]. However, it is currently unknown whether such a phagocytic defect is inherent or modulated by the environment.

Due to the highly heterogeneous nature of human SLE, no mouse model can completely recapitulate the broad spectrum of disease presentations in human subjects [398, 399]. Although the mouse models of SLE (Table 4) have contributed significantly to a better understanding of disease development and treatment, most studies have focused on lymphocytic involvements in lupus rather than that of myeloid cells [400, 401]. To improve the effectiveness of murine models, the latest technologies for genetic studies will include use of the CRISPR/Cas9 system, which allows for rapid assessment of the genetic impact

on lupus development [402]. Furthermore, humanized mice are being developed to bridge the gap between mouse model and human disease [403, 404].

Monocytes and macrophages are key components involved in the regulation of numerous diseases that are inflammatory or autoimmune in nature. The roles of these cells in the pathogenesis of myocarditis and DCM is still unclear. We hypothesize that the functions of monocytes and macrophages are driven both by endogenous and by exogenous factors in the heart during myocarditis development. We speculate that the fates and functions of the myocardial infiltrating cells determine the outcomes of DCM. In chapter 5, we will discuss the background of our work, our core findings, and discussing the broader implications of our results.

Table 4. Murine models of SLE

Category	Name	Phenotype
Spontaneous SLE model	NZB/NZWF1 (BW) [405]	Produce autoantibodies (predominantly ANA and anti-dsDNA) and develop immune complex glomerulonephritis and mild vasculitis. This model does not recapitulate the full spectrum of SLE manifestation in human and disease development is slow [406].
	NZM2410 [407]	Produce autoantibodies and develop immune complex glomerulonephritis only. Used extensively to define genetics of lupus [407, 408].
	NZM2328 [409]	Produce autoantibodies and develop acute glomerulonephritis followed by chronic nephritis [410, 411].
	MRL/lpr [412]	Develop a full spectrum of autoantibodies (anti-Sm, anti-Ro, anti-La, ANA and anti-dsDNA), as well as involves multiple organs including arthritis, skin rash and cerebritis [413, 414].
	BXSB [415, 416]	SLE only occur in male mice. Produce autoantibodies and develop immune complex glomerulonephritis only [415, 416].
	SNF1 [417]	Produce autoantibodies and develop immune complex glomerulonephritis only [417].
Induced SLE model	Pristane-induced [418]	Induce over-production of type I IFNs, similar to human SLE [419]. Produce many types of autoantibodies and develop immune complex glomerulonephritis as well as mild erosive arthritis [420].
	Resiquimod cream-induced [421, 422]	Induce over-production of type I IFNs in only BALB/c strain. Produce autoantibodies, develop immune complex glomerulonephritis as well as enlarged spleen [422].
	Graft-versus-host induction [423]	Depend on the strain used, autoantibodies and immune complex nephritis can be induced [423].
	Antibody induced	The injection of anti-glomerular basement membrane antibodies can induce rapid onset immune complex glomerulonephritis in mice [424, 425].

Chapter 5

The roles of monocyte and macrophage in myocarditis

This chapter is currently under review at *Cell Report*, entitled:

The cardiac microenvironment instructs divergent monocyte fates and functions in myocarditis.

Xuezhou Hou, Guobao Chen, William Bracamonte-Baran, Hee Sun Choi, Nicola L. Diny, Jungeun Sung, Taejoon Won, Megan Key Wood, David Hughes, Monica V. Talor, David Joel Hackam, Karin Klingel, Giovanni E. Davogustto, Heinrich Taegtmeyer, Isabelle Coppens, Jobert G. Barin, Daniela Čiháková.

Summary

Two types of monocytes, Ly6C^{hi} and Ly6C^{lo}, infiltrate the heart in murine experimental autoimmune myocarditis (EAM). We discovered a previously unappreciated role for cardiac fibroblasts in facilitating monocyte-to-macrophage differentiation of both Ly6C^{hi} and Ly6C^{lo} cells, allowing these macrophages to perform divergent functions in myocarditis progression. During the acute phase of EAM, IL-17A is highly abundant. It signals through cardiac fibroblasts to attenuate efferocytosis of Ly6C^{hi} monocyte-derived macrophages (MDMs) and simultaneously prevents Ly6C^{lo} monocyte-to-macrophage differentiation. We demonstrated an inverse clinical correlation between heart IL-17A levels and efferocytic receptor expressions in humans with heart failure. In the absence of IL-17A signaling, Ly6C^{hi} MDMs act as robust phagocytes and are less pro-inflammatory, whereas, Ly6C^{lo} monocytes resume their differentiation into MHCII^{+} macrophages. We propose that MHCII^{+} Ly6C^{lo} MDMs are associated with the reduction of cardiac fibrosis and prevention of the myocarditis sequalae.

Keywords

monocytes, macrophages, heart, myocarditis, Ly6C, MerTK

Introduction

Myocarditis remains a leading cause of heart failure in children and young adults [426, 427]. A recent global estimate of myocarditis incidence is approximately 1.5 million cases annually [428]. However, the actual myocarditis incidence could be significantly underestimated due to the heterogeneous clinical manifestations and a wide spectrum of disease presentations [429]. Between 9-16% of patients with myocarditis develop dilated cardiomyopathy (DCM). Yet no biomarkers are currently available to identify myocarditis patients at risk of developing DCM [57, 430, 431]. To date, treatment of myocarditis and prevention of its sequelae, DCM, remain vital goals in the quest to reduce morbidity and mortality in patients.

In the experimental autoimmune myocarditis (EAM) model as well as human clinical studies, we and others have reported that monocytes and macrophages comprise approximately three quarters of the infiltrating cells in the injured myocardium [432, 433]. Cardiac tissue-resident macrophages originate from precursors that develop in the embryonic yolk sac and fetal liver and maintain locally as self-renewing populations to perform tissue-specific functions. After birth, a proportion of embryonically-derived cardiac resident macrophages are progressively replaced by monocyte-derived macrophages (MDMs) that originate in the bone marrow (BM) [116, 118, 119, 147, 149, 434]. BM-derived circulating monocytes in mice consist of two subsets: the ‘classical’ inflammatory Ly6C^{hi} monocytes and the ‘non-classical’ patrolling Ly6C^{lo} monocytes. The

former resemble human $CD14^{hi}CD16^{-}$ and/or $CD14^{+}CD16^{+}$ monocytes, while the latter has similar characteristics to human $CD14^{-}CD16^{hi}$ monocytes [169, 170, 176, 317, 435-438]. Cardiac injury triggers massive $Ly6C^{hi}$ monocytes mobilization, trafficking and extravasation into the heart where they promote inflammation associated with tissue repair and remodeling [119, 171, 184, 272, 439-441].

It is challenging to distinguish tissue-resident macrophages from recruited MDMs when they co-exist in the same inflammatory niche. It is known that $Ly6C^{hi}$ monocytes are precursors to cardiac macrophages during cardiac injury [119, 245]. However, whether patrolling $Ly6C^{lo}$ monocytes also contribute to the macrophage pool is controversial. Ablation of $Ly6C^{lo}$ monocytes in a mouse model of myocardial infarction (MI) resulted in depletion of other monocyte and macrophage populations [245]. Moreover, it is unclear whether the phenotype and function of either $Ly6C^{hi}$ or $Ly6C^{lo}$ MDMs differ from one another. The mechanism through which extrinsic stimuli influence monocytes survival, proliferation, differentiation and function in the context of cardiac damage and inflammation is not understood.

We previously identified an important role of IL-17A in driving myocarditis progression to DCM [442]. IL-17A-deficient or IL-17 receptor alpha (IL17Ra)-deficient mice developed myocarditis with similar severity as WT animals. Remarkably, they have preserved cardiac functions and were protected from myocardial fibrosis and DCM [442]. We also reported that anti-IL-17A treatment during EAM onset can prevent DCM development in WT mice [442]. IL-17A signaling to cardiac fibroblasts results in the induction of

granulocyte-macrophage colony-stimulating factor (GM-CSF) and CCL2, which drives Ly6C^{hi} monocyte chemotaxis and accumulation in the heart, worsening DCM outcomes [247, 442]. The pathogenic role of IL-17A in the development of cardiac fibrosis and heart failure has also been confirmed in MI (Chen et al, 2018).

In order to better understand the underlying mechanisms of how recruited monocytes drive DCM, we fate-mapped the accumulating monocyte subsets in the heart during myocardial inflammation. We found that IL-17A-activated cardiac fibroblasts significantly arrested Ly6C^{lo} monocyte-to-macrophage differentiation and proliferation. We also discovered that IL-17A signaling through cardiac fibroblasts can downregulate efferocytosis receptors expressed by Ly6C^{hi} MDMs, negatively affecting their phagocytic function during inflammation resolution. Furthermore, both intrinsic and extrinsic factors modulate distinct transcriptomic profiles of Ly6C^{hi} and Ly6C^{lo} MDMs, signifying their potential functional differences in the context of myocarditis. Our work provides evidence that cardiac fibroblasts play a decisive role in MDM ontogeny and function during cardiac injury. Our findings provide new insights into monocyte and macrophage biology and their roles in the context of chronic cardiac inflammation.

Results

Infiltrating monocytes contribute to three subsets of macrophages during myocarditis

We created parabiotic mice to elucidate the contribution of infiltrating monocytes to cardiac macrophage populations under the influences of an inflammatory microenvironment during myocarditis development. The circulations of CD45.1 and CD45.2 mice were surgically joined, EAM was induced in CD45.1 mice 2 days prior to parabiosis (Figure 6A). On day 21 of EAM, we confirmed by histology that only CD45.1 parabionts developed severe myocardium infiltration (Figure 6B). Flow cytometric analysis at day 21 showed a significantly elevated total number of infiltrating non-neutrophilic myeloid cells in the CD45.1 EAM hearts compared to their CD45.2 parabiotic partners (Figure 6C). We also observed that CD45.1 EAM hearts had more total F4/80^{hi}CD64^{+} macrophages compared to non-EAM CD45.2 hearts, indicating cardiac macrophage expansion in response to inflammation (Figure 6D). We found a higher frequency of CD45.2^{+} MDMs in the CD45.1 EAM mice, compared to CD45.1^{+} MDMs in the CD45.2 non-EAM mice (Figure 6E, F; see gating strategy in Figure 7A). However, a higher frequency of CD45.2^{+} MDMs in the CD45.1 EAM mice did not reflect a higher frequency of total CD45.2^{+} infiltrating monocytes (Figure 6E). In addition, Ly6C^{hi} to Ly6C^{lo} monocyte ratio in the hearts between parabionts did not differ significantly (Figure 6G). Resident tissue macrophages can be further divided into three subsets, based on their expression of CCR2 and MHCII [119]. We found that infiltrating CD45.2^{+} monocytes predominantly differentiated into CCR2^{+}MHCII^{+} macrophages, though they possess the capacity to replenished all three macrophage subsets in the EAM hearts (Figure 6E, H). However, the heart infiltrating CD45.1^{+} monocytes in the non-EAM CD45.2 mice can only differentiate into MHCII^{+} macrophages (Figure 6E, H). Taken together, our data supports the idea that during cardiac inflammation, infiltrating monocytes readily differentiate into

macrophages and these monocyte-derived cells can replenish all three macrophage subpopulations.

During cardiac inflammation, mature Ly6C^{hi} monocytes arise from common monocyte progenitors (cMoPs) in the BM before trafficking to the heart [198]. We examined the mature monocyte population in the BM in response to cardiac inflammation (see gating strategy in Figure 7B). We found a substantial presence of CD45.1^{+} grafted cells in the CD45.2 parabiont BM, whereas CD45.2^{+} monocytes were relatively rare in the CD45.1 EAM parabiont BM (Figure 7C, D). We speculated that this could be due to undifferentiated CD45.1^{+} Ly6C^{hi} monocytes homing back to the CD45.1 BM in the absence of inflammation [170]. Alternatively, a systemic response to adjuvants used for EAM induction in CD45.1^{+} parabionts could increase monocyte infiltration into non-EAM parabiont BM. Another possible explanation is that EAM BM is saturated with inflammatory cells which prevented CD45.2^{+} monocytes from infiltrating CD45.1 BM. Nevertheless, the ratio of Ly6C^{hi} to Ly6C^{lo} monocytes was highly comparable between parabionts in the BM (Figure 7E). Collectively, the similarity of monocyte ratios in the BM between EAM and naïve mice suggests the local cardiac inflammatory milieu is instrumental in monocyte to macrophage differentiation in the heart.

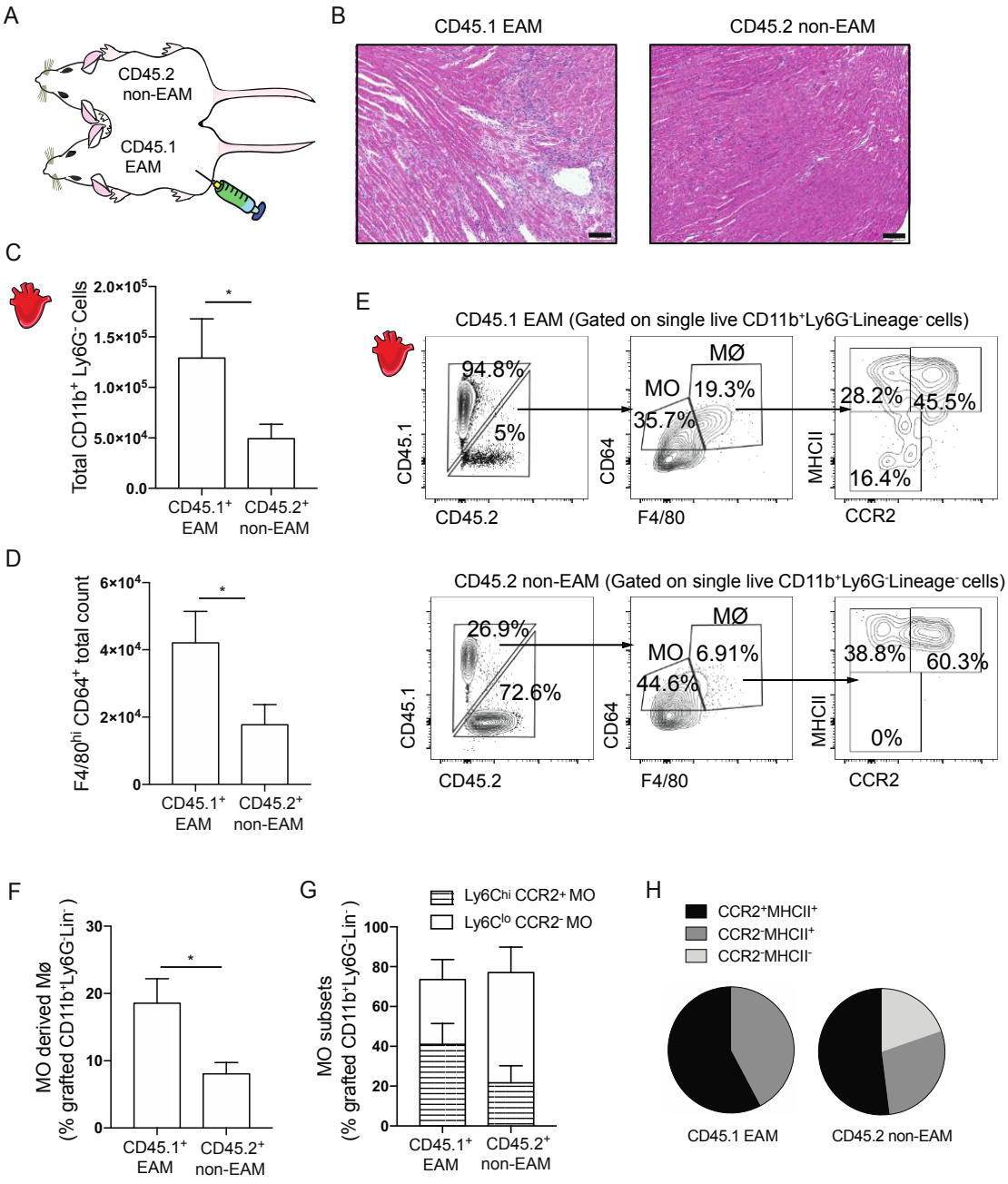

Figure 6. Monocyte dynamics during myocarditis

(A) Schematics of parabiosis mice. (B) Representative images of H&E-stained heart sections of the median animal from day 21 EAM induced CD45.1 mice and CD45.2 non-EAM pairs. Bars: 100 µm. (C) Comparison of total grafted $CD11b^{+}Ly6G^{-}$myeloid cell

counts between parabionts. (D) Comparison of total count of cardiac macrophages between parabionts. (E) Flow cytometry plots showing (Top left) Percentage of $CD45.2^{+}CD11b^{+}Ly6G^{-}$Lineage (CD3e, B220, NKp46, CD90.2 and Ter119)$^{-}$ grafted cells infiltrating the CD45.1 EAM hearts; (Top middle) Percentage of grafted cells in the hearts that differentiated into macrophages or remained as monocytes; (Top right) Percentage of grafted cell derived macrophage subsets each defined by CCR2 and MHCII expressions. (Bottom left) Percentage of $CD45.1^{+}CD11b^{+}Ly6G^{-}Lineage^{-}$ grafted cells infiltrating the CD45.2 non-EAM hearts; (Bottom middle) Percentage of grafted cells in the hearts that differentiated into macrophages or remained as monocytes; (Bottom right) Percentage of grafted cell derived macrophage subsets each defined by CCR2 and MHCII expressions. (F) Percentages of grafted monocyte-derive macrophages out of total grafted $CD11b^{+}Ly6G^{-}Lineage^{-}$ myeloid cells. (G) Percentages of grafted $Ly6C^{hi}$ and $Ly6C^{lo}$ cells out of total grafted $F4/80^{-}CD64^{+}$ monocytes. (H) Comparison of grafted MDM subsets defined by CCR2 and MHCII expressions between parabiotic mice. Data are representative of two independent experiments with biological triplicates. All data are presented as mean $\pm$ SD; n = 3. (C, D, F, G) Groups were compared using Student's *t* test. *, $P < 0.05$. See also Figure 7.

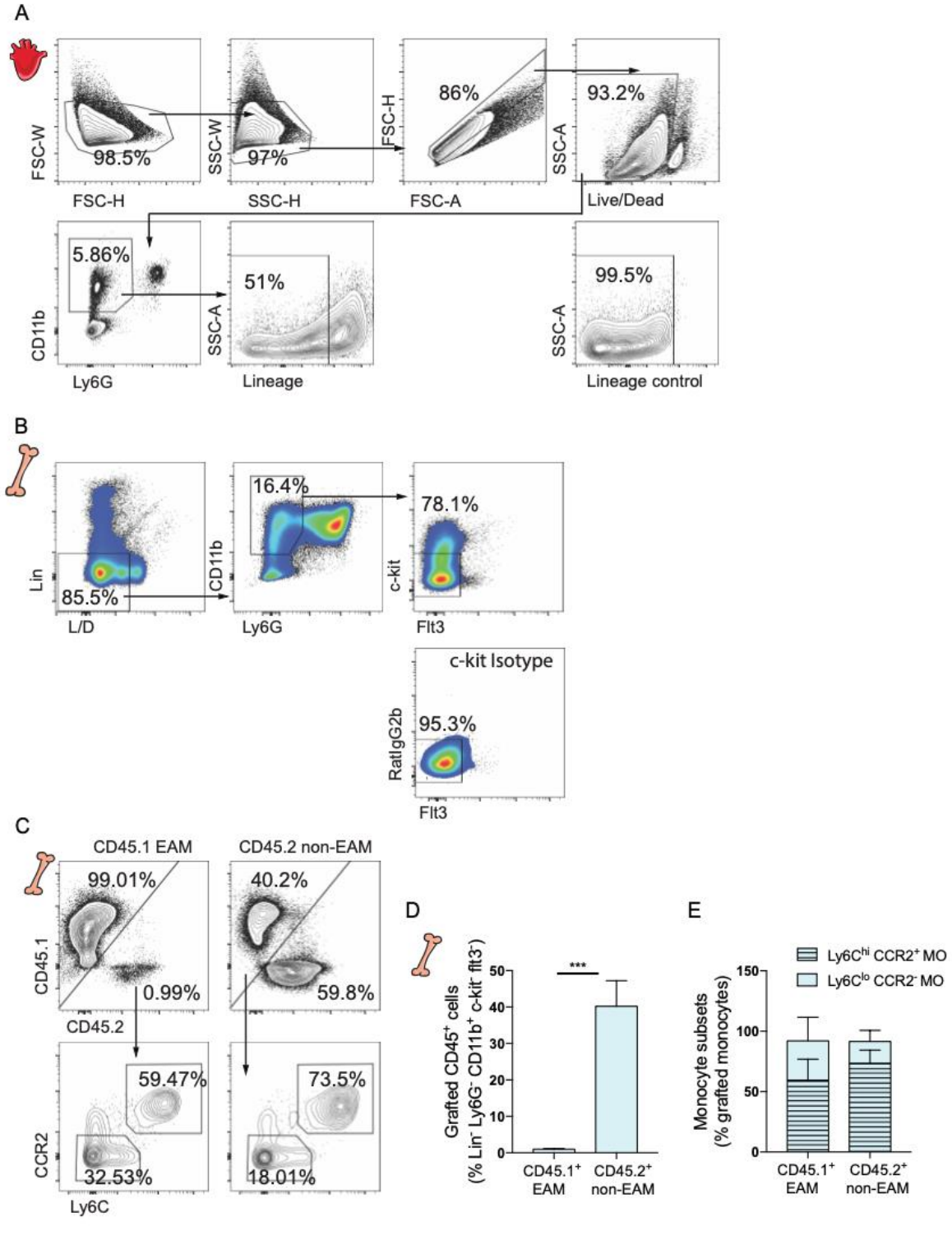
A
FSC-W
FSC-H
98.5%
SSC-W
SSC-H
97%
FSC-H
FSC-A
86%
SSC-A
Live/Dead
93.2%
CD11b
Ly6G
5.86%
SSC-A
Lineage
51%
SSC-A
Lineage control
99.5%
B
Lin
L/D
85.5%
CD11b
Ly6G
16.4%
c-kit
Flt3
78.1%
c-kit Isotype
RatIgG2b
Flt3
95.3%
C
CD45.1 EAM
CD45.2 non-EAM
CD45.1
CD45.2
99.01%
0.99%
40.2%
59.8%
CCR2
Ly6C
59.47%
32.53%
73.5%
18.01%
D
Grafted CD45+ cells
(% Lin- Ly6G- CD11b+ c-kit- flt3-)
***
CD45.1+ EAM
CD45.2+ non-EAM
E
Monocyte subsets
(% grafted monocytes)
Ly6Chi CCR2+ MO
Ly6Clo CCR2- MO
CD45.1+ EAM
CD45.2+ non-EAM

Figure 7. Characterization of monocytes and/or macrophages in murine hearts and bone marrows during EAM development

(A) Representative gating strategy showing identification of $CD11b^{+}Ly6G^{-}Lin^{-}$ myeloid cells in the hearts. (B) Representative gating strategy showing identification of mature $Lin^{-}CD11b^{+}Ly6G^{-}c\text{-}kit^{-}Flt3^{-}$ monocytes in the BM. (C) Flow cytometry plots showing grafted $Lin^{-}CD11b^{+}Ly6G^{-}c\text{-}kit^{-}Flt3^{-}$ monocytes that consist of both $Ly6C^{hi}CCR2^{+}$ and $Ly6C^{lo}CCR2^{-}$ populations in the bone marrow (BM). (D) Percentages of grafted $Lin^{-}CD11b^{+}Ly6G^{-}c\text{-}kit^{-}Flt3^{-}$ monocytes in the BM. (E) Percentages of grafted $Ly6C^{hi}$ and $Ly6C^{lo}$ monocytes out of total grafted monocytes in the BM. (A) (B) Lineage includes CD3e, B220, NKp46, CD90.2 and Ter119. Data are representative of two independent experiments with biological triplicates. All data are presented as mean $\pm$ SD. Groups were compared using Student's *t* test. ***, $P < 0.001$.

Cardiac fibroblasts facilitate Ly6C^{hi} and Ly6C^{lo} monocyte-to-macrophage differentiation

The results from the parabiosis experiments suggested that MDMs in an inflamed cardiac environment are a highly heterogenous population. Whether macrophage heterogeneity is instigated by monocyte intrinsic differences and/or extrinsic environmental factors is not yet known. We and others have recently reported that cardiac fibroblasts play a key sentinel role in the myocardium. Cardiac fibroblasts produce myelotropic chemokines and cytokines such as GM-CSF and CCL2 in response to cardiac injury in myocarditis [247, 442]. This immune modulatory property of cardiac fibroblasts was also confirmed in MI and Kawasaki disease [443, 444]. To examine whether Ly6C^{hi} and Ly6C^{lo} monocytes have the capacity to differentiate into macrophages and whether cardiac fibroblasts facilitate this differentiation process, we established an *in vitro* co-culture system. We harvested primary cardiac fibroblasts from naïve WT mice and co-cultured them with FACS-sorted IL-17Ra$^{-/-}$ EAM splenic Ly6C^{hi} or Ly6C^{lo} monocytes for up to 160 hours (Figure 8A; see gating strategy in Figure 9A). Due to the relative paucity of monocytes in blood, we used spleen as a surrogate source of monocytes. Using flow cytometry, we found that approximately 80% of the Ly6C^{hi} monocytes quickly differentiated to become macrophages, while almost all Ly6C^{lo} monocytes remained undifferentiated over the first 40 hours of culture (Figure 8B, C). However, when we assessed their phenotypic changes at 160 hours, approximately 30% of the Ly6C^{lo} monocytes had become macrophages (Figure 8D, E). Neither Ly6C^{hi} nor Ly6C^{lo} monocytes were able to survival long-term nor differentiate into macrophages in the absence of cardiac fibroblasts (Figure 8D, E). Ly6C^{hi} and Ly6C^{lo} MDMs were morphologically similar and resembled macrophages after 160 hours of co-culture with cardiac fibroblasts (Figure 8F). To better understand how

monocytes and cardiac fibroblasts interact *in vitro*, we used live-cell time-lapsed imaging to track CFSE-labeled ($CFSE^+$) $Ly6C^{hi}$ and $Ly6C^{lo}$ monocytes co-cultured with $CFSE^-$ cardiac fibroblasts. We found that $CFSE^+Ly6C^{hi}$ monocytes started to cluster around cardiac fibroblasts as early as 9 hours into co-culture. They adhered strongly to the cardiac fibroblasts and became static when adhesions formed (Figure 8G). In contrast, $CFSE^+Ly6C^{lo}$ monocytes were motile and they formed transient clusters around cardiac fibroblasts. $Ly6C^{lo}$ monocytes also lose CFSE at a higher rate, indicating faster proliferation when compared to $Ly6C^{hi}$ monocytes (Figure 8H). Flow cytometric analysis confirmed that $Ly6C^{lo}$ monocytes indeed proliferate faster than $Ly6C^{hi}$ monocytes (Figure 9B, C). Next, we used transmission electron microscopy (EM) to examine whether MDMs and cardiac fibroblasts establish cell-to-cell connections, which would suggest the presence of molecular adhesion structures. We observed that the cytoplasm of both $Ly6C^{hi}$ and $Ly6C^{lo}$ MDMs contained a large number of electron-lucent vesicles (Figure 8I, J). Each subset of MDMs formed close cell-to-cell contact with cardiac fibroblasts (Figure 8K, L). Interestingly, these close cell-to-cell interactions are important for driving monocyte to macrophage differentiation. We demonstrated a significant reduction in monocyte-to-macrophage differentiation when monocyte-fibroblast contacts are inhibited by a transwell barrier (Figure 9D, E). We also showed that $Ly6C^{hi}$ monocytes induced cardiac fibroblasts to significantly upregulate *Ccl2* mRNA levels compared to $Ly6C^{lo}$ monocytes, ensuring a feed-forward loop for a continuous supply of pro-inflammatory monocytes to accumulate in an inflamed microenvironment (Figure 9F). Taken together, $Ly6C^{hi}$ and $Ly6C^{lo}$ monocytes establish close physical contact with cardiac fibroblasts and

these cell-to-cell interactions play a role in facilitating Ly6C^{hi} and Ly6C^{lo} monocytes survival and differentiation into macrophages.

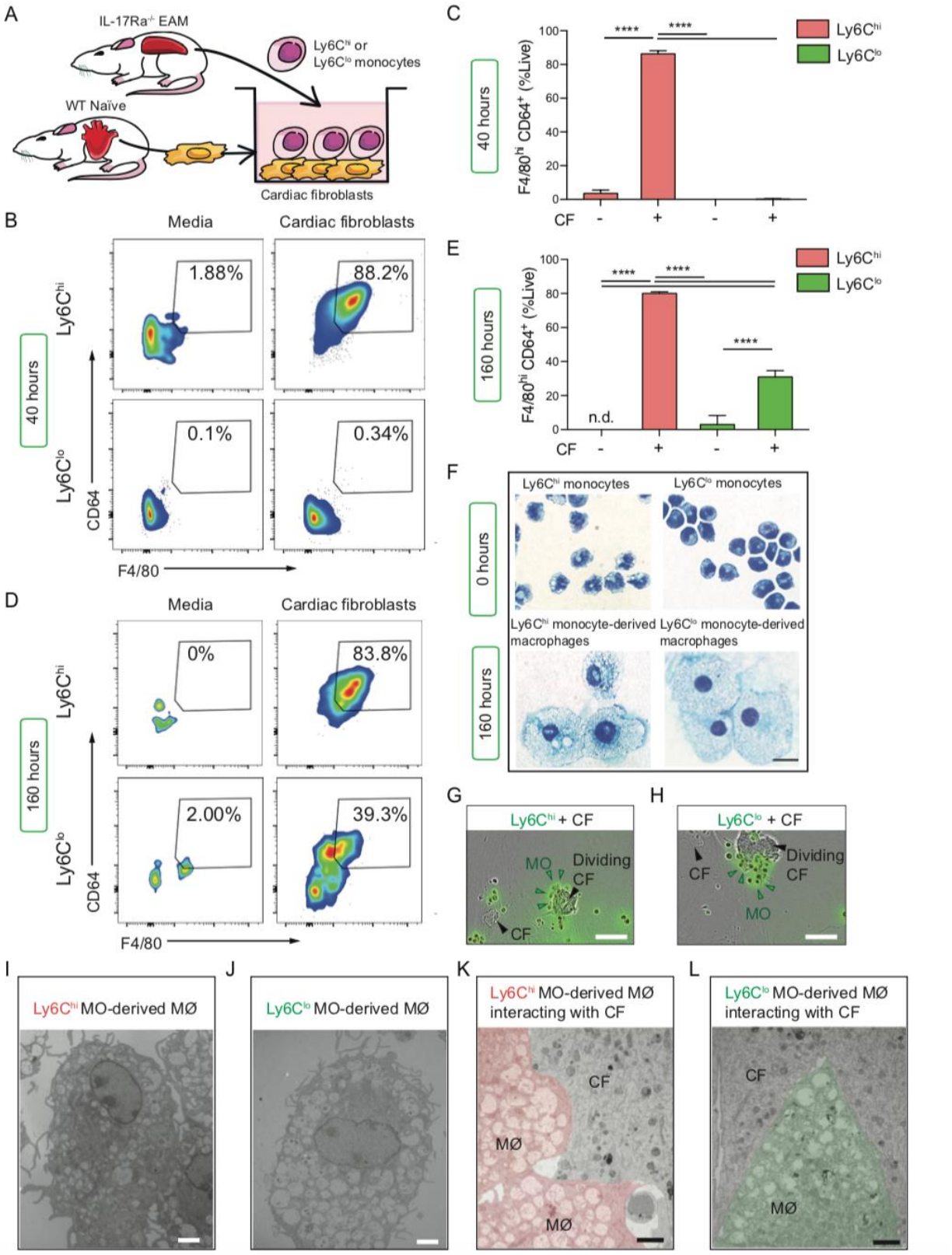
A
IL-17Ra-/- EAM
Ly6Chi or
Ly6Clo monocytes
WT Naïve
Cardiac fibroblasts
B
Media
Cardiac fibroblasts
40 hours
Ly6Chi
Ly6Clo
1.88%
88.2%
0.1%
0.34%
CD64
F4/80
C
40 hours
F4/80hi CD64+ (%Live)
Ly6Chi
Ly6Clo
****
****
CF
D
Media
Cardiac fibroblasts
160 hours
0%
83.8%
2.00%
39.3%
E
160 hours
n.d.
****
F
0 hours
160 hours
Ly6Chi monocytes
Ly6Clo monocytes
Ly6Chi monocyte-derived macrophages
Ly6Clo monocyte-derived macrophages
G
Ly6Chi + CF
MO
Dividing CF
CF
H
Ly6Clo + CF
CF
Dividing CF
MO
I
Ly6Chi MO-derived MØ
J
Ly6Clo MO-derived MØ
K
Ly6Chi MO-derived MØ interacting with CF
CF
MØ
MØ
L
Ly6Clo MO-derived MØ interacting with CF
CF
MØ

Figure 8. Direct contact with cardiac fibroblasts facilitate Ly6C^{hi} and Ly6C^{lo} monocyte-to-macrophage differentiation

(A) Schematics of the monocytes and cardiac fibroblasts co-culture system. Cardiac fibroblasts were harvested from WT naïve mice, whereas monocytes were sorted from EAM IL-17Ra$^{-/-}$ mice. (B) Flow cytometric analysis showing differentiation of viable Ly6C^{hi} and Ly6C^{lo} monocytes to become F4/80^{hi}CD64^{+} cells at 40 hours via flow cytometry. (C) Quantification of the frequency of macrophage differentiation at 40 hours. (D) Differentiation of viable Ly6C^{hi} and Ly6C^{lo} monocyte derived cells were assayed at 160 hours via flow cytometry. (E) Quantification of the frequency of macrophage differentiation at 160 hours. (F) Giemsa staining of monocytes morphologies before culture and after 160 hours co-culture with cardiac fibroblasts. Bars: (black) 8 μm (G) IncuCyte Imaging showing CFSE^{+}Ly6C^{hi} and (H) CFSE^{+}Ly6C^{lo} monocytes are in close contact when interacting with cardiac fibroblasts. Bars: (white) 50 μm. Representative images of EM images showing (I) Ly6C^{hi} and (J) Ly6C^{lo} MDMs, and (K) Ly6C^{hi} and (L) Ly6C^{lo} MDMs are in close contacts with cardiac fibroblasts. Images taken at 160 hours of co-culture. Bars: (white) 2 μm; (black) 2 μm. (A – F) Data are representative of five independent experiments with technical triplicates. (C, E) Data are presented as mean ± SD; n = 3. Groups were compared using one-way ANOVA followed by Tukey test. ****, P < 0.0001. See also Figure 9.

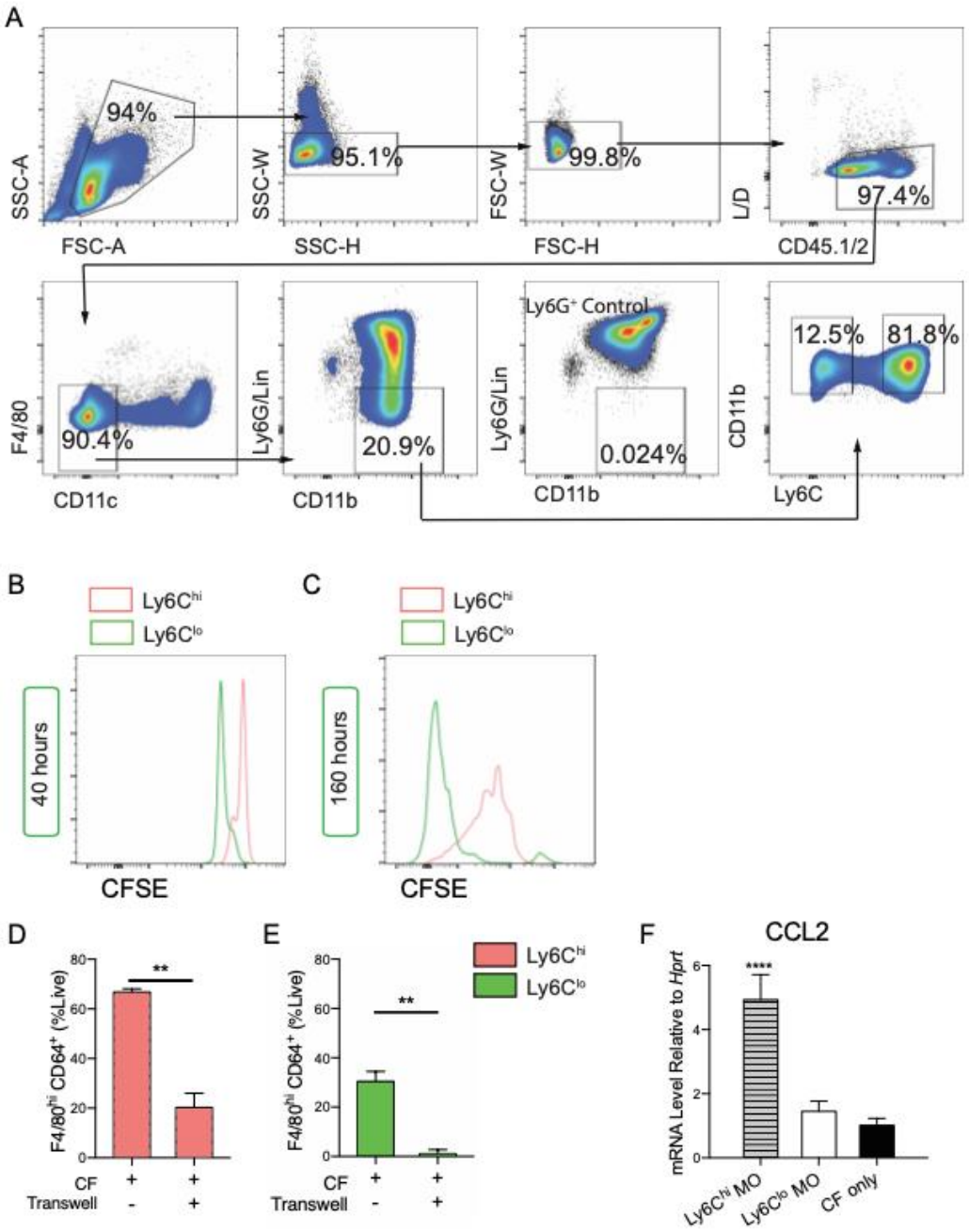

Figure 9. *In vitro* co-culture of splenic Ly6C^{hi} or Ly6C^{lo} monocytes with cardiac fibroblasts

(A) Representative gating strategies of FACS sorted Ly6C^{hi} and Ly6C^{lo} monocytes from WT (or IL-17Ra$^{-/-}$) EAM spleens. These monocytes were used for all adoptive transfers and *in vitro* co-culture experiments. Cells were gated stringently to obtain pure

populations. Lineage marks include CD3e, CD19, NKp46, CD49b. (B) Histograms of MFI showing CFSE staining of viable Ly6C^{hi} and Ly6C^{lo} monocytes at 40 hours and (C) at 160 hours. (D) A transwell co-culture was established with cardiac fibroblasts in the lower chamber and either Ly6C^{hi} or Ly6C^{lo} monocytes on the upper chamber. Cells were separated with a 0.4-micron pore size membrane. We examined Ly6C^{hi} and (E) Ly6C^{lo} monocyte-to-macrophage differentiation at 40 hours and 160 hours respectively. (F) Separately, cardiac fibroblasts were harvested in 40 hours and *Ccl2* mRNA levels were assessed. (D – F) Data are presented as mean $\pm$ SD. Data are representative of two independent experiments with technical triplicates. (C, D) Groups were compared using Student's *t* test. **, $P < 0.01$. (E) Groups were compared using one-way ANOVA followed by Tukey test. ****, $P < 0.0001$.

Inflammatory monocytes are the main precursors for monocyte-derived macrophages during myocarditis in both mice and humans

Given that cardiac fibroblasts facilitate the differentiation of both Ly6C^{hi} and Ly6C^{lo} monocytes into macrophages, we next sought to investigate whether both Ly6C^{hi} and Ly6C^{lo} monocytes could differentiate *in vivo* during EAM development. We FACS-sorted splenic CD45.2^{+} Ly6C^{hi} or Ly6C^{lo} monocytes from WT mice on day 14 of EAM, and intracardially injected them into CD45.1 WT recipients at the peak of EAM (Figure 10A). Both Ly6C^{hi} and Ly6C^{lo} monocytes and monocyte-derived cells of donor origin persisted in the myocardium 40 hours after the injection (Figure 10B, C). Approximately 50% of the injected Ly6C^{hi} monocytes had differentiated into F4/80^{hi}CD64^{+} macrophages (Figure 10D, C), whereas less than 1% of the Ly6C^{lo} monocytes differentiated into macrophages (Figure 10D, F). We employed Barnes-Hut Stochastic Neighbor Embedding (bh-SNE) analysis to visualize monocyte to macrophage differentiation [445, 446]. We confirmed that CD45.2^{+} Ly6C^{lo} monocytes were mostly unable to differentiate into F4/80^{hi}CD64^{+} macrophages, while CD45.2^{+} Ly6C^{hi} monocytes contributed significantly to the cardiac macrophage pool during EAM (Figure 10G, H). We also examined Ly6C^{hi} and Ly6C^{lo} monocytes differentiation at 160 hours *in vivo*, and found that very few injected monocytes were present in the myocardium, indicating a high local turn-over rate. Notably, we did not find evidence suggesting Ly6C^{lo} monocyte-to-macrophage differentiation (*data not shown*). Upon immunofluorescence examination of endomyocardial biopsy samples from a patient with giant cell myocarditis, we found the expression of CD68, a pan macrophage marker, coincided with CD14 but not CD16. This suggest that the inflammatory CD14^{+}CD16$^{-/+}$ but not the patrolling CD14^{-}CD16^{+} monocyte populations are the likely

source of macrophages in giant cell myocarditis (Figure 11A, B). In parallel, we examined endomyocardial biopsies from three patients who had left ventricular assist devices implanted as a result of heart failure with various etiologies (Table 5). Flow cytometric analysis from all three patients indicated that $CD14^{+}CD68^{+}$, but not $CD16^{+}CD68^{+}$ macrophages are present in the heart (Figure 11C). Further supporting the hypothesis that $CD14^{+}CD16^{-}$ monocytes are the main source of cardiac macrophages in human myocarditis. In conclusion, human $CD14^{+}$ and mouse $Ly6C^{hi}$ monocyte subsets are the major contributors to the cardiac macrophage population during myocarditis development.

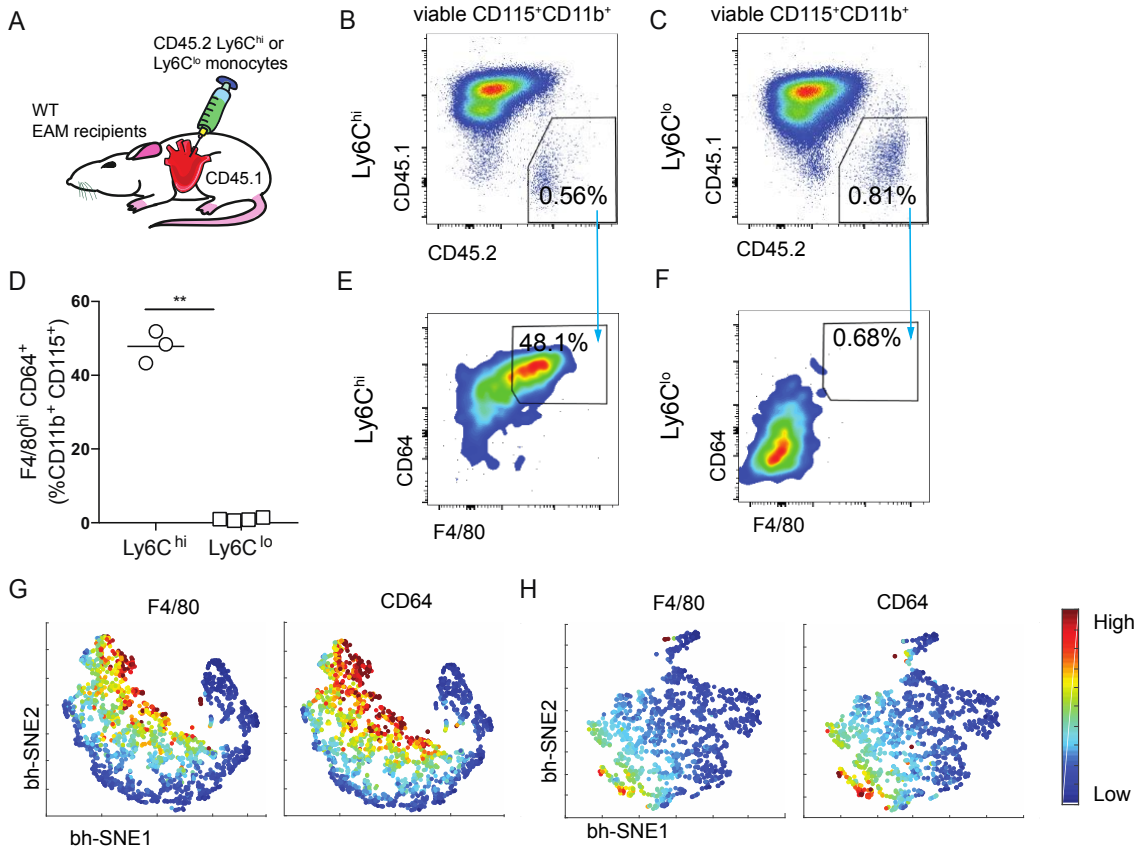

Figure 10. Inflammatory monocytes are the main precursors for monocyte-derived macrophages during myocarditis in both mice and humans

(A) Schematics of intracardiac injection of Ly6C^{hi} or Ly6C^{lo} CD45.2^{+} splenic monocytes into the heart of a CD45.1 day 21 EAM WT recipient mice. (B) Gating of concatenated Ly6C^{hi} and (C) Ly6C^{lo} donor cells from total viable CD115^{+}CD11b^{+} population. (D) Quantification of the percentages of injected Ly6C^{hi} or Ly6C^{lo} monocytes differentiated into macrophages. (E) Flow cytometric analysis of the frequencies of Ly6C^{hi} MDMs and (F) Ly6C^{lo} MDMs out of viable CD45.2^{+}CD115^{+}CD11b^{+} population. F4/80 and CD64 expression intensities of (G) Ly6C^{hi} MDMs and (H) Ly6C^{lo} MDMs using *bh-SNE* dimensional reduction algorithm. (D) Data are presented as mean $\pm$ SD; n = 3 – 4. Groups were compared using Student's *t* test. **, P <0.01. Data are representative of three independent experiments. See also Figure 11, Table 5.

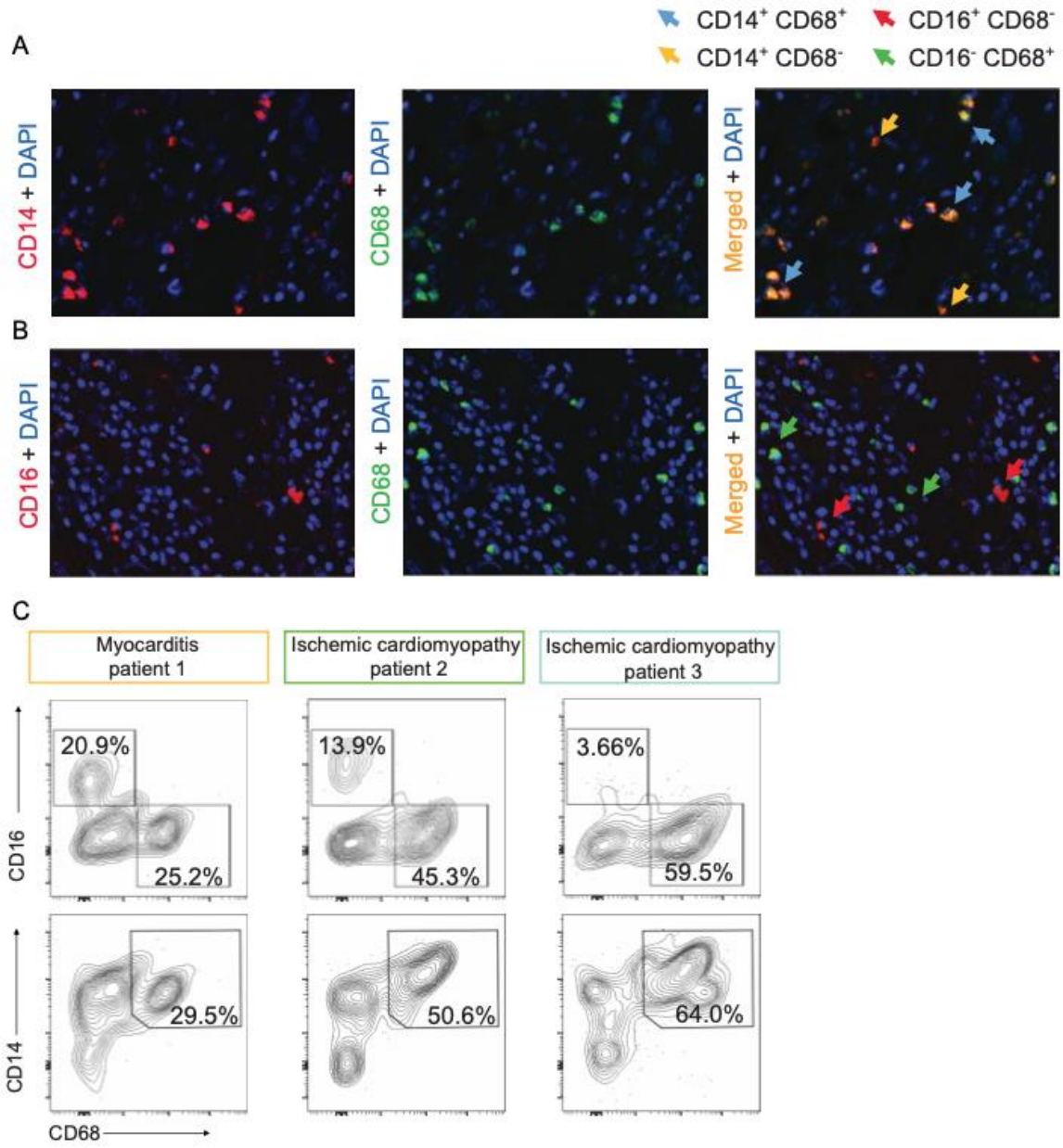

Figure 11. Examination of human macrophage ontogeny

(A) Immunofluorescent (IF) staining of CD14 (red) and CD68 (green) in a human giant cell myocarditis biopsy sample showing numerous $CD14^{+}CD68^{+}$ double positive cells (blue arrows) and some $CD14^{+}CD68^{-}$ single positive cells (yellow arrows). (B) Immunofluorescent (IF) staining of CD16 (red) and CD68 (green) in a human giant cell myocarditis biopsy sample showing numerous $CD16^{-}CD68^{+}$ single positive cells (green

arrows) and few $CD16^{+}CD68^{-}$ single positive cells (red arrows). (C) Gating of $CD16^{+}$ or $CD14^{+}$ and $CD68^{+}$ from viable $CD45^{+}CD11b^{+}$ myeloid cells in the hearts of three patients with ventricular assist device explant.

Sample	Myocarditis patient 1	Ischemic cardiomyopathy patient 2	Ischemic cardiomyopathy patient 3
Age	32	61	57
Race/Ethnicity	Caucasian	Caucasian	Caucasian
Gender	Male	Male	Male
Etiology	Viral myocarditis	Ischemic	Ischemic
Type of VAD	HM II 10600	3000 rpm	8000 rpm
Diabetes	No	No	Yes
Height	175 cm	170 cm	180 cm
Weight	86.63 Kg	86.63 Kg	100.69 Kg
LVIDd	3.9 cm	6.6 cm	6.5 cm
LVPWd	1.3 cm	0.9 cm	1.0 cm
IVSd	1.6 cm	1.1 cm	1.0 cm
EF			
Troponin level		<0.15	
Days on VAD	1167	270	432
Explant reason	OHT	OHT	OHT
Dead	No	No	No
BNP		185	376
CKMB		1.7	0.5
Tissue Amount (mg)	307.5 (LV)	294.1 (LV)	339.6 (LV)
Path explant		cardiomegaly, concentric LVH, posterior wall fibrosis, fatty infiltration of IVS, mild fibrous epicarditis CAD	cardiomegaly with concentric biventricular hypertrophy, CAD, fibrosis

Table 5. Patient information part I.

Patient information from individuals presenting with end stage heart failure who underwent implantation of a Left Ventricular Assist Device at the Texas Heart Institute. Tissues were collected for flow cytometry assessments. Gray Fill: Data Not available; OHT: Orthotopic Heart Transplant.

IL-17A signaling through cardiac fibroblasts inhibits Ly6C^{lo} monocyte-to-macrophage differentiation and Ly6C^{lo} proliferation

Given the differentiation capacity of Ly6C^{lo} monocytes shown above *in vitro*, we next sought to understand what factors limit their differentiation *in vivo*. EAM is a Th17 driven disease and IL-17A induces production of myelotropic cytokines and chemokines by cardiac stroma cells [247]. We speculated that IL-17A might play a role in determining monocyte fate during EAM. Since monocytes require cardiac fibroblasts to differentiate into macrophages, we co-cultured FACS-sorted IL-17Ra$^{-/-}$ EAM Ly6C^{hi} and Ly6C^{lo} splenic monocytes with either cardiac fibroblasts alone or IL-17A stimulated cardiac fibroblasts for 160 hours. We found that IL-17A stimulated cardiac fibroblasts significantly inhibited Ly6C^{lo} monocyte-to-macrophage differentiation, while its effect on Ly6C^{hi} monocyte differentiation was minimal (Figure 12A). Using CFSE labeling, we found that proliferation of Ly6C^{lo} monocytes was almost completely inhibited by cardiac fibroblasts stimulated with IL-17A, whereas proliferation of Ly6C^{hi} monocytes was minimally affected (Figure 12B). We described previously that cardiac fibroblasts are potent producers of granulocyte-macrophage colony-stimulating factor (GM-CSF) upon IL-17A stimulation [247]. We found that while treatment with recombinant GM-CSF only marginally suppressed Ly6C^{hi} monocyte-to-macrophage differentiation (Figure 12C), it completely recapitulated the inhibitory effect of IL-17A through cardiac fibroblasts on Ly6C^{lo} monocyte-to-macrophage differentiation (Figure 12D). IL-17A-induced inhibition of Ly6C^{lo} monocyte-to-macrophage differentiation could be reversed with anti-GM-CSF treatment (Figure 12D). Similarly, GM-CSF did not change proliferation of Ly6C^{hi} monocytes and MDMs, while completely inhibiting proliferation of undifferentiated Ly6C^{lo} monocytes (Figure 12E, F). Treatment of anti-GM-CSF to IL-17A-stimulated cardiac fibroblasts

restored proliferation of Ly6C^{lo} monocytes (Figure 12F). We further validated all of our major *in vitro* findings using splenic monocytes from WT animals and showed that monocytes responded to environmental cues similarly regardless of their sources (**Error! Reference source not found.**). To summarize, GM-CSF acts as a downstream mediator of IL-17A signaling through cardiac fibroblasts that exhibits minor inhibitory effects on Ly6C^{hi} monocyte differentiation and proliferation, but substantially inhibits Ly6C^{lo} monocyte differentiation and proliferation *in vitro*.

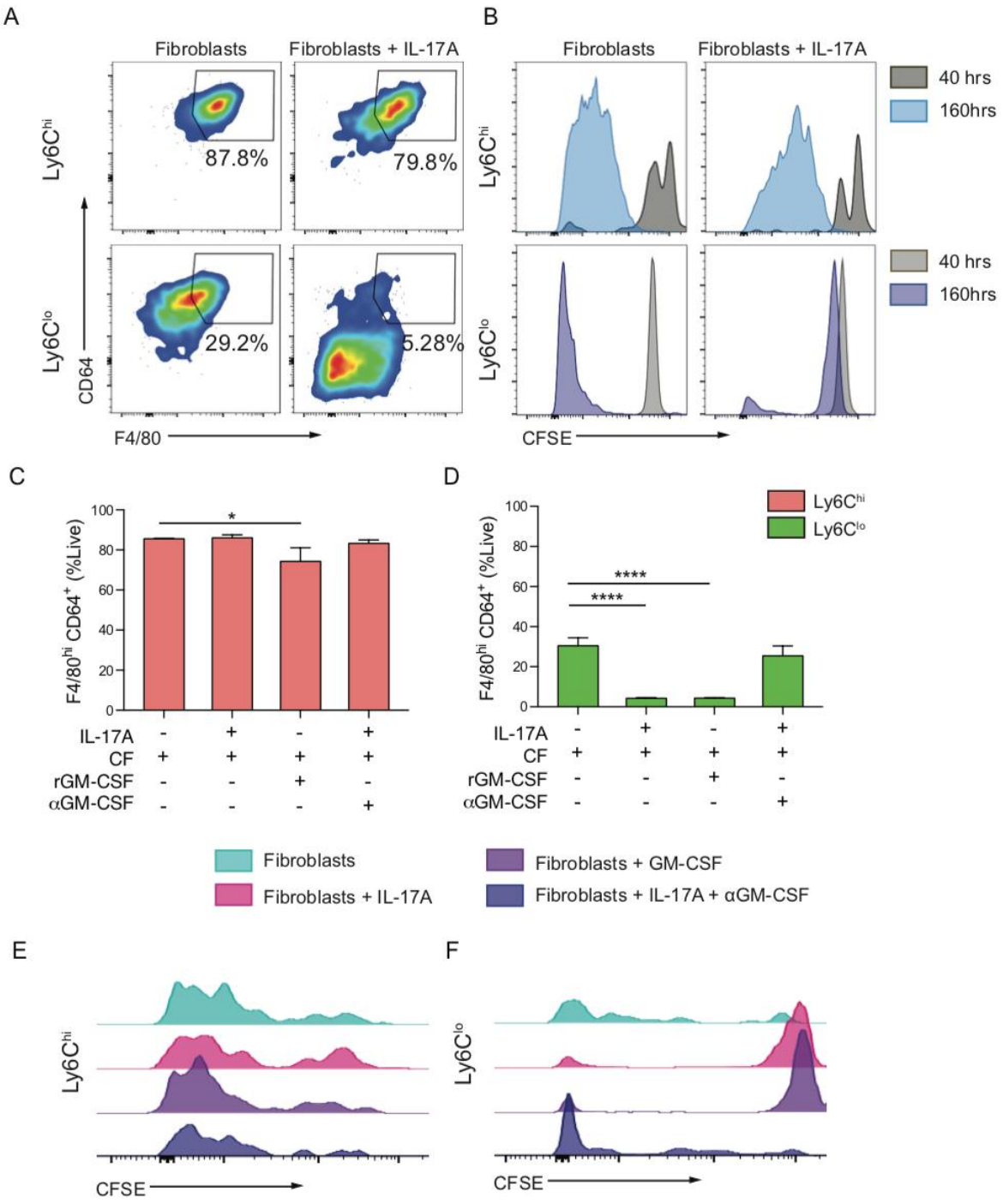

Figure 12. IL-17A signaling through cardiac fibroblasts inhibits Ly6C^{lo} monocyte-to-macrophage differentiation and Ly6C^{lo} monocyte proliferation

All co-cultured cells were assessed using flow cytometry at 160 hours. (A) Gating of concatenated $Ly6C^{hi}$ and $Ly6C^{lo}$ monocyte-derived macrophages out of viable $CD45^{+}CD11b^{+}$. (B) Histograms of mean fluorescent intensity (MFI) showing CFSE staining of the viable $Ly6C^{hi}$ cells and $Ly6C^{lo}$ cells after co-culturing with either cardiac fibroblasts or IL-17A treated cardiac fibroblasts. (C) Percentages of macrophages derived from $Ly6C^{hi}$ monocytes (D) and $Ly6C^{lo}$ monocytes with cardiac fibroblasts only, IL-17A stimulated cardiac fibroblasts, recombinant GM-CSF supplemented cardiac fibroblasts and IL-17A stimulated cardiac fibroblasts treated with anti-GM-CSF, respectively. (E) Histograms of MFI showing CFSE staining of the viable $Ly6C^{hi}$ monocyte-derived macrophages and (F) $Ly6C^{lo}$ monocytes with cardiac fibroblasts only, IL-17A stimulated cardiac fibroblasts, recombinant GM-CSF supplemented cardiac fibroblasts and IL-17A stimulated cardiac fibroblasts treated with anti-GM-CSF, respectively. (C, D) Data are presented as mean $\pm$ SD. Data are representative of three independent experiments with technical triplicates. (C – D) Groups were compared using one-way ANOVA followed by Dunnett test. *, $P < 0.05$ ****, $P < 0.0001$. See also Figure 13.

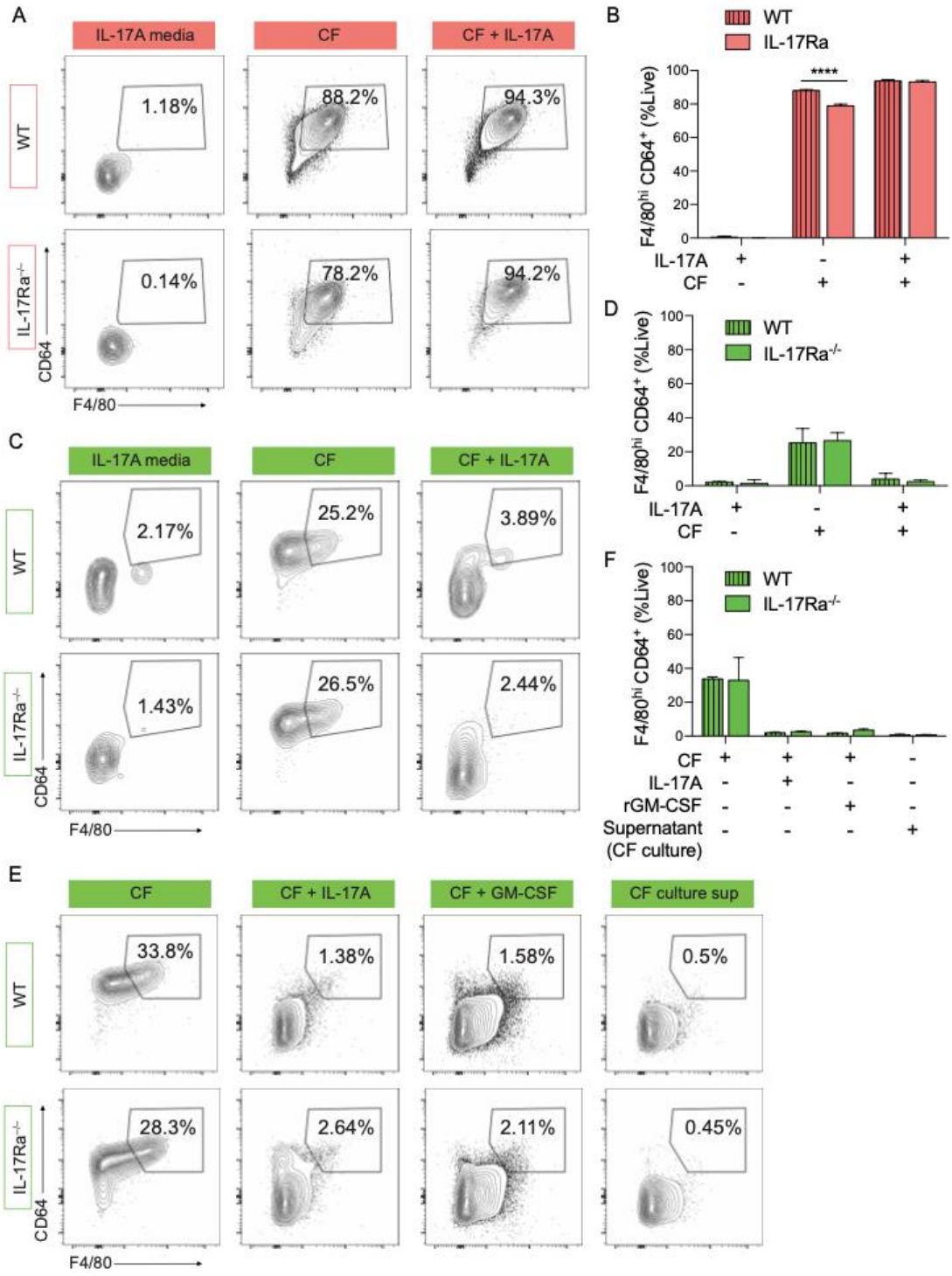
A
IL-17A media
CF
CF + IL-17A
WT
IL-17Ra-/-
1.18%
88.2%
94.3%
0.14%
78.2%
94.2%
CD64
F4/80
B
WT
IL-17Ra
F4/80hi CD64+ (%Live)
****
IL-17A
CF
C
2.17%
25.2%
3.89%
1.43%
26.5%
2.44%
D
WT
IL-17Ra-/-
F
CF
IL-17A
rGM-CSF
Supernatant (CF culture)
E
CF + GM-CSF
CF culture sup
33.8%
1.38%
1.58%
0.5%
28.3%
2.64%
2.11%
0.45%

Figure 13. Validation of WT monocyte differentiation *in vitro*

Cardiac fibroblasts were harvested from WT naïve mice, whereas monocytes were sorted from either EAM WT or EAM IL-17Ra$^{-/-}$ mice. (A) Flow cytometry plots showing differentiation status of splenic Ly6C^{hi} monocyte from either WT or IL-17Ra$^{-/-}$ mice. (B) Quantification of the percentages of macrophages derived from Ly6C^{hi} monocytes in culture. (C) Flow cytometry plots showing differentiation status of splenic Ly6C^{lo} monocyte from either WT or IL-17Ra$^{-/-}$ mice. (D) Quantification of the percentages of macrophages derived from Ly6C^{lo} monocytes in culture. (E) Flow cytometry plots showing the inhibitory effects of IL-17A and GM-CSF on Ly6C^{lo} monocyte-to-macrophage differentiation, regardless of monocyte source. Cardiac fibroblasts supernatant alone cannot promote WT and IL-17Ra$^{-/-}$Ly6C^{lo} monocyte-to-macrophage differentiation. (F) Quantification of the percentages of macrophages derived from Ly6C^{lo} monocytes in culture.

The absence of IL-17A signaling enables Ly6C^{lo} monocyte-to-macrophage differentiation *in vivo*

We next aimed to test *in vivo* whether eliminating IL-17A signaling during EAM would enable Ly6C^{lo} monocytes to undergo differentiation. To begin, we intracardially injected either FACS-sorted CD45.2^{+}Ly6C^{hi} or Ly6C^{lo} monocytes into CD45.1 IL17Ra$^{-/-}$ recipients during the peak of EAM (Figure 14A). Both monocyte subsets were present in the myocardium after 40 hours post injection (Figure 14B, C). Strikingly, while most of the Ly6C^{hi} monocytes differentiated into F4/80^{hi}CD64^{+} macrophages, approximately 30% of the Ly6C^{lo} monocytes also differentiated into macrophages (Figure 14D – F). The bh-SNE algorithm further confirmed that while Ly6C^{hi} monocytes contributed in substantial numbers to the cardiac macrophage pool, a non-negligible proportion of Ly6C^{lo} monocytes had also differentiated into F4/80^{hi}CD64^{+} macrophages (Figure 14G, H). In addition, we examined whether the Ly6C^{lo} monocytes are able to traffic through blood and differentiate in the myocardium. We retro-orbitally injected FACS sorted CD45.1^{+}Ly6C^{lo} monocytes into either CD45.2 WT or IL17Ra$^{-/-}$ recipients during the peak of EAM (Figure 14I). CD45.1^{+}Ly6C^{lo} monocytes could be found in the myocardium after 40 hours post injection (Figure 14J, K). Consistent to our finding, approximately 30% of the Ly6C^{lo} monocytes had differentiated into F4/80^{hi}CD64^{+} macrophages in IL17Ra$^{-/-}$ recipients but not in WT (Figure 14L – N). Therefore, our results indicate that the absence of IL-17A signaling enables Ly6C^{lo} monocyte-to-macrophage differentiation. Again, underlining the inhibitory role of IL-17A on Ly6C^{lo} monocyte-to-macrophage differentiation.

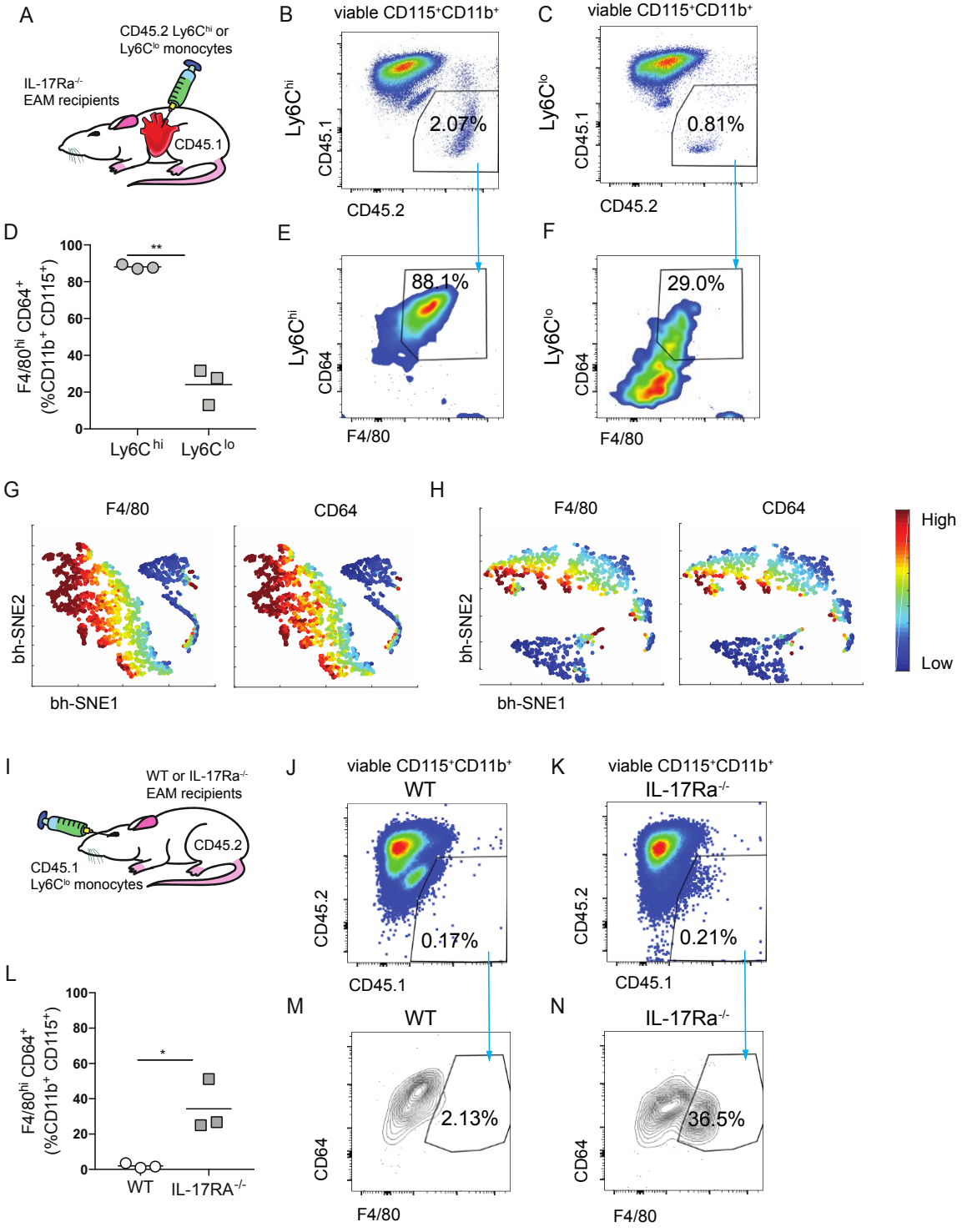
A
CD45.2 Ly6C^hi or
Ly6C^lo monocytes
IL-17Ra^-/-
EAM recipients
CD45.1
B
viable CD115+CD11b+
Ly6C^hi
CD45.1
2.07%
CD45.2
C
viable CD115+CD11b+
Ly6C^lo
CD45.1
0.81%
CD45.2
D
F4/80^hi CD64+
(%CD11b+ CD115+)
**
Ly6C^hi
Ly6C^lo
E
Ly6C^hi
CD64
88.1%
F4/80
F
Ly6C^lo
CD64
29.0%
F4/80
G
F4/80
CD64
bh-SNE2
bh-SNE1
H
F4/80
CD64
bh-SNE2
bh-SNE1
High
Low
I
WT or IL-17Ra^-/-
EAM recipients
CD45.2
CD45.1
Ly6C^lo monocytes
J
viable CD115+CD11b+
WT
CD45.2
0.17%
CD45.1
K
viable CD115+CD11b+
IL-17Ra^-/-
CD45.2
0.21%
CD45.1
L
F4/80^hi CD64+
(%CD11b+ CD115+)
*
WT
IL-17RA^-/-
M
WT
CD64
2.13%
F4/80
N
IL-17Ra^-/-
CD64
36.5%
F4/80

Figure 14. Ly6C^{lo} monocyte-to-macrophage differentiation can be initiated in vivo in the absence of IL-17A signaling through cardiac fibroblasts

(A) Schematics of intracardiac injection of Ly6C^{hi} or Ly6C^{lo} CD45.2 monocytes into CD45.1 day 21 EAM IL-17Ra$^{-/-}$ recipient mice. (B) Gating of concatenated Ly6C^{hi} and (C) Ly6C^{lo} donor cells from total viable CD115^{+}CD11b^{+} population. (D) Percentages of injected Ly6C^{hi} or Ly6C^{lo} monocytes differentiated into macrophages. (E) Frequencies of Ly6C^{hi} monocyte-derived macrophages and (F) Ly6C^{lo} monocyte-derived macrophages out of viable CD45.2^{+}CD115^{+}CD11b^{+} population. F4/80 and CD64 expression intensities of (G) Ly6C^{hi} monocyte-derived and (H) Ly6C^{lo} monocyte-derived macrophages using bh-SNE dimensional reduction algorithm. (D) Groups were compared using Student's *t* test. **, P < 0.01. Data are representative of two independent experiments with biological triplicates.

Distinct gene expression profiles in Ly6C^{hi} and Ly6C^{lo} monocyte-derived macrophage subsets *in vitro*

To explore the molecular differences between these MDM subpopulations, we next characterized the changes in gene expression that occurred during Ly6C^{lo} and Ly6C^{hi} monocyte-to-macrophage differentiation after being co-cultured with cardiac fibroblasts (condition 1 and 2). In addition, we also examined the effect of IL-17A stimulated cardiac fibroblasts on Ly6C^{hi} MDMs (condition 3). Since there were very few Ly6C^{lo} MDMs in the co-culture with IL-17A stimulated cardiac fibroblasts, this condition was not included for this analysis. We performed microarray-based transcriptomic profiling of RNA isolated from FACS sorted macrophages derived from the three conditions in triplicate (see gating strategy in Figure 15A). Gene expression profiles of the three MDM subsets were evaluated by principal component analysis (PCA) and hierarchical clustering analysis (Figure 16A, B). Both analyses demonstrated distinct gene expression profiles for the three MDM subsets, suggesting that both the microenvironment and monocyte intrinsic properties are determining factors. Differential gene expression analysis showed that consistent with both PCA and hierarchical clustering analysis, Ly6C^{lo} MDMs versus Ly6C^{hi} MDMs from IL-17A treated cardiac fibroblast culture had the greatest number of differentially expressed genes (n = 1057). Whereas Ly6C^{lo} MDMs versus Ly6C^{hi} MDMs from non-treated cardiac fibroblasts culture had the lowest number of differentially expressed genes (n = 644) (Figure 15B). We found that IL-17A signaling through cardiac fibroblasts significantly up-regulated genes encoding inflammatory chemokines, cytokines, growth factors, *Il6*/*Stat3* and the NFκB pathway in Ly6C^{hi} MDMs (Figure 16C – E). Moreover, IL-17A *trans*-signaling through cardiac fibroblasts up-regulated genes in Ly6C^{hi} MDMs known to promote tissue fibrosis such as *Osm*, as well as genes related to

extracellular matrix degradation including *Mmp9* and *Timp1* (Figure 16F). In contrast, Ly6C^{lo} MDMs uniquely upregulated genes associated with class II antigen processing, including *Cd74*, *H2-Ab1* (Figure 16D). Flow cytometric analysis showed that *in vitro* Ly6C^{lo} MDMs indeed express MHCII, strongly suggesting their antigen presenting capabilities (Figure 16G). Ly6C^{lo} MDMs also express significantly more MHCII than Ly6C^{hi} MDMs when injected intracardially into EAM IL17Ra$^{-/-}$ recipients (Figure 15C). Furthermore, MHCII^{+}Ly6C^{lo} MDMs contribute to the increased proportion of MHCII^{+} macrophage in IL17Ra$^{-/-}$ mice during the resolution phase of EAM at day 28 (Figure 16H). We also validated that Ly6C^{lo} MDMs do not carry a dendritic cell signature (Figure 15D). IL-17A signaling through cardiac fibroblasts significantly up-regulated many genes encoding both M1 and M2 markers in the Ly6C^{hi} MDMs, highlighting that the classic M1/M2 paradigm cannot simply characterize macrophages activation complexity during disease states (Figure 15E) [447, 448]. We conclude that IL-17A *trans*-signaling through cardiac fibroblasts promotes pro-inflammatory and pro-tissue remodeling characteristics in Ly6C^{hi} MDMs. Interestingly, Ly6C^{lo} MDMs upregulate genes associated with antigen presentation and have elevated surface expression of MHCII both *in vitro* and *in vivo*. Our findings suggest that Ly6C^{hi} and Ly6C^{lo} MDMs represent distinct subsets that have unique roles and functions in the inflamed heart.

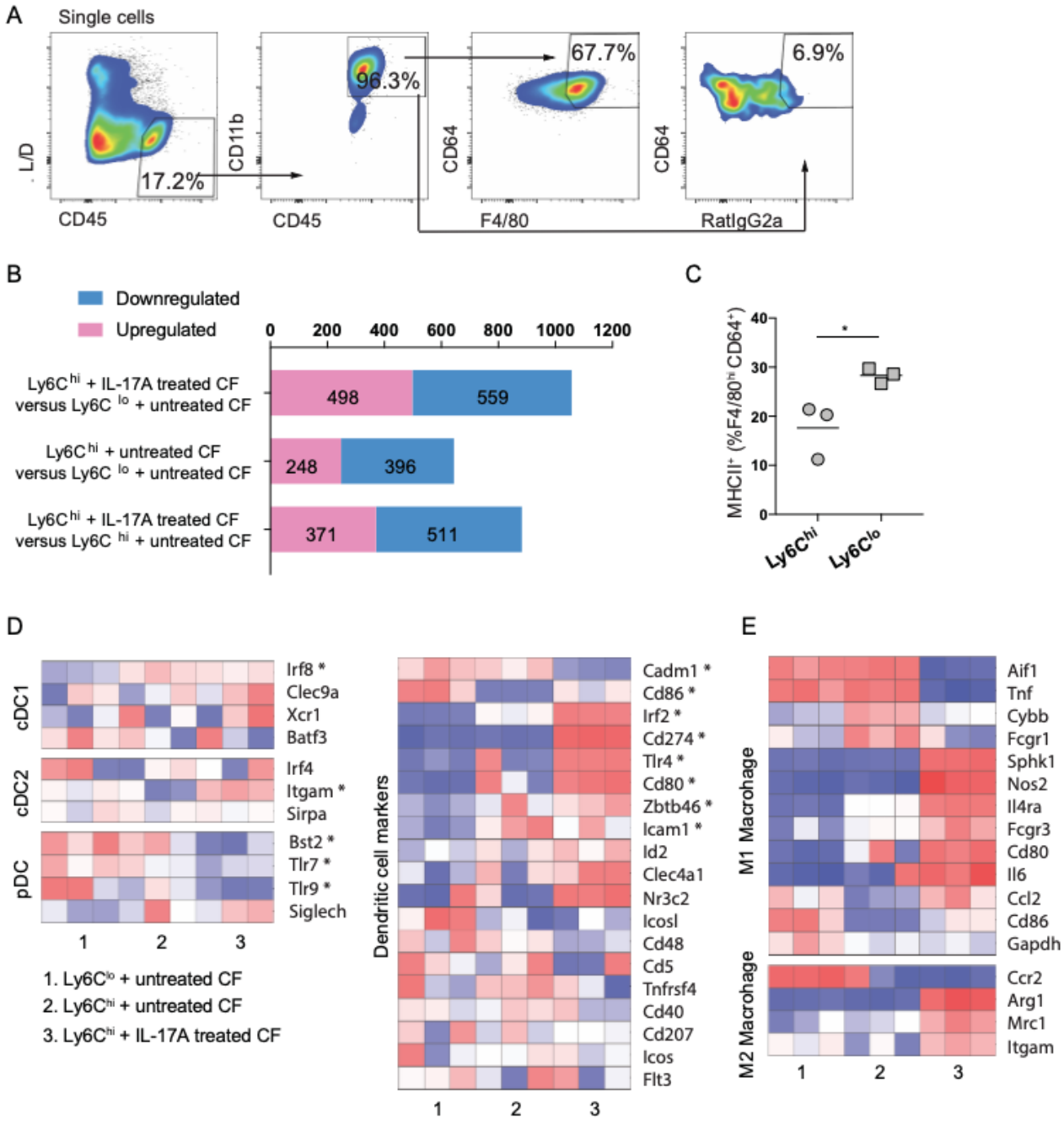

Figure 15. Validating the identities of in vitro derived macrophage subsets

(A) Representative gating strategy used to FACS sort $CD45^{+}CD11b^{+}CD64^{+}F4/80^{hi}$ macrophages from the heart for *in vitro* monocyte-fibroblast co-culture. F4/80 isotype control RatIgG2a was included. (B) Bar graph displaying the number of differentially regulated genes, using a threshold of 2 × fold change and p value<0.05. (C) Frequencies

of MHCII^{+} subset out of total intracardially injected MDMs in IL-17Ra$^{-/-}$ recipient mice were assessed by flow cytometry. (D) Heat maps showing relative fold changes in genes associated with dendritic cells and (E) M1/M2 dichotomy of macrophages. (C) Data are presented as mean $\pm$ SD, and representative of two independent experiments with biological triplicates. Groups were compared using Student's *t* test. *, $P < 0.05$. (D) * Represent selected genes displayed on the heat maps have a one-way ANOVA p value<0.05 among groups compared.

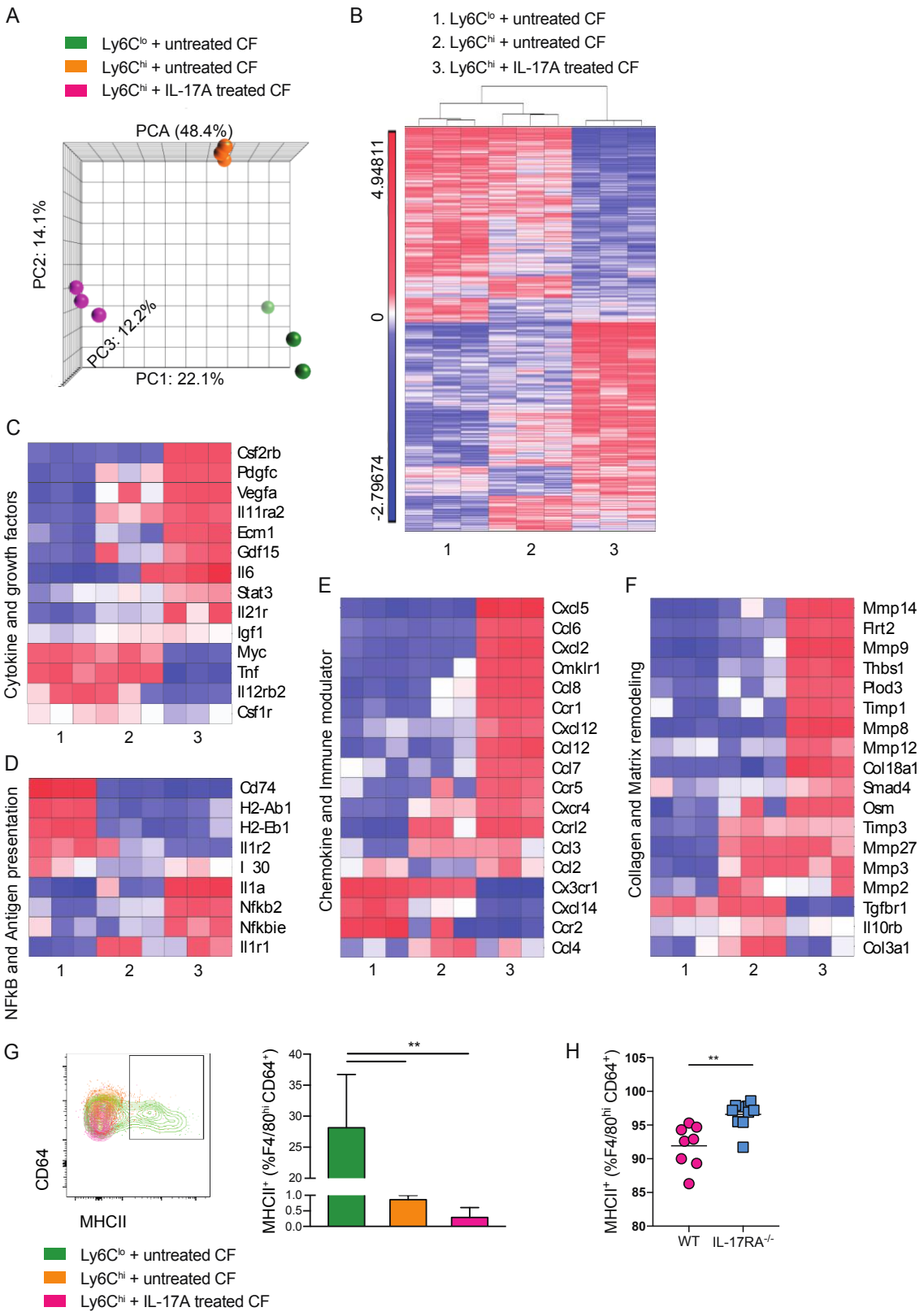
A
Ly6C^lo + untreated CF
Ly6C^hi + untreated CF
Ly6C^hi + IL-17A treated CF
PCA (48.4%)
PC2: 14.1%
PC3: 12.2%
PC1: 22.1%
B
1. Ly6C^lo + untreated CF
2. Ly6C^hi + untreated CF
3. Ly6C^hi + IL-17A treated CF
4.94811
0
-2.79674
1
2
3
C
Cytokine and growth factors
Csf2rb
Pdgfc
Vegfa
Il11ra2
Ecm1
Gdf15
Il6
Stat3
Il21r
Igf1
Myc
Tnf
Il12rb2
Csf1r
1
2
3
D
NFkB and Antigen presentation
Cd74
H2-Ab1
H2-Eb1
Il1r2
I 30
Il1a
Nfkb2
Nfkbie
Il1r1
1
2
3
E
Chemokine and Immune modulator
Cxcl5
Ccl6
Cxcl2
Cmklr1
Ccl8
Ccr1
Cxcl12
Ccl12
Ccl7
Ccr5
Cxcr4
Ccrl2
Ccl3
Ccl2
Cx3cr1
Cxcl14
Ccr2
Ccl4
1
2
3
F
Collagen and Matrix remodeling
Mmp14
Flrt2
Mmp9
Thbs1
Plod3
Timp1
Mmp8
Mmp12
Col18a1
Smad4
Osm
Timp3
Mmp27
Mmp3
Mmp2
Tgfbr1
Il10rb
Col3a1
1
2
3
G
CD64
MHCII
MHCII+ (%F4/80hi CD64+)
40
35
30
25
20
1.0
0.5
0.0
**
Ly6C^lo + untreated CF
Ly6C^hi + untreated CF
Ly6C^hi + IL-17A treated CF
H
MHCII+ (%F4/80hi CD64+)
105
100
95
90
85
80
**
WT
IL-17RA-/-

Figure 16. Distinct gene expression profiles in Ly6C^{hi} and Ly6C^{lo} monocyte-derived macrophage subsets differentiated in vitro in the presence of untreated or IL-17A-treated cardiac fibroblasts

(A) PCA analysis of microarray experiments. The principal components and their fraction of overall variability of the data (%) are shown on the x-axis, the y-axis and the z-axis. (B) Supervised hierarchical clustering highlighting differential gene expression profiles among three groups of *in vitro* MDMs, using a threshold of 2-fold change and p-value < 0.05. Sample number scheme is identical to the legend in all heat maps below. (C) Heat maps showing relative fold changes in genes associated with cytokines and growth factors, (D) NFκB pathway and antigen presentation, (E) chemokines and immune modulating activities and (F) collagen production and matrix remodeling. (G) Gating of MHCII^{+}CD64^{+} macrophages derived from monocyte-fibroblast co-culture. Frequencies of MHCII^{+} subset out of total *in vitro* co-culture derived macrophages were assessed by flow cytometry. (H) Hearts from day 28 EAM mice. Frequencies of MHCII^{+} out of F4/80^{hi}CD64^{+} macrophages were assessed by flow cytometry. (B – F) All genes displayed on the heat maps have one-way ANOVA p value < 0.05 among groups compared. (G) Data are presented as mean ± SD; n = 3. (H) Data are presented as mean ± SD; n = 8 – 9. (G) Data are representative of three independent experiments with technical triplicates. Groups were compared using one-way ANOVA followed by Dunnett test. **, P < 0.01. (H) Groups were compared using Student's *t* test. **, P < 0.01. See also Figure 15.

IL-17A *trans*-signaling through cardiac fibroblasts down-regulates MerTK expression on monocytes and monocyte-derived macrophages

The clearance of apoptotic cells during inflammation resolution is critical for proper wound repair and tissue remodeling. The myeloid-epithelial-reproductive receptor tyrosine kinase (MerTK) is a major apoptotic cell receptor on macrophages, known to play a role in the clearance of dying cells, a process called efferocytosis [449, 450]. Efferocytosis is also known to induce an anti-inflammatory phenotype in macrophages and diminish proinflammatory cytokine release [451-453]. EM results showed engulfed apoptotic cells or large cell debris inside Ly6C^{hi} MDMs (Figure 17A, B). Their phagocytic index was significantly elevated compared to the Ly6C^{lo} MDMs derived from the co-culture (Figure 17C). This indicates that Ly6C^{hi} MDMs are professional phagocytes. Consistent with our finding that IL-17A modulates the replenishment of the tissue macrophage pool with circulating monocytes, we observed an increase in the percentage of F4/80^{hi}CD64^{+} macrophages in IL-17Ra$^{-/-}$ EAM hearts compared to WT EAM hearts (Figure 17D; see gating strategy in Figure 18A). In general, macrophages express considerably higher levels of MerTK than monocytes in the hearts (Figure 18B). We found higher MerTK expression levels in both the macrophage and monocyte compartments from IL17Ra$^{-/-}$ hearts compared to WT (Figure 17E, F). This suggests that IL-17A plays a role in down-regulating MerTK expression on monocytes and macrophages. Furthermore, we found significantly less soluble Mer (sMer) present in IL17Ra$^{-/-}$ mice sera than WT animals, indicating that IL-17A might influence the rate at which MerTK is proteolytically cleaved from the surface of the cell (Figure 17G). In order to confirm that IL-17A signaling through cardiac fibroblasts was responsible for modulation of MerTK, we assessed MerTK

expression *in vitro*. We confirmed that *in vitro* MerTK was predominantly expressed by Ly6C^{hi} but not Ly6C^{lo} monocytes and MDMs (Figure 17H). Moreover, IL-17A signaling through cardiac fibroblasts resulted in a significant down-regulation of MerTK expression on Ly6C^{hi} monocytes and MDMs (Figure 17H). In addition, we observed that sMer was significantly elevated in the co-culture supernatants when IL-17A signaling was present (Figure 17I). Our findings suggest that IL-17A stimulated cardiac fibroblasts can suppress macrophages' phagocytic function by promoting MerTK cleavage resulting in reduced surface MerTK expression. Our results also suggest that Ly6C^{hi} MDMs in WT EAM hearts have compromised phagocytic activities during heart inflammation. We retro-orbitally injected FITC conjugated latex beads in both IL17Ra$^{-/-}$ and WT EAM mice. We found significantly more FITC^{+} macrophages in the hearts of IL17Ra$^{-/-}$ compared to WT, indicating enhanced phagocytic activity in an IL-17A signaling deficient environment (Figure 17J, K). Human myocarditis patients were reported to have high serum IL-17A, as well as an abundant presence of Th17 cells in their hearts and blood [454]. Indeed, we found higher frequencies of IL-17A expressing infiltrating leukocytes in the hearts of myocarditis patients compared to patients with ischemic cardiomyopathy (Figure 18C, D; Table 6 and Table 7). We therefore hypothesized that myocarditis patients could have lower MerTK expression in their cardiac myeloid population. In a cohort of heart failure patients, we found a significant reduction in myeloid MerTK expression in patients with myocarditis as compared to those with ischemic heart failure, similar to our finding in murine model (Figure 17L; Table 6 and Table 7). In conclusion, IL-17A signals through cardiac fibroblasts to promote MerTK cleavage on Ly6C^{hi} MDMs, thus compromising the processes of efferocytosis. With reduced phagocytic ability as a result of surface MerTK

modulation, we predict that macrophages are less efficient in clearing apoptotic cells efficiently and more likely to exhibit a proinflammatory phenotype, which in turn could promote irreversible cardiac remodeling and fibrosis.

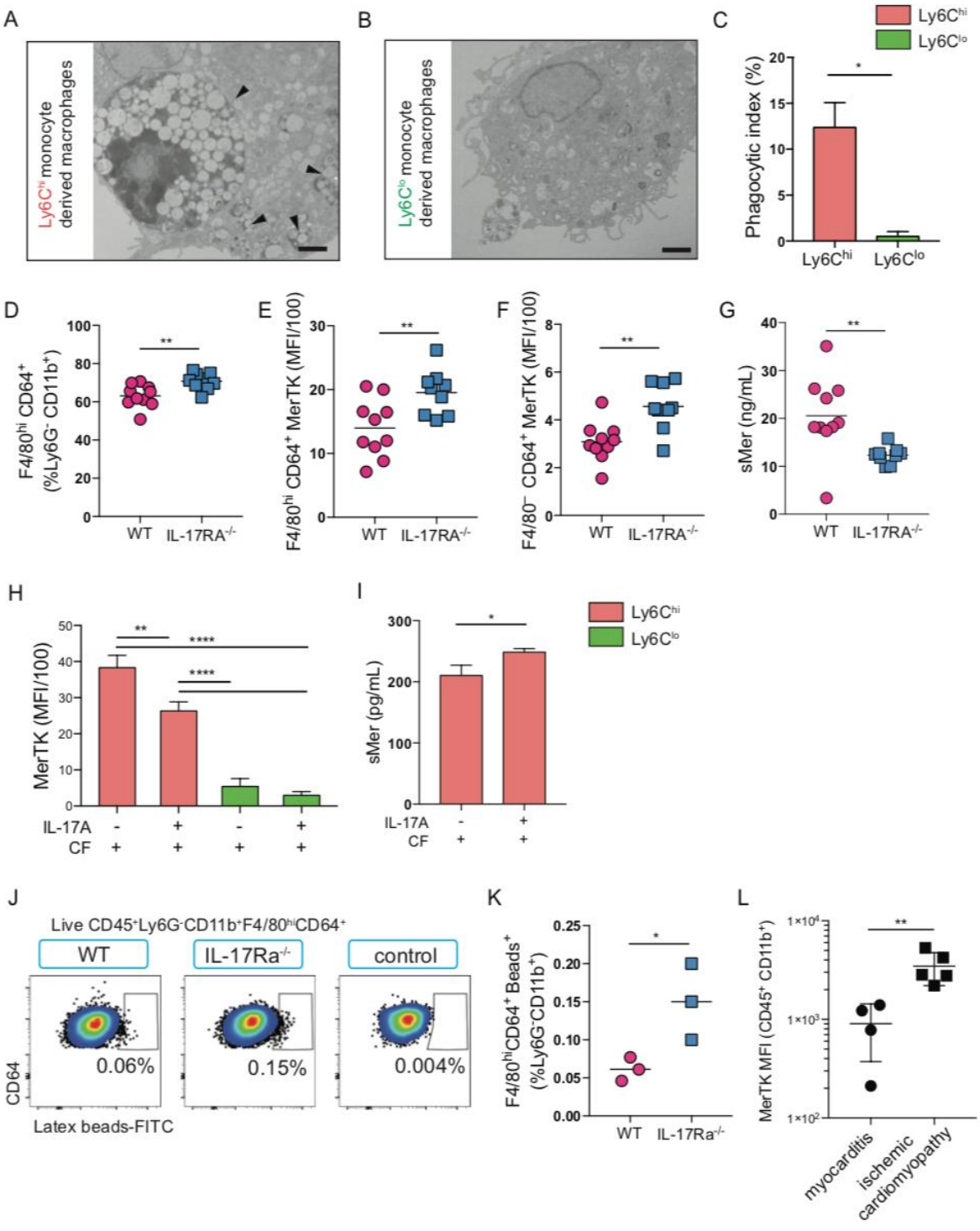

Figure 17. IL-17A signaling through cardiac fibroblasts downregulates MerTK expression on monocytes and monocyte-derived macrophages

(A) Representative images of EM showing apoptotic cells or apoptotic cellular debris internalized by Ly6C^{hi} MDMs (arrowheads) and (B) engulfed cellular debris were largely absent in Ly6C^{lo} MDMs. Bars: (black) 2 μm. (C) Macrophage phagocytic index was calculated using the following formula: (Number of engulfed apoptotic cells/Total number of macrophages) × (Number of macrophages with engulfed apoptotic cells/Total number of macrophages) × 100. (D – G) Hearts from day 21 EAM mice. (D) Frequencies of F4/80^{hi}CD64^{+} macrophages out of viable CD45^{+}Ly6G^{-}CD11b^{+} cells were assessed by flow cytometry. (E) MerTK MFI of F4/80^{hi}CD64^{+} macrophages in the hearts. (F) MerTK MFI of F4/80^{-}CD64^{+} monocytes in the hearts. (G) Concentration of soluble Mer (sMer) detected in WT and IL-17Ra$^{-/-}$ EAM mice sera using an ELISA. (H – I) Cardiac fibroblasts were harvested from WT naïve mice, whereas monocytes were sorted from EAM IL-17Ra$^{-/-}$ mice. (H) MFI of MerTK expression of Ly6C^{hi} or Ly6C^{lo} monocytes and MDMs *in vitro* after 160 hours post-co-culture with cardiac fibroblasts stimulated with or without IL-17A. (I) sMer detected in supernatants of the monocyte-fibroblast co-culture by ELISA. (J) Flow cytometric analysis of the frequencies of FITC^{+}F4/80^{hi}CD64^{+} macrophages in the myocardium of WT, IL-17Ra$^{-/-}$ and non-treated controls. (K) Quantification of the percentages of FITC^{+}F4/80^{hi}CD64^{+} macrophages out of viable CD45^{+}Ly6G^{-}CD11b^{+} cells. (L) MerTK MFI in patients with either myocarditis or ischemic cardiomyopathy. (D – G) Data are representative of five independent experiments. Results are presented as mean ± SD; n = 8 – 9. (H – I) Data are representative of three independent experiments with technical triplicates. Results are presented as mean ± SD; n = 3. (J, K) Data are representative of two independent experiments. Results are presented as mean ± SD; n = 3. (C – G, I, K, L) Groups were compared using Student's *t* test. *, $P < 0.05$ **, $P < 0.01$.

(H) Groups were compared using one-way ANOVA followed by Dunnett test. **, P < 0.01 ****, P < 0.0001. See also Figure 18, Table 6 and 7.

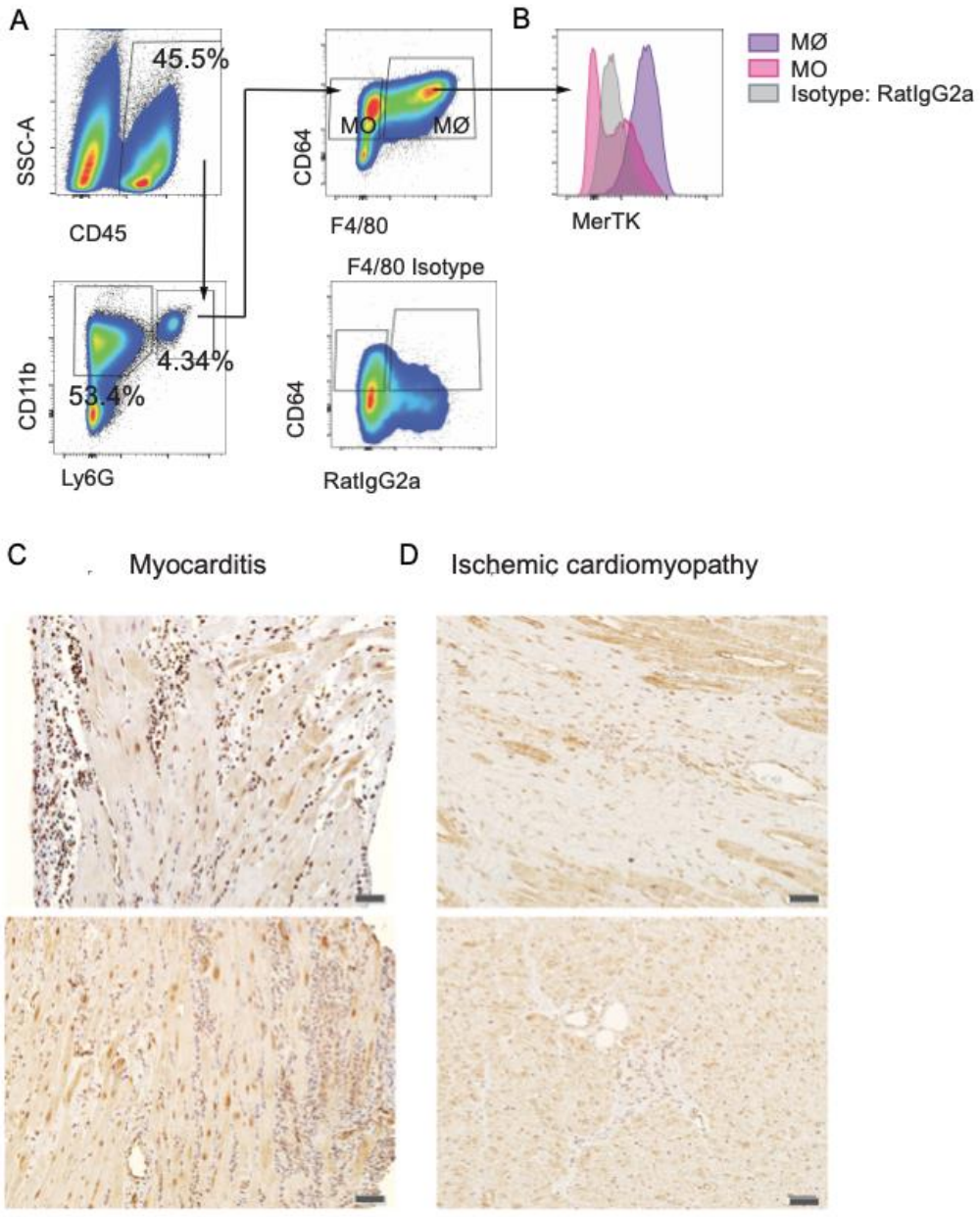

Figure 18. Murine MerTK expression levels by monocytes and macrophages and IL-17A levels in human endomyocardial biopsies

(A) Flow cytometry gating of concatenated $CD45^{+}Ly6G^{-}CD11b^{+}F4/80^{hi}CD64^{+}$ macrophages and $CD45^{+}Ly6G^{-}CD11b^{+}F4/80^{-}CD64^{+}$ monocytes in the hearts. Appropriate F4/80 isotype control was shown. (B) Macrophages and monocytes' MerTK expression level as compared to isotype control for MerTK. (C) Representative immunohistochemistry staining for human IL-17A in heart tissue implant samples of selected two myocarditis patients and (D) two ischemic cardiomyopathy patients.

Sample	Myocarditis patient I	Myocarditis patient II	Myocarditis patient III	Myocarditis patient IV
Age	43	25	15	63
Race/Ethnicity		Hispanic	African American	Caucasian
Gender	Male	Male	Male	Male
Etiology	Viral	Viral	Viral	Viral
Type of VAD	HM XVE	HM II	HM II	Jarvik 2
Diabetes	No	No	No	Yes
Height	188 cm	172 cm	185 cm	183 cm
Weight	100.01 Kg	100.69 Kg	113.39 Kg	87.54 Kg
LVIDd		7.0 cm	7.2 cm	6.7 cm
LVPWd		1.1 cm	0.8 cm	0.7 cm
IVSd		1.1 cm	0.9 cm	0.7 cm
EF	10 – 15%	<20%	<15%	<15%
Troponin level		<0.15		
Days on VAD	50	502	1121	600
Explant reason	OHT	OHT	To Jarvik, died 2d after	OHT
Dead	Yes	No	Yes	No
BNP		423	1163	
CKMB		0.2		2.2
Tissue Amount (mg)	44	130	231.4	245.5
Path Implant		focal interstitial edema, minimal hypertrophy	myocyte hypertrophy	myocyte hypertrophy and lysis

Table 6. Patient information part II

Viral myocarditis patient information from individuals presenting with end stage heart failure who underwent Left Ventricular Assist Device explant and orthotopic heart

transplant at the Texas Heart Institute. Tissues were collected for IHC and flow cytometry assessments. Gray Fill: Data Not available; OHT: Orthotopic Heart Transplant.

Sample	Ischemic cardiomyopathy patient I	Ischemic cardiomyopathy patient II	Ischemic cardiomyopathy patient III	Ischemic cardiomyopathy patient IV	Ischemic cardiomyopathy patient V
Age	61	59	64	56	72
Race/Ethnicity	Caucasian	Caucasian	Hispanic	Caucasian	Caucasian
Gender	Male	Male	Male	Male	Male
Etiology	Ischemic	Ischemic	Ischemic	Ischemic	Ischemic
Type of VAD	HM II	HW	HM II	HM II	HW
Diabetes	No	No	Yes	Yes	Yes
Height	170 cm	170 cm	170 cm	180 cm	178 cm
Weight	77.11 Kg	73.48 Kg	90.71 Kg	97.97 Kg	69.39 Kg
LVIDd	6.92 cm	7.2 cm	7.0 cm	8.0 cm	6.9 cm
LVPWd	1.1 cm	1.1 cm	1.0 cm	1.1 cm	1.0 cm
IVSd	0.63 cm	0.9 cm	1.1 cm	1.0 cm	1.1 cm
EF	20%	30%	<15%	20%	<20%
Troponin level	0.06	<0.15	<0.15		<0.15
Days on VAD	270	452	363	432	182
Explant reason	OHT	OHT	OHT	OHT	OHT
Dead	No	No	yes	No	No
BNP	2983	222	1130	283	240
CKMB	1.6	1.2	5.9		0.2
Tissue Amount (mg)	273	251	240.6	271.9	218
Path Implant	myocyte hypertrophy	Myocyte hypertrophy, interstitial and replacement-type myocardial fibrosis	severe myocyte hypertrophy with extensive fibrosis	myocyte hypertrophy, patchy interstitial fibrosis	Replacement type myocardial fibrosis

Table 7. Patient information part III

Ischemic cardiomyopathy patient information from individuals presenting with end stage heart failure who underwent Left Ventricular Assist Device explant and orthotopic heart transplant at the Texas Heart Institute. Tissues were collected for IHC and flow cytometry assessments. OHT: Orthotopic Heart Transplant.

Discussion

Monocytes and macrophages are key effector cells in the injured myocardium during human myocarditis and EAM [432, 433]. Although both Ly6C^{hi} and Ly6C^{lo} monocytes infiltrate the myocardium during EAM, we found that an excessive accumulation of Ly6C^{hi} rather than Ly6C^{lo} monocytes in the heart leads to adverse cardiac remodeling and the development of DCM [247]. However, it was unknown whether both infiltrating Ly6C^{hi} and Ly6C^{lo} monocytes contribute to the adverse cardiac tissue remodeling during development of EAM. Moreover, the role of the local pro-inflammatory cardiac microenvironment in influencing Ly6C^{hi} and Ly6C^{lo} monocyte fate and function was not well understood. We used three fate-mapping strategies to evaluate the phenotypic and functional changes of monocytes in the heart during myocarditis: parabiosis, adoptive transfer of monocytes, and an *in vitro* co-culture system.

Under steady-state, adult cardiac tissue macrophages in mice are of mixed embryonic and hematopoietic origins [115-119]. In cases of aging or perturbed homeostasis, a greater proportion of embryonic derived macrophages are replaced by infiltrating monocytes, changing the landscape of macrophage dynamics in the heart. [119, 149, 441]. Our parabiosis fate-mapping results reveal that monocytes extravasate into hearts during EAM and readily differentiate into macrophages, which contributes to the increase in cardiac macrophage number during EAM. It was previously reported that cardiac CCR2^{-} macrophages including MHCII^{+} and MHCII^{-} populations are largely embryonically-derived, whereas cardiac CCR2^{+} macrophages represent a haematopoietically derived

lineage at steady-state [119, 455]. Embryonically derived macrophages are shown to have regenerative and reparative properties [455, 456], whereas $CCR2^{+}$ macrophages are thought to initiate inflammation and contribute to adverse cardiac remodeling [457, 458]. We report here that infiltrating monocytes predominantly contribute to the $CCR2^{+}MHCII^{+}$ macrophage compartment. Albeit to a lesser extent, they are also able to differentiate into $CCR2^{-}MHCII^{+}$ macrophages, with very few becoming $CCR2^{-}MHCII^{-}$ macrophages in the chronically inflamed heart.

$Ly6C^{hi}$ monocytes are known to replenish the macrophage pool during cardiac injury; however, the contribution of $Ly6C^{lo}$ monocytes to the cardiac macrophage pool has not been previously described [119, 171, 184, 245, 272, 439-441]. Here we show that both $Ly6C^{hi}$ and $Ly6C^{lo}$ monocytes have the capability to differentiate into macrophages, a process driven by direct contact with cardiac fibroblasts. Previously, we demonstrated that IL-17A can stimulate cardiac fibroblasts to produce significant amounts of GM-CSF [247]. Evidence from EAM, Kawasaki syndrome, and the mouse model of MI show that cardiac fibroblasts are potent producers of GM-CSF [247, 444, 459, 460]. An accumulating body of literature indicates that GM-CSF plays a key role in signaling myelopoiesis in response to tissue injury. GM-CSF also induces a pathogenic transcriptional signature in pro-inflammatory monocytes propelling the inflammatory cascade resulting in further tissue damage [247, 459, 461]. Here, we are the first to show a profound inhibitory role of IL-17A as it works *in trans* through cardiac fibroblast-derived GM-CSF on $Ly6C^{lo}$ monocyte-to-macrophage differentiation *in vitro*. We also confirmed *in vivo* the inhibitory effect of IL-17A signaling on $Ly6C^{lo}$ monocyte-to-macrophage

differentiation. We hypothesize that these Ly6C^{lo} MDMs have distinct functions in myocarditis compared to Ly6C^{hi} MDMs.

Gene expression profiling results substantiate that Ly6C^{hi} and Ly6C^{lo} MDMs represent distinct cell types, possibly driven partly by intrinsic properties. Recent studies have demonstrated that Ly6C^{hi} and Ly6C^{lo} monocytes are phenotypically heterogenous populations. Intrinsic properties such as transcription factors regulate Ly6C^{hi} and Ly6C^{lo} monocyte fate and function during steady state or tissue injury [462-466]. However, we found that IL-17A signaling through cardiac fibroblasts accentuates a proinflammatory and pro-tissue remodeling gene profile in Ly6C^{hi} MDMs. These macrophages up-regulate genes such as *Il6*, *Mmp9*, *Timp1* and *Osm*, all of which have been implicated in cardiac dysfunction and maladaptive cardiac remodeling [467-472]. Unexpectedly, we found that Ly6C^{lo} MDMs are enriched with genes associated with class II antigen processing. We confirm that Ly6C^{lo} MDMs express higher levels of MHCII than their Ly6C^{hi} counterparts *in vitro*. IL17Ra$^{-/-}$ mice develop EAM similar to their WT counterparts, but are protected from DCM, cardiac fibrosis and dysfunction [442]. *In vivo*, IL17Ra$^{-/-}$ EAM hearts contain more MHCII expressing macrophages than WT EAM controls during disease resolution, coinciding with DCM protection in IL17Ra$^{-/-}$ mice. The anti-inflammatory and proangiogenic properties of Ly6C^{lo} monocytes were previously investigated, and their roles in the resolution of cardiac inflammation were frequently highlighted [171, 245, 247]. This suggests that MHCII^{+}Ly6C^{lo} MDMs might be beneficial in disease resolution and contribute to the protection of IL17Ra$^{-/-}$ mice from DCM and heart failure. The functions of Ly6C^{lo} MDMs was placed under scrutiny recently. It has been implicated that they are

the precursors for wound healing macrophages in a soft tissue injury model [177]. Paradoxically, they were also shown to give rise to inflammatory macrophages in an autoimmune arthritis model [350]. We offer clues that Ly6C^{lo} MDMs are a non-inflammatory and non-tissue-remodeling population. The increased presence of these macrophages and an increased Ly6C^{lo} to Ly6C^{hi} ratio in EAM myocardium correlate with DCM protection in IL17Ra$^{-/-}$ mice [247]. Although phagocytic activity of Ly6C^{lo} MDMs is unremarkable, their potential antigen presentation capability predicts their immune regulatory role in the heart. Whether MHCII^{+} Ly6C^{lo} MDMs play a role in effector/memory T cell or regulatory T cell activation in the heart require further examination. Recent evidence indicated that MHCII^{+} macrophages loaded with cardiac myosin peptide are not effective in stimulating proliferation of autoreactive CD4^{+} T cell [473]. However, the beneficial effects of macrophages and regulatory T cells interactions during inflammation resolution and tissue regeneration have been reported [474, 475]. Currently, it remains unfeasible to selectively deplete Ly6C^{lo} monocytes in mice. However, further experiments utilizing Nr4a1$^{-/-}$, CX3CR1$^{-/-}$ or S1PR5$^{-/-}$ mice with reduced Ly6C^{lo} monocytes can help to better assess specific functional role of Ly6C^{lo} monocytes-derived macrophage in the context of myocarditis [218, 232, 476].

Macrophage function can be shaped by both progenitor origin and tissue microenvironment [113, 455]. We tested the hypothesis that upon IL-17A stimulation, cardiac fibroblasts play a role in modulating macrophage function. Recent data directly links the level of efferocytosis receptors on monocytes and macrophages to phagocytosis-dependent wound healing and restoration of organ function [477-480].

Uncontrolled cellular necrosis and apoptosis during cardiac injury are integral components that contribute to adverse tissue healing and remodeling. Inefficient phagocytic clearance can also lead to exposure of self-antigens, which contribute further to autoimmune reactivity [481]. One of these efferocytosis receptors, MerTK, has been shown to be up-regulated on phagocytic cells during inflammation and plays an essential role in apoptotic cell recognition and clearance [449, 482-484]. Moreover, efferocytosis triggers a shift in macrophage activation making them phenotypically less proinflammatory [452, 453, 485]. Notably, our *in vivo* and *in vitro* results suggest that IL-17A signaling through cardiac fibroblasts lead to MerTK shedding and the release of soluble Mer, which significantly reduces surface MerTK expression on Ly6C^{hi} monocytes and MDMs. Cardiomyocytes have been shown to induce shedding of macrophage MerTK to suppress phagocytosis [486]. This highlights another mechanism by which IL-17A through cardiac fibroblasts can induce MerTK shedding, and in turn contributes to cardiac pathology in autoimmune myocarditis. Moreover, we showed that myeloid MerTK was significantly lower in human myocarditis patients when compared to ischemic patients. These findings warrant future studies to determine whether sMer can be used as a biomarker in clinical settings to differentiate patients with myocarditis from those with other types of cardiac diseases.

Taken together, we underscore the fates of Ly6C^{hi} and Ly6C^{lo} monocyte subsets as a result of changes in the cardiac microenvironment. We demonstrate how the local cardiac milieu instructs cardiac fibroblasts to facilitate monocyte differentiation and proliferation as well as regulate the phenotype and function of monocytes and MDMs. Monocytes are

versatile immune cells playing a multi-faceted role in a wide range of inflammatory disorders [175, 177, 245, 296, 487, 488]. Our findings have broader implications for inflammatory diseases in the heart and other organs. We recently reported that IL-17A signaling to cardiac fibroblasts is associated with severe fibrosis and post-infarct death [444], which demonstrates a potential parallel concept that warrants future investigation. Ultimately, we anticipate that further studies of macrophage-cardiac fibroblast interactions will provide new insights into the development of targeted therapies that prevent deleterious inflammatory responses.

Material and Methods

Patients

Endomyocardial biopsies from the apex of the left ventricle were obtained from patients with end stage heart failure (AHA stage D) of various etiologies. Biopsies were from patients who were undergoing either an implantation of Left Ventricular Assist Device (LVAD), or an orthotopic heart transplant after LVAD explant at the Texas Heart Institute. Details including patients' age and gender are summarized in Table S1 – 3. Informed consent was obtained from human subjects and the study protocol was approved by the Committee for the Protection of Human Subjects (University of Texas Health Science Center at Houston. IRB #HSC-MS-05-0074). Samples were properly preserved in cryovials embedded in liquid nitrogen (-190^{o}C) and then kept at -80^{o}C in the tissue bank at the Texas Heart Institute, Houston, TX as previously described [489]. Aliquots of the samples were shipped frozen and processed in house. Reported diagnoses corresponded to clinical charts, based on standard histology (H&E), clinical presentation,

hemodynamic parameters, and routine clinical biochemical and serology parameters. Patient's information of all samples was processed with random non-linked code relabeling in a database at the time of preservation. Furthermore, for each sample, a separate random non-linked code was assigned for the analyses process. Separately, one paraffin embedded, virus negative, acute giant cell myocarditis left ventricle transmural endomyocardial biopsy sample in Figure S3A and S3B were provided by Dr. Karin Klingel. The sample was taken for routine diagnostic purposes to identify infectious agents in the myocardium as described before [490]. Informed consent was obtained from human subjects and the study was approved by local ethic committee (Project-No.253/2009BO2). Diagnosis of giant cell myocarditis was based on established criteria [18].

Mice

IL-17Ra$^{-/-}$ mice on BALB/c background were provided by Amgen Inc. (Thousand Oaks, CA) and Dr. J. Kolls (Children's Hospital, University of Pittsburgh Medical Center, Pittsburgh, PA) [247, 491]. CByJ.SJL(B6)-Ptprc^{a}/J (CD45.1) mice (006584) and WT BALB/cJ (000651) mice were purchased from The Jackson Laboratory. IL-17Ra$^{-/-}$ mice were crossed to CByJ.SJL(B6)-Ptprc^{a}/J (CD45.1) mice and bred to homozygosity at both loci. All mice were housed and maintained in the Johns Hopkins University School of Medicine specific pathogen-free vivarium. 6–10 weeks old healthy naïve male mice were randomly selected as the subjects of all of our studies. All experiments involving animals were in compliance with the Animal Welfare Act and strictly followed the Guide for the Care and Use of Laboratory Animals. The Animal Care and Use Committee of The Johns Hopkins University has approved all procedures and protocols used in this study.

Primary adult cardiac fibroblasts isolation and culture

50U heparin was injected *i.p.* into 6 – 10-week-old male BALB/cJ naïve mice prior to sacrifice. Hearts were cannulated through the aorta and perfused for 3 minutes with 37°C perfusion buffer at 4 mL/minute: 7.03g/L NaCl, 1.1 g/L KCl, 0.082 g/L KH_2PO_4, 0.085 g/L Na_2HPO_4, 0.144 g/L $MgSO_4$, 2.38 g/L HEPES, 0.39 g/L $NaHCO_3$, 1 g/L glucose, 3.74 g/L Taurine, 1 g/L 2,3-Butanedione monoxime (all Sigma), and for 8 min with Collagenase II and Protease XIV (Worthington) and 0.03M $CaCl_2$. Hearts were cut into small pieces and cells separated by gently pipetting for 3 minutes or until no large tissue pieces were observed. Cells were filtered through a 100 µm filter and washed in DMEM (Gibco). Cells were plated in DMEM with 20% FBS (GE Healthcare Life Sciences), nonessential amino acids (Sigma), Penicillin/Streptomycin, 2 mM L-Glutamine, and 25mM HEPES (all Quality Biological). Cells were incubated in a humidified 5% CO_2 incubator at 37°C from here on. Non-adherent cells were washed away after 1 hour. Fibroblasts from second passage were used in experiments. The purity of cardiac fibroblast cultures was confirmed by qPCR and flow cytometry. Cells and supernatants were harvested at the indicated time points after addition of recombinant mouse cytokine IL-17A at 50 ng/mL or recombinant mouse GM-CSF at 50ng/mL (Peprotech). LEAF™ Purified anti-GM-CSF at 50µg/mL was used (MP1-22E9, BioLegend). Monocytes and fibroblasts separation in the co-culture was achieved by 0.4 µM transwell inserts (Corning).

Parabiosis surgery

Pairs of mice were anesthetized with inhaled isoflurane, 4.0–5.0% v/v induction (Baxter). Fur was removed thoroughly from the entire flank region using clippers. Anesthesia in surgical pairs was maintained with intramuscular injections of ketamine (80 mg/kg) and

xylazine (16 mg/kg). The mice were laid supine and the site was disinfected with betadine followed by 70% EtOH. We administered buprenorphine (0.1 mg/kg) intraperitoneally for initial analgesia, and at 12 hours postoperatively. Longitudinal incisions were made through the skin starting from the elbow joint and extended down to the knee joint. Non-absorbable 4-0 interrupted sutures were placed around the knee and elbow joints. Pairs where attached from the elbow joints first. To increase skin anastomosis, we used a continuous 5-0 absorbable vicryl sutures through the muscular layer and connect the pairs further, before attaching the knee joints. Surgical stapler was used to connect the skins of the pairs. Baytril was used upon completion of the procedure. Animals were provided with moistened chow and gel food diet supplement every other day until sacrifice at 19 to 20 days after parabiosis.

EAM induction

To induce EAM, we injected mice with 125 μg myosin heavy chain α peptide MyHCα$_{614-629}$ (Ac-SLKLMATLFSTYASAD; Genscript) [492] emulsified in CFA (Sigma-Aldrich) supplemented with 5mg/mL heat-killed *Mycobacterium tuberculosis* strain H37Ra (Difco) on days 0 and 7. On the first day of immunization, mice also received a dose of 500 ng pertussis toxins intraperitoneally (List Biologicals) [83].

EAM histopathology assessments

Myocarditis severity was evaluated by histology on days 21. Heart tissues were fixed in SafeFix solution (Thermo Fisher Scientific), embedded and cut into 5 μm serial sections. Sections were stained with H&E and ventricular inflammation was scored via a microscope by two independent blinded investigators and averaged using the following criteria for hematopoietic infiltrates: grade 0, no inflammation; grade 1, <10% of the heart

section is involved; grade 2, 10–30%; grade 3, 30–50%; grade 4, 50–90%; grade 5, >90% [83].

Isolation of Splenic Ly6C^{hi} and Ly6C^{lo} monocytes

Spleens from WT or IL-17Ra$^{-/-}$ BALB/c mice on day 14 of EAM were dissected and mechanically disrupted. Cells were filtered through 40 µm cell strainers and washed. Histopaque 1119 and 1077 (Sigma) were used to isolate mononuclear cells. Anti-Ly6G MicroBead kit (Miltenyi Biotech) was used to deplete Ly6G^{+} cells, and CD11b MicroBead kit (Miltenyi Biotech) was used to positively enrich CD11b^{+} cells. Single-cell suspensions were stained with LIVE/DEAD stain (ThermoFisher), washed, FcγRII/III blocked with a-CD16/CD32, and stained with fluorochrome-conjugated antibodies (eBioscience, BioLegend, BD Pharmingen). Cells were sorted on an AriaIIu cell sorter. Sorted cells from IL-17Ra$^{-/-}$ BALB/c mice spleens were used for *in vitro* co-culture with primary cardiac fibroblasts, major outcomes were validated with sorted cells from WT BALB/c mice spleens co-cultured with cardiac fibroblasts. Sorted cells from WT BALB/c mice spleens were used in intracardiac transfer experiments (see below).

Cell staining and light microscopy

Modified Giemsa staining was achieved by using Differential Quik Stain Kit, following the manufacturer's instructions (Polysciences). Cell staining images were acquired on Olympus BX43 microscope with a camera (DP72) using CellSens Standard software (version 1.4.1; Olympus).

IncuCyte ZOOM imaging

Once the monocyte-fibroblast co-cultures were established, the plates were placed into the IncuCyte ZOOM^{TM} (Essen Bioscience) apparatus and images of cells were recorded

with 20× magnification undisturbed every 1 hour for a total duration of 160 hours. Cardiac fibroblasts alone were used as controls and triplicated wells were included in all data acquisitions.

Transmission electron microscopy

Co-cultured cells were washed with PBS and fixed in 2.5% glutaraldehyde dissolved in 0.1 M Na cacodylate. Samples were then processed by the Johns Hopkins Microscope Facility [493] before examination using the Philips CM120 transmission electron microscope. Images were captured using Advanced Microscopy Techniques V602 software. The phagocytic index was calculated according to the following formula: phagocytic index = (total number of engulfed cells/total number of counted macrophages) × (number of macrophages containing engulfed cells/total number of counted macrophages) × 100. Approximately 60 total macrophages derived from each monocyte subset were counted, numbers were acquired from two separate assessments.

Immunofluorescence microscopy

Human paraffin-embedded giant cell myocarditis biopsy sample slides were processed using xylene and rehydrated with decreasing concentration of ethyl alcohol and rinsed with distilled water. After blocking with 1% BSA and 0.1% tween-20 in 1× PBS, tissues were incubated with anti-CD14-biotin sheep antibodies (R & D systems) and anti-CD68 mouse antibodies (Abcam). We then used NL-637 Streptavidin and donkey NL-557 anti-mouse IgG (R & D systems) as secondary antibodies diluted in 0.05% Evans Blue for counterstaining. DAPI was used for staining nuclei. Finally, Sudan Black was used to suppress auto-fluorescence as a result of tissue fixation and paraffin treatment. Images were acquired using Zeiss Axio Imager.A2. microscope with AxioCam MRm at 20×

magnification. We used AxioVision Rel. 4.8 software to acquire images and Adobe Photoshop version 12.0 to process images.

Intracardiac injection

WT or IL-17Ra$^{-/-}$ BALB/c mice on day 21 of EAM were depilated and anesthetized with 3.5% isoflurane (Baxter). The mice were subsequently endotracheally intubated, 100% oxygen and 2% isoflurane were provided to the animals throughout the operation by mechanical ventilation (Model 845, Harvard Apparatus). Pre-operational analgesics (0.05 mg/kg Buprenorphine, Reckitt Benckiser) and paralytics (1 mg/kg Succinylcholine, Henry Schein) were administered prior to operation. Mice were subjected to a thoracotomy, typically around the 4th or 5th intercostal space to expose the heart ventricles. Roughly 1.5 – 2 x 10^5 cells were injected with a 29G ½ insulin syringe (BD) into 2 – 3 ventricular locations. Mice were placed under the heat lamp to recover post-surgery, post-operational analgesics (0.05 mg/kg Buprenorphine, Reckitt Benckiser) were administered. Mice were sacrifice at 40 hours and 160 hours post-surgery to assess cell transfer outcomes.

Retro-orbital injection of monocytes

WT or IL-17Ra$^{-/-}$ BALB/c mice on day 21 of EAM were depilated and anesthetized with 100% oxygen and 3.5% isoflurane (Baxter). Mice were subjected to an injection into the ophthalmic venous sinus. Roughly 4 – 5 x 10^5 FACS sorted monocytes were injected with a 29G ½ insulin syringe (BD).

Retro-orbital injection of liposomes and latex beads

We administered a single treatment of 10 µl Clodrosome® (clodronate loaded liposomes; Encapsula Nano Sciences) per gram of animal weight seventeen hours prior to latex microsphere labeling to better visualize FITC$^+$ macrophages *in vivo*. 0.5-µm FITC-

conjugated (yellow gold) plain microspheres (2.5% solids [wt/vol]; Polysciences, Inc.) were diluted 1:25 in 1XPBS. We administered 250 µl of the diluted latex beads to examine macrophage phagocytic activity *in vivo*. Hearts were harvested 24 hours post bead administration.

Quantitative reverse transcription PCR

Cell mRNAs were extracted in TRIzol (Invitrogen), and reverse transcribed using High-Capacity cDNA Reverse Transcription Kit (Applied Biosystems). Target cDNAs were amplified with Power SYBR Green PCR Master Mix (Bio-Rad) and real time cycle thresholds were detected via MyiQ2 themocycler running on an iQ5 software (Bio-Rad). Target genes fold induction were calculated using the $2^{-\Delta\Delta Ct}$ method by normalizing cycle thresholds to the *Hprt* housekeeping gene and medium controls [494]. Verified *Ccl2* primer sequences were acquired from the PrimerBank (Harvard Medical School, Massachusetts General Hospital and The Center for Computational and Integrative Biology), and commercially synthesized (Integrated DNA Technologies). *Ccl2* forward primer sequence (5' to 3'): TTAAAAACCTGGATCGGAACCAA, and reverse primer sequence (5' to 3'): GCATTAGCTTCAGATTTACGGGT.

Flow cytometry analysis and *Barnes-Hut Stochastic Neighbor Embedding* analysis

Hearts of naïve or EAM mice were perfused through the ventricles with PBS for 3 minutes. GentleMACS C Tubes were used to mechanically disassociate the tissue according to manufacturer's instructions (Miltenyi Biotech). Single cell suspensions were achieved using enzymatic digestion by 3000 U Collagenase II and 300 U DNase I (Worthington) dissolved in 5mL HBSS. Splenocytes, blood, and BM cells (femurs and tibias) were isolated by mechanical disruption, followed by red blood cell lysis using ACK buffer

(ThermoFisher). Heart samples were filtered through 40 μm filters, whereas the other tissues were filtered through 70 μm filters. Cells were then stained with LIVE/DEAD (ThermoFisher), FcγRII/III blocked with α-CD16/CD32, and stained with fluorochrome-conjugated antibodies (eBioscience, BioLegend and BD Pharmingen). Alternatively, we used APC Annexin V Apoptosis Detection Kit with 7-AAD (BioLegend) instead of LIVE/DEAD. CellTrace™ CFSE Kit was used to track cell proliferation both *in vivo* and *in vitro* (ThermoFisher). Samples were acquired on a BD LSRII or LSRFortessa 4-laser cytometers running FACSDiva 6.0 (BD Immunocytometry) and analyzed using FlowJo 10.4 software. We ran an interactive visualization tool called *cyt* in Matlab to analyze high-dimensional flow cytometry data [445, 446]. bh-SNE is an unsupervised non-linear dimensionality reduction embedding technique [445].

Microarray

Ly6C^{hi} and Ly6C^{lo} *in vitro* co-culture derived macrophages in triplicate were FACS sorted and cells were lysed using RLT buffer (Qiagen). RNA was extracted using RNeasy micro kit. RNA samples were labeled using Thermal Fisher 3' IVT Pico Reagent kit (Affymetrix) according to manufacturer's guidelines and probed using the Affymetrix Mouse Clariom S Array. RNA concentration and integrity were determined with Agilent Bioanalyzer Pico Chip.

Statistical analysis

GraphPad Prism 7 software was used for statistical analysis. Statistical analysis details are described in the figure legends. To determine if datasets show a normal distribution, either the D'Agostino-Pearson or the Shapiro-Wilk normality test was used. P values were considered statistically significant at $P<0.05$.

Microarray gene expression analysis

Raw data generated from Clariom S Arrays were processed using Affymetrix Expression Console Software. CEL files containing feature intensity values were converted into summarized expression values by Partek Genomic Suite Software including background adjustment, quantile normalization and summarization across all chips. All samples passed QC thresholds for hybridization, labeling and the expression of spiked in controls. The variances, both between and within groups, in log2 transformed expression values were analyzed by one-way ANOVA. PCA graph was generated using Partek Genomic Suite Software, heat maps were generated using TIBCO Spotfire Software. The complete normalized data set is available on GEO under Series accession number GSE118861.

Author contribution

Conceptualization and Methodology, X.H., J.G.B., and D. C.; Software, Validation, Formal Analysis, Data Curation and Visualization, X.H.; Investigation, X.H., G.C., W.B., H.S.C., N.L.D., J.S., M.V.T., T.W., D.H., M.K.W. and I.C.; Resources, D.J.H., K.K., G.E.D. and H.T.; Writing – Original Draft and Writing – Review & Editing, X.H., and D. C.; Supervision, Project Administration and Funding Acquisition, D. C.

Chapter 6

Conclusions and future directions

In addition to myocardium, valves and an electrical conduction system, the heart depends on a complex network of cells, including cardiomyocytes, cardiac fibroblasts that produce extracellular matrix, endothelial cells and tissue macrophages, to provide the structure and function that allows the heart to pump oxygen and nutrients throughout the body [495]. As we begin to understand this complex network there has been an increasing interest in the roles played by the cardiac tissue macrophages in maintaining cardiac function [117, 118, 147, 152, 153, 496]. Resident cardiac macrophages remove senescent and dying cells under steady-state and actively participate in the cardiac conduction system that maintains cardiac rhythm [497, 498]. Currently many attempts have been made to create immunotherapies that target macrophages. Unfortunately, global suppression or depletion of macrophage has been shown to have an adverse effect by contributing to heart failure [495]. Thus, it is imperative to dissect the functions of macrophage subsets to develop more specific treatments. Many new exciting technologies such as CRISPR/Cas9 gene editing, single cell sequencing, mass cytometry and intravital microscopy are available to transform our research and provide the opportunity to develop new therapies and biomarkers.

My current work has demonstrated that, through direct contact, cardiac fibroblasts play a kely role in the monocyte-to-macrophage differentiation of both Ly6C^{hi} and Ly6C^{lo} cells recruited to the heart. Ly6C^{hi} monocyte-derived macrophages differentiate to primaryilgy

phagocytic cells, whereas Ly6C^{lo} monocyte-derived macrophages transform to cells that predominantly express MHCII and show the potential for antigen presentation. Furthermore, a cardiac milieu rich in IL-17A can induce GM-CSF production from cardiac fibroblasts which inhibits Ly6C^{lo} monocyte-to-macrophages differentiation downstream. IL-17A signaling through cardiac fibroblasts also enhances MerTK proteolytic cleavage, which dampens phagocytic capabilities of Ly6C^{hi} monocyte-derived macrophages. IL-17A is the most dominant cytokine produced in the myocardium of both mice and humans with myocarditis. It has been shown previously that IL-17A is essential for EAM progression into DCM [442]. Therefore, we hypothesize that reduced macrophage phagocytic activity as a result of IL-17A signaling contributes to myocarditis pathogenesis. We found that MHCII is highly and most predominantly expressed by Ly6C^{lo} monocyte-derived macrophages, coinciding with higher MHCII expression in the macrophage compartment in IL-17Ra$^{-/-}$ EAM mice when compared to WT controls. However, we were unable to elucidate the exact role of Ly6C^{lo} monocyte-derived macrophages during myocarditis at this time.

Several questions remain unanswered. Are these Ly6C^{lo} monocyte-derived macrophages presenting antigens to T effector cells or to T regulatory cells? Do Ly6C^{lo} monocyte-derived macrophages travel to the draining lymph nodes or remain static in the myocardium during antigen presentation? Do Ly6C^{lo} monocyte-derived macrophages contribute to steady state cardiac macrophage pool? We plan to use latex bead labeling to track blood Ly6C^{lo} monocytes establishment in the myocardium during EAM [177, 299, 499]. However, several caveats exist for this technique. First, labeling kinetics declines steadily over time and less than 5% of the blood Ly6C^{lo} monocytes are still labeled by day

7 [499]. EAM is a chronic disease that requires 7 days to induce and 14 more days to fully develop (Figure 1). Therefore, Ly6C^{lo} monocytes should ideally be labeled between the initiation and the peak of cardiac infiltration (day 12 to day 21) to fully capture the change of Ly6C^{lo} monocytes during EAM. Unfortunately, it has been shown that latex beads label similar percentages of Ly6C^{hi} and Ly6C^{lo} monocytes *in vivo* during the first few hours [499]. This means that labeled Ly6C^{hi} monocytes can established themselves as macrophages in the myocardium, which could severely confound the result and its interpretation. Alternatively, we can utilize IL-17Ra$^{-/-}$Nr4a1$^{-/-}$ EAM mice to determine if these IL-17Ra deficient mice will continue to develop DCM when Ly6C^{lo} monocytes are absent.

Previously we uncovered a protective role for IL-13 in EAM development. IL-13$^{-/-}$ EAM mice were shown to have a decreased number of anti-inflammatory macrophages present in the myocardium [500]. Recently I have shown that the IL-13 receptor IL-13Ra1 is highly expressed by macrophages in the naïve heart (Figure 19A). Heart ILCs are the most predominant IL-13 producers in naïve hearts (Figure 19B). The percentage of ILCs wanes as EAM progresses, which surprisingly coincides with IL-13Ra1 down-regulation on macrophages as well (data not shown). We are currently investigating whether macrophage phenotypes are altered in ILC deficient Rag2$^{-/-}\gamma c^{-/-}$ mice.

In summary, our findings demonstrate that monocyte and macrophage fates and functions are fine-tuned by both intrinsic and environmental factors. Macrophages constitute a double-edged sword in cardiac injury and inflammation. It is still largely unknown whether macrophage heterogeneity and remarkable versatility is a consequence of changes at a single cell level (genetic and epigenetic alteration) or at a

population level (proliferation, cell death, recruitment or egress). Technologies are currently still limited that would allow us to readily and precisely distinguish tissue-resident macrophages from monocyte-derived macrophages upon establishment of tissue residency. Therefore, it is essential to develop more advanced methods to answer these questions.

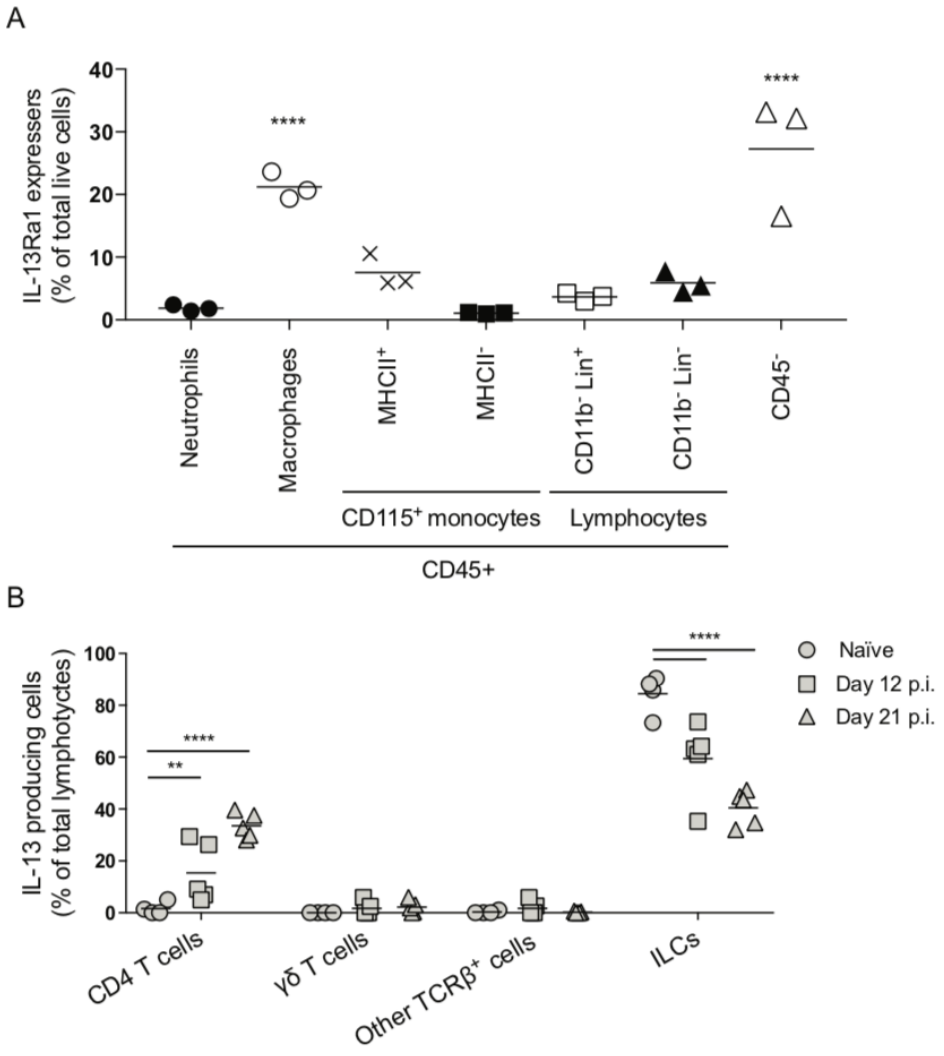

Figure 19. IL-13Ra1 expressing cells and IL-13 producing cells during EAM development

(A) Percentages of IL-13Ra1 expressing cells out of total live cells in naïve mice myocardium. (B) Percentages of IL-13 producing cells out of overall lymphocytic population during EAM development.

The ongoing debates about the role of cardiac fibroblasts

Since cardiac fibroblasts play a role in facilitating monocyte-to-macrophage differentiation, we will discuss here what is currently known about cardiac fibroblasts.

It is estimated that about 10% of the total cells in adult mouse myocardium are fibroblasts [249]. We are beginning to understand the ontogeny and fundamental role of cardiac tissue-resident fibroblasts in disease and health. There are two opposing theories describing the origin of resident fibroblasts. One states that cardiac fibroblasts originate from a variety of cell types (including endothelial cells [501, 502], pericytes and leukocytes [503-505]) that requires further trans-differentiation to become activated. The other states that adult cardiac resident fibroblasts originate from the epicardium during embryogenesis and contribute to activated fibroblasts or myofibroblasts during injury [506]. A recent genetic lineage tracing study that supports the latter theory showed that cardiac resident fibroblasts are the primary source of activated fibroblasts after MI and pressure overload [507].

It is now clear that cardiac fibroblasts are potent producers of pro-inflammatory cytokines, chemokines and extracellular matrix during cardiac inflammation and heart failure [247, 508]. Specifically, GM-CSF production by fibroblasts has been implicated in the pathogenesis of EAM, MI and Kawasaki disease [247, 460, 509]. Cardiac fibroblasts are highly plastic and heterogenous. We have recently demonstrated that cardiac inflammation triggers the expansion of $CD45^{-}CD31^{-}CD29^{+}mEFSK4^{+}PDGF\alpha^{+}Sca\text{-}1^{+}periostin^{+}$ fibroblast population in mice, which is a major producer of GM-CSF as well as CCL2 [508]. Fibroblasts co-expressing GM-CSF and CCL2 could also be found in human myocardial biopsy samples in both myocarditis and ischemic heart failure patients

[508]. Ablation of GM-CSF production in fibroblasts or fibroblast subsets that produce GM-CSF protects mice from heart failure [508, 510]. We therefore speculate that fibroblast-specific ablation of GM-CSF production permits Ly6C^{lo} monocytes to become reparative macrophages in the heart to promote adequate cardiac remodeling and inflammation resolution.

Before we propose that cardiac fibroblasts can be used as potential therapeutic targets, it is important to address whether macrophages can also influence cardiac fibroblast activation status. Interaction between macrophages and fibroblasts via both soluble factors and direct cell-cell contact is most likely not a one-way street. Therefore, a better understanding of the roles and functions of cardiac fibroblasts will be useful to target maladaptive fibrosis in human cardiovascular diseases.

Pericardial and peritoneal macrophages – two facets of a kind?

The heart is enclosed in the pericardium, a cavity filled with protective serosal fluid. Macrophages are found residing in human serosal fluid [511]. Recently, Kubes and colleagues demonstrated that F4/80^{+}GATA-6^{+} murine peritoneal macrophages are rapidly mobilized to promote tissue repair after acute sterile liver injury [512]. Thus, the concept that peritoneum serves as a reparative macrophage reservoir during acute injury can be potentially extended to other serosal populations, including pericardial cavities. It is unclear whether pericardial macrophages can actively infiltrate the myocardium during cardiac injury. Also, it will be interesting to know their specific function during heart inflammation.

We obtained pericardial effusion samples from 5 patients with chronic ischemic heart diseases who underwent coronary artery bypass grafting. Control blood samples were collected from a healthy donor, whose peripheral blood mononuclear cells (PBMCs) were isolated for comparison purposes. All patients in the study provided informed consent. Our preliminary data suggested that while $CD14^{+}CD16^{-}$ monocytes accounted for the most predominant population in blood [183, 513], pericardial effusion samples consisted almost entirely of $CD14^{+}CD16^{+}CD68^{+}CD64^{+}$ macrophage population (Figure 20). Additionally, the monocyte/macrophage population in pericardial effusion express high levels of CD206, HLA-DR and CD116 when compared to blood monocytes (Figure 20). Next, we compared peritoneal, pericardial and myocardial $F4/80^{hi}CD64^{+}$ macrophages in naïve mice. We found that peritoneal and pericardial macrophages express high levels of glycoprotein CD44 and GATA-6 (

Figure 21). These GATA-6^{+} macrophages can infiltrate the myocardium post MI (data not shown).

Although the origin of pericardial macrophages is unknown, similarity between peritoneal and pericardial macrophages suggests that pericardial macrophages may also carry reparative features. Together with embryonic macrophages and Ly6C^{lo} monocyte-derived macrophages, they could play protective roles during cardiac injury. Our initial findings warrant rigorous future studies to elucidate the ontogeny and function of these pericardial macrophages, as well as their identities distinct from myocardial macrophages, which may shed light on their roles in health and disease.

Our knowledge of tissue macrophages has evolved significantly over the past decade. We have gained an appreciation that macrophage activation is multifaceted in the context of tissue injury. Future therapeutic manipulation to improve disease outcomes require

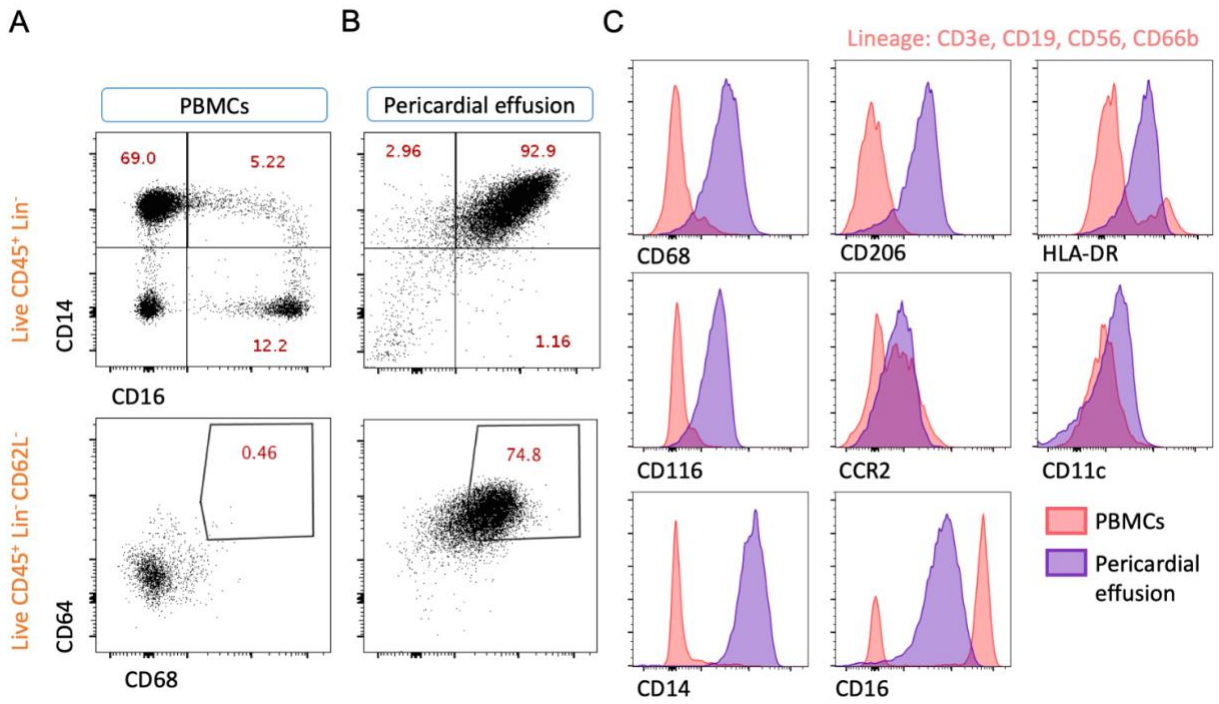

careful examination of macrophage subsets and functions. Our work studying the role of macrophages in myocarditis will advance our understanding of pathogenesis, diagnosis and treatment of chronic heart failure.

Figure 20. Pericardial macrophage phenotype

(A) Top panel shows flow cytometry gating of CD14 and CD16 from a healthy donor's total live $CD45^{+}Lin^{-}$ (lineage including CD3e, CD19, CD56 and CD66b) peripheral blood mononuclear cells (PBMCs). Lower panel shows $CD64^{+}CD68^{+}$ macrophages out of total live $CD45^{+}Lin^{-}CD62L^{-}$ PBMC. (B) Top panel shows representative gating of CD14 and CD16 cells from total live $CD45^{+}Lin^{-}$ cells present in the pericardial effusion fluid of patients with chronic ischemic heart diseases. Lower panel shows these patient's $CD64^{+}CD68^{+}$ macrophages out of total live $CD45^{+}Lin^{-}CD62L^{-}$ cells in the pericardial effusion. (C) Histograms of MFI showing different markers' expression of cells in healthy donor's PBMC versus pericardial effusion fluid of patients with chronic ischemic heart diseases.

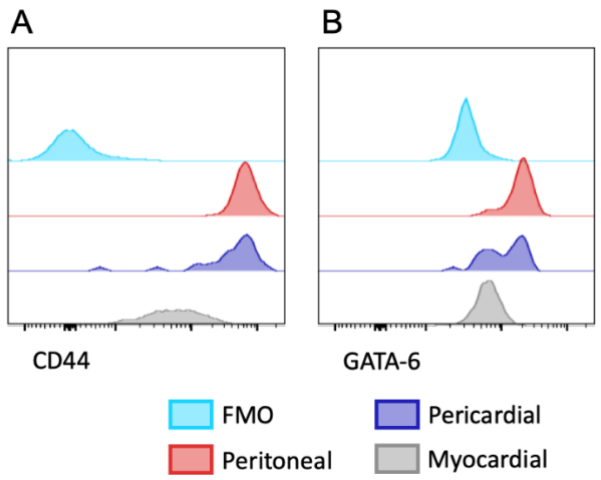

Figure 21. Pericardial macrophages are similar to peritoneal macrophages in CD44 and GATA-6 co-expression

(A) Histograms of CD44 MFI and (B) GATA-6 MFI showing murine (red) peritoneal macrophages, (purple) pericardial macrophages, and (grey) myocardial macrophages. All compared to (blue) fluorescent minus one (FMO) control.

Final remarks

Our work in the past has demonstrated that the recruitment of Ly6C^{hi} monocytes in large numbers to the myocardium contributes to a greater Ly6C^{hi} to Ly6C^{lo} monocyte/macrophage ratio in the heart which promotes EAM to DCM development (Figure 22A). Current results highlight that Ly6C^{hi} monocytes contribute to a macrophage population that is highly pro-inflammatory, pro-tissue remodeling and is deficient in phagocytic activities in an IL-17A rich cardiac environment. This supports our main hypothesis on which our work is based. However, we also found that IL-17A plays a suppressive role through signaling to cardiac fibroblasts by inhibiting Ly6C^{lo} monocytes to become MHCII^{+} macrophages (Figure 22B). While the role of Ly6C^{lo} monocyte-derived MHCII^{+} macrophages warrants future in-depth examination, we hypothesize that they are associated with DCM protection in IL-17A deficient animals. In summary, our finding has filled significant gaps in the knowledge describing the pathogenesis of myocarditis and DCM.

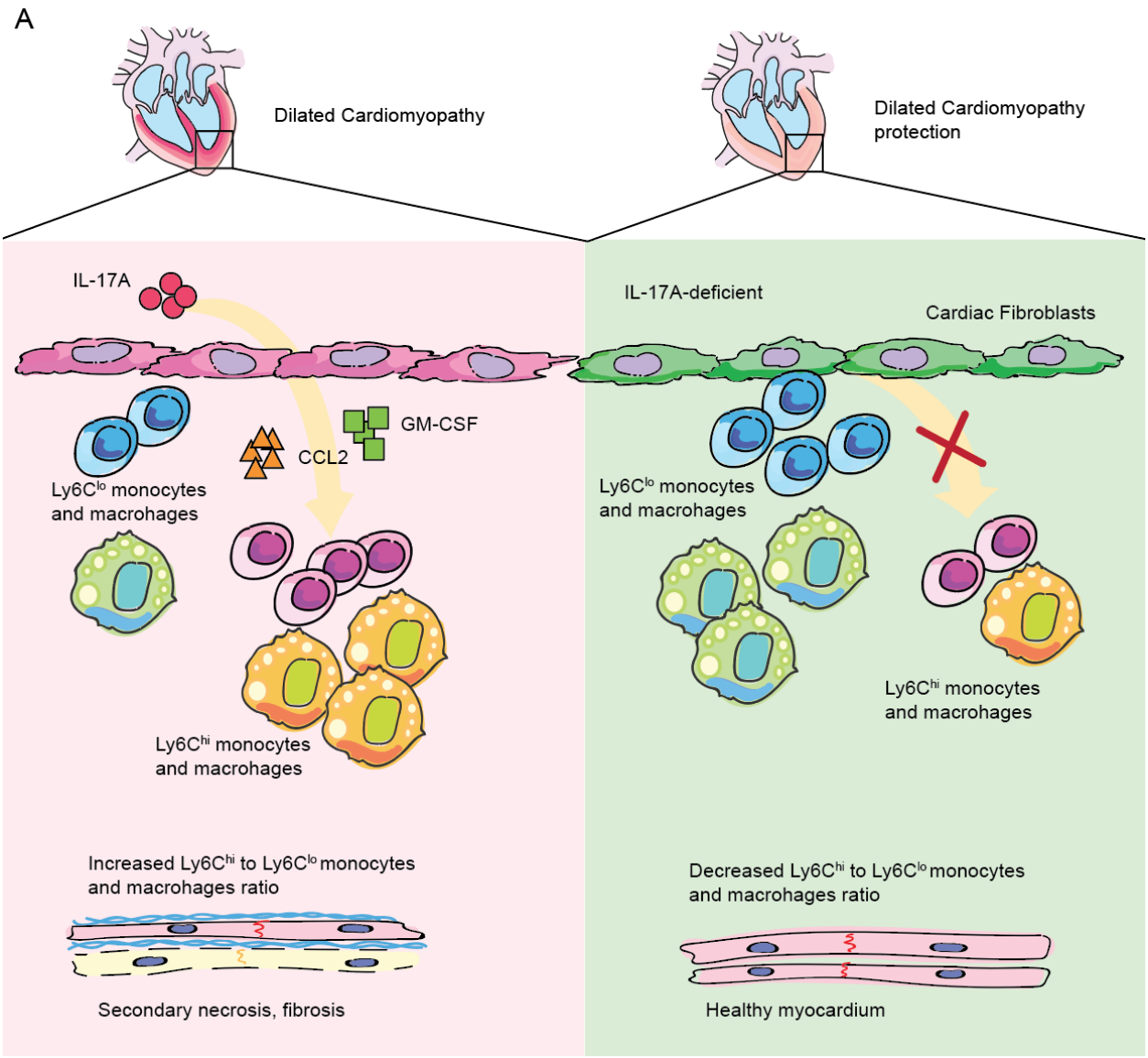
A
Dilated Cardiomyopathy
Dilated Cardiomyopathy protection
IL-17A
IL-17A-deficient
Cardiac Fibroblasts
GM-CSF
CCL2
Ly6C^lo monocytes and macrohages
Ly6C^hi monocytes and macrohages
Ly6C^lo monocytes and macrohages
Ly6C^hi monocytes and macrohages
Increased Ly6C^hi to Ly6C^lo monocytes and macrohages ratio
Secondary necrosis, fibrosis
Decreased Ly6C^hi to Ly6C^lo monocytes and macrohages ratio
Healthy myocardium

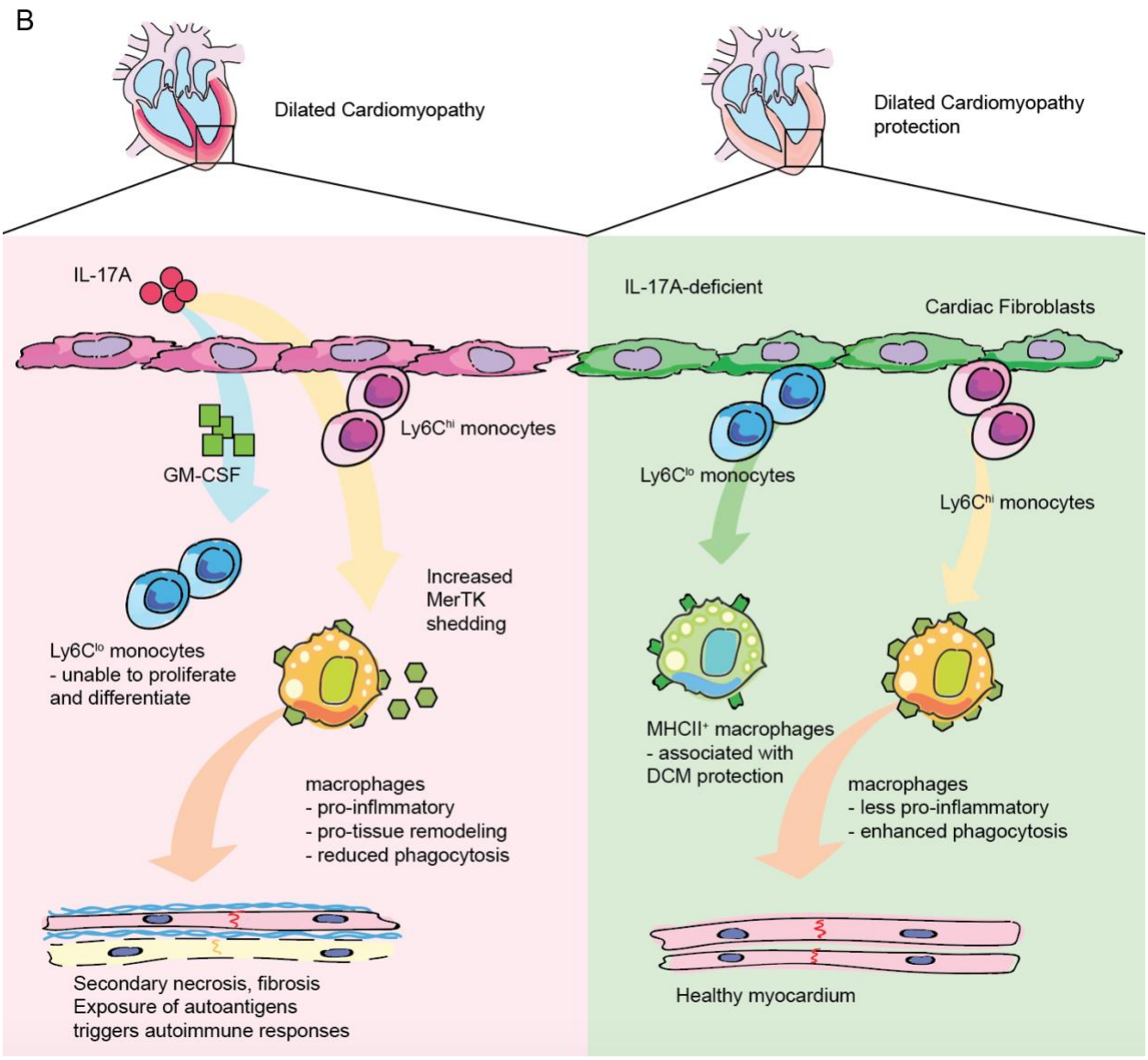

Figure 22. Past and current models explaining the disease pathogenesis of EAM and DCM

(A) Past model suggesting that the Ly6C^{hi} to Ly6C^{lo} ratio is associated with EAM to DCM progression. (B) Current model detailing the fates and functions of monocytes in EAM to DCM progression.

Reference

1. Drory, Y., et al., *Sudden unexpected death in persons less than 40 years of age.* Am J Cardiol, 1991. **68**(13): p. 1388-92.
2. Cooper, L.T., Jr., et al., *The global burden of myocarditis: part 1: a systematic literature review for the Global Burden of Diseases, Injuries, and Risk Factors 2010 study.* Glob Heart, 2014. **9**(1): p. 121-9.
3. Kindermann, I., et al., *Update on myocarditis.* J Am Coll Cardiol, 2012. **59**(9): p. 779-92.
4. Leone, O., et al., *2011 consensus statement on endomyocardial biopsy from the Association for European Cardiovascular Pathology and the Society for Cardiovascular Pathology.* Cardiovasc Pathol, 2012. **21**(4): p. 245-74.
5. Richardson, P., et al., *Report of the 1995 World Health Organization/International Society and Federation of Cardiology Task Force on the Definition and Classification of cardiomyopathies.* Circulation, 1996. **93**(5): p. 841-2.
6. Aretz, H.T., *Myocarditis: the Dallas criteria.* Hum Pathol, 1987. **18**(6): p. 619-24.
7. Aretz, H.T., et al., *Myocarditis. A histopathologic definition and classification.* Am J Cardiovasc Pathol, 1987. **1**(1): p. 3-14.
8. Kindermann, I., et al., *Predictors of outcome in patients with suspected myocarditis.* Circulation, 2008. **118**(6): p. 639-48.
9. Maisch, B., et al., *Inflammatory dilated cardiomyopathy (DCMI).* Herz, 2005. **30**(6): p. 535-44.
10. Rose, N.R., *Myocarditis: infection versus autoimmunity.* J Clin Immunol, 2009. **29**(6): p. 730-7.
11. Baboonian, C. and T. Treasure, *Meta-analysis of the association of enteroviruses with human heart disease.* Heart, 1997. **78**(6): p. 539-43.
12. Bock, C.T., K. Klingel, and R. Kandolf, *Human parvovirus B19-associated myocarditis.* N Engl J Med, 2010. **362**(13): p. 1248-9.
13. Caforio, A.L., et al., *A prospective study of biopsy-proven myocarditis: prognostic relevance of clinical and aetiopathogenetic features at diagnosis.* Eur Heart J, 2007. **28**(11): p. 1326-33.
14. Cambridge, G., et al., *Antibodies to Coxsackie B viruses in congestive cardiomyopathy.* Br Heart J, 1979. **41**(6): p. 692-6.
15. Mahrholdt, H., et al., *Cardiovascular magnetic resonance assessment of human myocarditis: a comparison to histology and molecular pathology.* Circulation, 2004. **109**(10): p. 1250-8.
16. Schultheiss, H.P., U. Kuhl, and L.T. Cooper, *The management of myocarditis.* Eur Heart J, 2011. **32**(21): p. 2616-25.
17. Baughman, K.L., *Diagnosis of myocarditis: death of Dallas criteria.* Circulation, 2006. **113**(4): p. 593-5.
18. Caforio, A.L., et al., *Current state of knowledge on aetiology, diagnosis, management, and therapy of myocarditis: a position statement of the European Society of Cardiology*

Working Group on Myocardial and Pericardial Diseases. Eur Heart J, 2013. **34**(33): p. 2636-48, 2648a-2648d.
19. Fabre, A. and M.N. Sheppard, *Sudden adult death syndrome and other non-ischaemic causes of sudden cardiac death.* Heart, 2006. **92**(3): p. 316-20.
20. Pollack, A., et al., *Viral myocarditis--diagnosis, treatment options, and current controversies.* Nat Rev Cardiol, 2015. **12**(11): p. 670-80.
21. Hales-Kharazmi, A., et al., *Utility of cardiac MRI in paediatric myocarditis.* Cardiol Young, 2018. **28**(3): p. 377-385.
22. Jue, J., et al., *Cardiac MRI and acute myocarditis.* QJM, 2017. **110**(3): p. 183-184.
23. Olimulder, M.A., J. van Es, and M.A. Galjee, *The importance of cardiac MRI as a diagnostic tool in viral myocarditis-induced cardiomyopathy.* Neth Heart J, 2009. **17**(12): p. 481-6.
24. Bozkurt, B., et al., *Current Diagnostic and Treatment Strategies for Specific Dilated Cardiomyopathies: A Scientific Statement From the American Heart Association.* Circulation, 2016. **134**(23): p. e579-e646.
25. Buslaeva, G.N., *[Clinico-radiographic diagnosis of acquired non-rheumatic myocarditis in children].* Pediatriia, 1981(9): p. 56.
26. Das, S.K., H.T. Colfer, and B. Pitt, *Long-term follow-up of patients with previous myocarditis using radionuclide ventriculography.* Heart Vessels Suppl, 1985. **1**: p. 195-8.
27. Dec, G.W., *How Should We Diagnose Myocarditis, and Is its Recognition Really Clinically Relevant?* J Am Coll Cardiol, 2016. **67**(15): p. 1812-1814.
28. Hawwa, N., Z.B. Popovic, and H.A. Isma'eel, *Discordant Electrocardiogram Left Ventricular Wall Thickness and Strain Findings in Influenza Myocarditis.* Echocardiography, 2015. **32**(12): p. 1880-4.
29. Ichikawa, R., et al., *The follow-up evaluation of electrocardiogram and arrhythmias in children with fulminant myocarditis.* Circ J, 2011. **75**(4): p. 932-8.
30. Lee, J.M., et al., *A case of reversible very low voltage electrocardiogram in fulminant myocarditis.* Korean Circ J, 2013. **43**(8): p. 565-8.
31. Lurz, P., et al., *Diagnostic performance of CMR imaging compared with EMB in patients with suspected myocarditis.* JACC Cardiovasc Imaging, 2012. **5**(5): p. 513-24.
32. Mlczoch, E., et al., *NT-pro BNP in acute childhood myocarditis.* J Pediatr, 2012. **160**(1): p. 178-9.
33. Nasser, N., et al., *NT-proBNP as a marker for persistent cardiac disease in children with history of dilated cardiomyopathy and myocarditis.* Pediatr Cardiol, 2006. **27**(1): p. 87-90.
34. Nensa, F., et al., *Feasibility of FDG-PET in myocarditis: Comparison to CMR using integrated PET/MRI.* J Nucl Cardiol, 2018. **25**(3): p. 785-794.
35. Nieminen, M.S., J. Heikkila, and J. Karjalainen, *Echocardiography in acute infectious myocarditis: relation to clinical and electrocardiographic findings.* Am J Cardiol, 1984. **53**(9): p. 1331-7.
36. O'Connell, J.B., et al., *Gallium-67 imaging in patients with dilated cardiomyopathy and biopsy-proven myocarditis.* Circulation, 1984. **70**(1): p. 58-62.
37. Pinamonti, B., et al., *Echocardiographic findings in myocarditis.* Am J Cardiol, 1988. **62**(4): p. 285-91.

38. Sarda, L., et al., *Myocarditis in patients with clinical presentation of myocardial infarction and normal coronary angiograms.* J Am Coll Cardiol, 2001. **37**(3): p. 786-92.
39. Urena, P.E., et al., *Ejection fraction by radionuclide ventriculography and contrast left ventriculogram. A tale of two techniques. SAVE Investigators. Survival and Ventricular Enlargement.* J Am Coll Cardiol, 1999. **33**(1): p. 180-5.
40. Friedrich, M.G., et al., *Cardiovascular magnetic resonance in myocarditis: A JACC White Paper.* J Am Coll Cardiol, 2009. **53**(17): p. 1475-87.
41. Dennert, R., H.J. Crijns, and S. Heymans, *Acute viral myocarditis.* Eur Heart J, 2008. **29**(17): p. 2073-82.
42. Elliott, P., et al., *Classification of the cardiomyopathies: a position statement from the European Society Of Cardiology Working Group on Myocardial and Pericardial Diseases.* Eur Heart J, 2008. **29**(2): p. 270-6.
43. Liu, P., et al., *Viral myocarditis: balance between viral infection and immune response.* Can J Cardiol, 1996. **12**(10): p. 935-43.
44. Maron, B.J., et al., *Contemporary definitions and classification of the cardiomyopathies: an American Heart Association Scientific Statement from the Council on Clinical Cardiology, Heart Failure and Transplantation Committee; Quality of Care and Outcomes Research and Functional Genomics and Translational Biology Interdisciplinary Working Groups; and Council on Epidemiology and Prevention.* Circulation, 2006. **113**(14): p. 1807-16.
45. Sagar, S., P.P. Liu, and L.T. Cooper, Jr., *Myocarditis.* Lancet, 2012. **379**(9817): p. 738-47.
46. Ansari, A., B.J. Maron, and D.G. Berntson, *Drug-induced toxic myocarditis.* Tex Heart Inst J, 2003. **30**(1): p. 76-9.
47. Franco-Paredes, C., et al., *Cardiac manifestations of parasitic infections part 1: overview and immunopathogenesis.* Clin Cardiol, 2007. **30**(4): p. 195-9.
48. Haddad, F., et al., *Active bacterial myocarditis: a case report and review of the literature.* J Heart Lung Transplant, 2007. **26**(7): p. 745-9.
49. Hidron, A., et al., *Cardiac involvement with parasitic infections.* Clin Microbiol Rev, 2010. **23**(2): p. 324-49.
50. Inayat, F., et al., *New drugs and new toxicities: pembrolizumab-induced myocarditis.* BMJ Case Rep, 2018. **2018**.
51. Laubli, H., et al., *Acute heart failure due to autoimmune myocarditis under pembrolizumab treatment for metastatic melanoma.* J Immunother Cancer, 2015. **3**: p. 11.
52. Schultz, J.C., et al., *Diagnosis and treatment of viral myocarditis.* Mayo Clin Proc, 2009. **84**(11): p. 1001-9.
53. Tayal, U. and S.K. Prasad, *Myocardial remodelling and recovery in dilated cardiomyopathy.* JRSM Cardiovasc Dis, 2017. **6**: p. 2048004017734476.
54. Varricchi, G., et al., *Cardiotoxicity of immune checkpoint inhibitors.* ESMO Open, 2017. **2**(4): p. e000247.
55. Bhatt, A., et al., *Myocarditis along with acute ischaemic cerebellar, pontine and lacunar infarction following viper bite.* BMJ Case Rep, 2013. **2013**.
56. Cihakova, D. and N.R. Rose, *Pathogenesis of myocarditis and dilated cardiomyopathy.* Adv Immunol, 2008. **99**: p. 95-114.

57. Mason, J.W., et al., *A clinical trial of immunosuppressive therapy for myocarditis. The Myocarditis Treatment Trial Investigators.* N Engl J Med, 1995. **333**(5): p. 269-75.
58. Frustaci, A. and C. Chimenti, *Immunosuppressive therapy in myocarditis.* Circ J, 2015. **79**(1): p. 4-7.
59. Frustaci, A., et al., *Immunosuppressive therapy for active lymphocytic myocarditis: virological and immunologic profile of responders versus nonresponders.* Circulation, 2003. **107**(6): p. 857-63.
60. Fairweather, D. and N.R. Rose, *Coxsackievirus-induced myocarditis in mice: a model of autoimmune disease for studying immunotoxicity.* Methods, 2007. **41**(1): p. 118-22.
61. Fairweather, D., K.A. Stafford, and Y.K. Sung, *Update on coxsackievirus B3 myocarditis.* Curr Opin Rheumatol, 2012. **24**(4): p. 401-7.
62. Ginsberg, F. and J.E. Parrillo, *Eosinophilic myocarditis.* Heart Fail Clin, 2005. **1**(3): p. 419-29.
63. Enko, K., et al., *Fulminant eosinophilic myocarditis associated with visceral larva migrans caused by Toxocara canis infection.* Circ J, 2009. **73**(7): p. 1344-8.
64. Pieroni, M., et al., *Clozapine-induced hypersensitivity myocarditis.* Chest, 2004. **126**(5): p. 1703-5.
65. Roehrl, M.H., et al., *Eosinophilic myocarditis in hypereosinophilic syndrome.* Am J Hematol, 2011. **86**(7): p. 607-8.
66. Cooper, L.T., et al., *The role of endomyocardial biopsy in the management of cardiovascular disease: a scientific statement from the American Heart Association, the American College of Cardiology, and the European Society of Cardiology. Endorsed by the Heart Failure Society of America and the Heart Failure Association of the European Society of Cardiology.* J Am Coll Cardiol, 2007. **50**(19): p. 1914-31.
67. Barin, J.G., et al., *Fatal eosinophilic myocarditis develops in the absence of IFN-gamma and IL-17A.* J Immunol, 2013. **191**(8): p. 4038-47.
68. Ekstrom, K., et al., *Long-term outcome and its predictors in giant cell myocarditis.* Eur J Heart Fail, 2016. **18**(12): p. 1452-1458.
69. Cooper, L.T., Jr., G.J. Berry, and R. Shabetai, *Idiopathic giant-cell myocarditis--natural history and treatment. Multicenter Giant Cell Myocarditis Study Group Investigators.* N Engl J Med, 1997. **336**(26): p. 1860-6.
70. Kandolin, R., et al., *Diagnosis, treatment, and outcome of giant-cell myocarditis in the era of combined immunosuppression.* Circ Heart Fail, 2013. **6**(1): p. 15-22.
71. Larsen, B.T., et al., *Atrial giant cell myocarditis: a distinctive clinicopathologic entity.* Circulation, 2013. **127**(1): p. 39-47.
72. Hulten, E., et al., *Cardiac sarcoidosis-state of the art review.* Cardiovasc Diagn Ther, 2016. **6**(1): p. 50-63.
73. Kandolin, R., et al., *Cardiac sarcoidosis: epidemiology, characteristics, and outcome over 25 years in a nationwide study.* Circulation, 2015. **131**(7): p. 624-32.
74. Cooper, L.T., Jr., *Giant cell and granulomatous myocarditis.* Heart Fail Clin, 2005. **1**(3): p. 431-7.
75. Valantine, H.A., et al., *Cardiac sarcoidosis: response to steroids and transplantation.* J Heart Transplant, 1987. **6**(4): p. 244-50.

76. Felker, G.M., et al., *Underlying causes and long-term survival in patients with initially unexplained cardiomyopathy.* N Engl J Med, 2000. **342**(15): p. 1077-84.
77. Herskowitz, A., et al., *Demographic features and prevalence of idiopathic myocarditis in patients undergoing endomyocardial biopsy.* Am J Cardiol, 1993. **71**(11): p. 982-6.
78. Kasper, E.K., et al., *The causes of dilated cardiomyopathy: a clinicopathologic review of 673 consecutive patients.* J Am Coll Cardiol, 1994. **23**(3): p. 586-90.
79. Jefferies, J.L. and J.A. Towbin, *Dilated cardiomyopathy.* Lancet, 2010. **375**(9716): p. 752-62.
80. Neu, N., et al., *Cardiac myosin induces myocarditis in genetically predisposed mice.* J Immunol, 1987. **139**(11): p. 3630-6.
81. Maisch, B., et al., *Diagnostic relevance of humoral and cytotoxic immune reactions in primary and secondary dilated cardiomyopathy.* Am J Cardiol, 1983. **52**(8): p. 1072-8.
82. Maisch, B., et al., *Diagnostic relevance of humoral and cell-mediated immune reactions in patients with acute viral myocarditis.* Clin Exp Immunol, 1982. **48**(3): p. 533-45.
83. Cihakova, D., et al., *Animal models for autoimmune myocarditis and autoimmune thyroiditis.* Methods Mol Med, 2004. **102**: p. 175-93.
84. Waldner, H., et al., *Fulminant spontaneous autoimmunity of the central nervous system in mice transgenic for the myelin proteolipid protein-specific T cell receptor.* Proc Natl Acad Sci U S A, 2000. **97**(7): p. 3412-7.
85. Fontes, J.A., et al., *Complete Freund's adjuvant induces experimental autoimmune myocarditis by enhancing IL-6 production during initiation of the immune response.* Immun Inflamm Dis, 2017. **5**(2): p. 163-176.
86. Huber, S.A., C.J. Gauntt, and P. Sakkinen, *Enteroviruses and myocarditis: viral pathogenesis through replication, cytokine induction, and immunopathogenicity.* Adv Virus Res, 1998. **51**: p. 35-80.
87. Fairweather, D., S. Frisancho-Kiss, and N.R. Rose, *Viruses as adjuvants for autoimmunity: evidence from Coxsackievirus-induced myocarditis.* Rev Med Virol, 2005. **15**(1): p. 17-27.
88. Zhou, N., Y. Yue, and S. Xiong, *Sex Hormone Contributes to Sexually Dimorphic Susceptibility in CVB3-Induced Viral Myocarditis via Modulating IFN-gamma(+) NK Cell Production.* Can J Cardiol, 2018. **34**(4): p. 492-501.
89. Gordon, S., *The macrophage: past, present and future.* Eur J Immunol, 2007. **37 Suppl 1**: p. S9-17.
90. Stefater, J.A., 3rd, et al., *Metchnikoff's policemen: macrophages in development, homeostasis and regeneration.* Trends Mol Med, 2011. **17**(12): p. 743-52.
91. Eom, D.S. and D.M. Parichy, *A macrophage relay for long-distance signaling during postembryonic tissue remodeling.* Science, 2017. **355**(6331): p. 1317-1320.
92. Bechade, C., Y. Cantaut-Belarif, and A. Bessis, *Microglial control of neuronal activity.* Front Cell Neurosci, 2013. **7**: p. 32.
93. Cunningham, C.L., V. Martinez-Cerdeno, and S.C. Noctor, *Microglia regulate the number of neural precursor cells in the developing cerebral cortex.* J Neurosci, 2013. **33**(10): p. 4216-33.
94. Hoshiko, M., et al., *Deficiency of the microglial receptor CX3CR1 impairs postnatal functional development of thalamocortical synapses in the barrel cortex.* J Neurosci, 2012. **32**(43): p. 15106-11.

95. Kettenmann, H., F. Kirchhoff, and A. Verkhratsky, *Microglia: new roles for the synaptic stripper.* Neuron, 2013. **77**(1): p. 10-8.
96. Li, Y., et al., *Reciprocal regulation between resting microglial dynamics and neuronal activity in vivo.* Dev Cell, 2012. **23**(6): p. 1189-202.
97. Paolicelli, R.C., et al., *Synaptic pruning by microglia is necessary for normal brain development.* Science, 2011. **333**(6048): p. 1456-8.
98. Parkhurst, C.N., et al., *Microglia promote learning-dependent synapse formation through brain-derived neurotrophic factor.* Cell, 2013. **155**(7): p. 1596-609.
99. Pascual, O., et al., *Microglia activation triggers astrocyte-mediated modulation of excitatory neurotransmission.* Proc Natl Acad Sci U S A, 2012. **109**(4): p. E197-205.
100. Schafer, D.P., et al., *Microglia sculpt postnatal neural circuits in an activity and complement-dependent manner.* Neuron, 2012. **74**(4): p. 691-705.
101. Schafer, D.P., E.K. Lehrman, and B. Stevens, *The "quad-partite" synapse: microglia-synapse interactions in the developing and mature CNS.* Glia, 2013. **61**(1): p. 24-36.
102. Sierra, A., et al., *Microglia shape adult hippocampal neurogenesis through apoptosis-coupled phagocytosis.* Cell Stem Cell, 2010. **7**(4): p. 483-95.
103. Squarzoni, P., et al., *Microglia modulate wiring of the embryonic forebrain.* Cell Rep, 2014. **8**(5): p. 1271-9.
104. Ueno, M., et al., *Layer V cortical neurons require microglial support for survival during postnatal development.* Nat Neurosci, 2013. **16**(5): p. 543-51.
105. DeFalco, T., et al., *Yolk-sac-derived macrophages regulate fetal testis vascularization and morphogenesis.* Proc Natl Acad Sci U S A, 2014. **111**(23): p. E2384-93.
106. Hutson, J.C., *Interactions between testicular macrophages and Leydig cells.* J Androl, 1998. **19**(4): p. 394-8.
107. Smith, L.B., P.J. O'Shaughnessy, and D. Rebourcet, *Cell-specific ablation in the testis: what have we learned?* Andrology, 2015. **3**(6): p. 1035-49.
108. Godwin, J.W., A.R. Pinto, and N.A. Rosenthal, *Macrophages are required for adult salamander limb regeneration.* Proc Natl Acad Sci U S A, 2013. **110**(23): p. 9415-20.
109. Yona, S. and S. Gordon, *From the Reticuloendothelial to Mononuclear Phagocyte System - The Unaccounted Years.* Front Immunol, 2015. **6**: p. 328.
110. van Furth, R., et al., *[Mononuclear phagocytic system: new classification of macrophages, monocytes and of their cell line].* Bull World Health Organ, 1972. **47**(5): p. 651-8.
111. Tremblay, M.E., R.L. Lowery, and A.K. Majewska, *Microglial interactions with synapses are modulated by visual experience.* PLoS Biol, 2010. **8**(11): p. e1000527.
112. N, A.G., et al., *Phagocytosis imprints heterogeneity in tissue-resident macrophages.* J Exp Med, 2017. **214**(5): p. 1281-1296.
113. Amit, I., D.R. Winter, and S. Jung, *The role of the local environment and epigenetics in shaping macrophage identity and their effect on tissue homeostasis.* Nat Immunol, 2016. **17**(1): p. 18-25.
114. Wynn, T.A., A. Chawla, and J.W. Pollard, *Macrophage biology in development, homeostasis and disease.* Nature, 2013. **496**(7446): p. 445-55.

115. Sheng, J., C. Ruedl, and K. Karjalainen, *Most Tissue-Resident Macrophages Except Microglia Are Derived from Fetal Hematopoietic Stem Cells.* Immunity, 2015. **43**(2): p. 382-93.
116. Schulz, C., et al., *A lineage of myeloid cells independent of Myb and hematopoietic stem cells.* Science, 2012. **336**(6077): p. 86-90.
117. Hoeffel, G., et al., *C-Myb(+) erythro-myeloid progenitor-derived fetal monocytes give rise to adult tissue-resident macrophages.* Immunity, 2015. **42**(4): p. 665-78.
118. Hashimoto, D., et al., *Tissue-resident macrophages self-maintain locally throughout adult life with minimal contribution from circulating monocytes.* Immunity, 2013. **38**(4): p. 792-804.
119. Epelman, S., et al., *Embryonic and adult-derived resident cardiac macrophages are maintained through distinct mechanisms at steady state and during inflammation.* Immunity, 2014. **40**(1): p. 91-104.
120. Moore, M.A. and D. Metcalf, *Ontogeny of the haemopoietic system: yolk sac origin of in vivo and in vitro colony forming cells in the developing mouse embryo.* Br J Haematol, 1970. **18**(3): p. 279-96.
121. Cline, M.J. and M.A. Moore, *Embryonic origin of the mouse macrophage.* Blood, 1972. **39**(6): p. 842-9.
122. McGrath, K.E., et al., *Circulation is established in a stepwise pattern in the mammalian embryo.* Blood, 2003. **101**(5): p. 1669-76.
123. Palis, J., et al., *Development of erythroid and myeloid progenitors in the yolk sac and embryo proper of the mouse.* Development, 1999. **126**(22): p. 5073-84.
124. Kasaai, B., et al., *Erythro-myeloid progenitors can differentiate from endothelial cells and modulate embryonic vascular remodeling.* Sci Rep, 2017. **7**: p. 43817.
125. Mass, E., et al., *Specification of tissue-resident macrophages during organogenesis.* Science, 2016. **353**(6304).
126. Takahashi, K., F. Yamamura, and M. Naito, *Differentiation, maturation, and proliferation of macrophages in the mouse yolk sac: a light-microscopic, enzyme-cytochemical, immunohistochemical, and ultrastructural study.* J Leukoc Biol, 1989. **45**(2): p. 87-96.
127. Gomez Perdiguero, E. and F. Geissmann, *Myb-independent macrophages: a family of cells that develops with their tissue of residence and is involved in its homeostasis.* Cold Spring Harb Symp Quant Biol, 2013. **78**: p. 91-100.
128. Sandberg, M.L., et al., *c-Myb and p300 regulate hematopoietic stem cell proliferation and differentiation.* Dev Cell, 2005. **8**(2): p. 153-66.
129. Sumner, R., et al., *Initiation of adult myelopoiesis can occur in the absence of c-Myb whereas subsequent development is strictly dependent on the transcription factor.* Oncogene, 2000. **19**(30): p. 3335-42.
130. Kierdorf, K., et al., *Microglia emerge from erythromyeloid precursors via Pu.1- and Irf8-dependent pathways.* Nat Neurosci, 2013. **16**(3): p. 273-80.
131. Perdiguero, E.G., et al., *The Origin of Tissue-Resident Macrophages: When an Erythro-myeloid Progenitor Is an Erythro-myeloid Progenitor.* Immunity, 2015. **43**(6): p. 1023-4.
132. Rantakari, P., et al., *Fetal liver endothelium regulates the seeding of tissue-resident macrophages.* Nature, 2016. **538**(7625): p. 392-396.

133. Tamoutounour, S., et al., *Origins and functional specialization of macrophages and of conventional and monocyte-derived dendritic cells in mouse skin.* Immunity, 2013. **39**(5): p. 925-38.
134. Zigmond, E., et al., *Ly6C hi monocytes in the inflamed colon give rise to proinflammatory effector cells and migratory antigen-presenting cells.* Immunity, 2012. **37**(6): p. 1076-90.
135. Medvinsky, A. and E. Dzierzak, *Definitive hematopoiesis is autonomously initiated by the AGM region.* Cell, 1996. **86**(6): p. 897-906.
136. Yokomizo, T. and E. Dzierzak, *Three-dimensional cartography of hematopoietic clusters in the vasculature of whole mouse embryos.* Development, 2010. **137**(21): p. 3651-61.
137. Kieusseian, A., et al., *Immature hematopoietic stem cells undergo maturation in the fetal liver.* Development, 2012. **139**(19): p. 3521-30.
138. Kumaravelu, P., et al., *Quantitative developmental anatomy of definitive haematopoietic stem cells/long-term repopulating units (HSC/RUs): role of the aorta-gonad-mesonephros (AGM) region and the yolk sac in colonisation of the mouse embryonic liver.* Development, 2002. **129**(21): p. 4891-9.
139. Bain, C.C., et al., *Constant replenishment from circulating monocytes maintains the macrophage pool in the intestine of adult mice.* Nat Immunol, 2014. **15**(10): p. 929-937.
140. Audzevich, T., et al., *Pre/pro-B cells generate macrophage populations during homeostasis and inflammation.* Proc Natl Acad Sci U S A, 2017. **114**(20): p. E3954-E3963.
141. Ginhoux, F. and M. Guilliams, *Tissue-Resident Macrophage Ontogeny and Homeostasis.* Immunity, 2016. **44**(3): p. 439-449.
142. Alliot, F., I. Godin, and B. Pessac, *Microglia derive from progenitors, originating from the yolk sac, and which proliferate in the brain.* Brain Res Dev Brain Res, 1999. **117**(2): p. 145-52.
143. Alliot, F., et al., *Microglial progenitors with a high proliferative potential in the embryonic and adult mouse brain.* Proc Natl Acad Sci U S A, 1991. **88**(4): p. 1541-5.
144. Bruttger, J., et al., *Genetic Cell Ablation Reveals Clusters of Local Self-Renewing Microglia in the Mammalian Central Nervous System.* Immunity, 2015. **43**(1): p. 92-106.
145. Gomez Perdiguero, E., et al., *Tissue-resident macrophages originate from yolk-sac-derived erythro-myeloid progenitors.* Nature, 2015. **518**(7540): p. 547-51.
146. Scott, C.L., et al., *Bone marrow-derived monocytes give rise to self-renewing and fully differentiated Kupffer cells.* Nat Commun, 2016. **7**: p. 10321.
147. Yona, S., et al., *Fate mapping reveals origins and dynamics of monocytes and tissue macrophages under homeostasis.* Immunity, 2013. **38**(1): p. 79-91.
148. Ensan, S., et al., *Self-renewing resident arterial macrophages arise from embryonic CX3CR1(+) precursors and circulating monocytes immediately after birth.* Nat Immunol, 2016. **17**(2): p. 159-68.
149. Molawi, K., et al., *Progressive replacement of embryo-derived cardiac macrophages with age.* J Exp Med, 2014. **211**(11): p. 2151-8.
150. Leid, J., et al., *Primitive Embryonic Macrophages are Required for Coronary Development and Maturation.* Circ Res, 2016. **118**(10): p. 1498-511.
151. Gautier, E.L., et al., *Gene-expression profiles and transcriptional regulatory pathways that underlie the identity and diversity of mouse tissue macrophages.* Nat Immunol, 2012. **13**(11): p. 1118-28.

152. Gosselin, D., et al., *Environment drives selection and function of enhancers controlling tissue-specific macrophage identities.* Cell, 2014. **159**(6): p. 1327-40.
153. Lavin, Y., et al., *Tissue-resident macrophage enhancer landscapes are shaped by the local microenvironment.* Cell, 2014. **159**(6): p. 1312-26.
154. Haldar, M., et al., *Heme-mediated SPI-C induction promotes monocyte differentiation into iron-recycling macrophages.* Cell, 2014. **156**(6): p. 1223-1234.
155. Gautier, E.L., et al., *Gata6 regulates aspartoacylase expression in resident peritoneal macrophages and controls their survival.* J Exp Med, 2014. **211**(8): p. 1525-31.
156. Okabe, Y. and R. Medzhitov, *Tissue-specific signals control reversible program of localization and functional polarization of macrophages.* Cell, 2014. **157**(4): p. 832-44.
157. Rosas, M., et al., *The transcription factor Gata6 links tissue macrophage phenotype and proliferative renewal.* Science, 2014. **344**(6184): p. 645-648.
158. Ghosn, E.E., et al., *Two physically, functionally, and developmentally distinct peritoneal macrophage subsets.* Proc Natl Acad Sci U S A, 2010. **107**(6): p. 2568-73.
159. Wang, Z., et al., *Gut flora metabolism of phosphatidylcholine promotes cardiovascular disease.* Nature, 2011. **472**(7341): p. 57-63.
160. Van den Bossche, J., L.A. O'Neill, and D. Menon, *Macrophage Immunometabolism: Where Are We (Going)?* Trends Immunol, 2017. **38**(6): p. 395-406.
161. Chen, H.H., et al., *IRF2BP2 Reduces Macrophage Inflammation and Susceptibility to Atherosclerosis.* Circ Res, 2015. **117**(8): p. 671-83.
162. Erbilgin, A., et al., *Identification of CAD candidate genes in GWAS loci and their expression in vascular cells.* J Lipid Res, 2013. **54**(7): p. 1894-905.
163. Wu, X.Q., et al., *Emerging role of microRNAs in regulating macrophage activation and polarization in immune response and inflammation.* Immunology, 2016. **148**(3): p. 237-48.
164. Capucha, T., et al., *Distinct Murine Mucosal Langerhans Cell Subsets Develop from Pre-dendritic Cells and Monocytes.* Immunity, 2015. **43**(2): p. 369-81.
165. Garber, M., et al., *A high-throughput chromatin immunoprecipitation approach reveals principles of dynamic gene regulation in mammals.* Mol Cell, 2012. **47**(5): p. 810-22.
166. Heinz, S., et al., *Simple combinations of lineage-determining transcription factors prime cis-regulatory elements required for macrophage and B cell identities.* Mol Cell, 2010. **38**(4): p. 576-89.
167. Ostuni, R. and G. Natoli, *Lineages, cell types and functional states: a genomic view.* Curr Opin Cell Biol, 2013. **25**(6): p. 759-64.
168. Winter, D.R. and I. Amit, *The role of chromatin dynamics in immune cell development.* Immunol Rev, 2014. **261**(1): p. 9-22.
169. Geissmann, F., S. Jung, and D.R. Littman, *Blood monocytes consist of two principal subsets with distinct migratory properties.* Immunity, 2003. **19**(1): p. 71-82.
170. Sunderkotter, C., et al., *Subpopulations of mouse blood monocytes differ in maturation stage and inflammatory response.* J Immunol, 2004. **172**(7): p. 4410-7.
171. Hilgendorf, I., et al., *Ly-6Chigh monocytes depend on Nr4a1 to balance both inflammatory and reparative phases in the infarcted myocardium.* Circ Res, 2014. **114**(10): p. 1611-22.

172. Palframan, R.T., et al., *Inflammatory chemokine transport and presentation in HEV: a remote control mechanism for monocyte recruitment to lymph nodes in inflamed tissues.* J Exp Med, 2001. **194**(9): p. 1361-73.
173. Varga, T., et al., *Tissue LyC6- macrophages are generated in the absence of circulating LyC6- monocytes and Nur77 in a model of muscle regeneration.* J Immunol, 2013. **191**(11): p. 5695-701.
174. Auffray, C., et al., *Monitoring of blood vessels and tissues by a population of monocytes with patrolling behavior.* Science, 2007. **317**(5838): p. 666-70.
175. Arnold, L., et al., *Inflammatory monocytes recruited after skeletal muscle injury switch into antiinflammatory macrophages to support myogenesis.* J Exp Med, 2007. **204**(5): p. 1057-69.
176. Carlin, L.M., et al., *Nr4a1-dependent Ly6C(low) monocytes monitor endothelial cells and orchestrate their disposal.* Cell, 2013. **153**(2): p. 362-75.
177. Olingy, C.E., et al., *Non-classical monocytes are biased progenitors of wound healing macrophages during soft tissue injury.* Sci Rep, 2017. **7**(1): p. 447.
178. Ancuta, P., et al., *Transcriptional profiling reveals developmental relationship and distinct biological functions of CD16+ and CD16- monocyte subsets.* BMC Genomics, 2009. **10**: p. 403.
179. Boyette, L.B., et al., *Phenotype, function, and differentiation potential of human monocyte subsets.* PLoS One, 2017. **12**(4): p. e0176460.
180. Cros, J., et al., *Human CD14dim monocytes patrol and sense nucleic acids and viruses via TLR7 and TLR8 receptors.* Immunity, 2010. **33**(3): p. 375-86.
181. Ingersoll, M.A., et al., *Monocyte trafficking in acute and chronic inflammation.* Trends Immunol, 2011. **32**(10): p. 470-7.
182. Wong, K.L., et al., *The three human monocyte subsets: implications for health and disease.* Immunol Res, 2012. **53**(1-3): p. 41-57.
183. Ziegler-Heitbrock, L., et al., *Nomenclature of monocytes and dendritic cells in blood.* Blood, 2010. **116**(16): p. e74-80.
184. Robbins, C.S., et al., *Extramedullary hematopoiesis generates Ly-6C(high) monocytes that infiltrate atherosclerotic lesions.* Circulation, 2012. **125**(2): p. 364-74.
185. Becker, A.J., C.E. Mc, and J.E. Till, *Cytological demonstration of the clonal nature of spleen colonies derived from transplanted mouse marrow cells.* Nature, 1963. **197**: p. 452-4.
186. Siminovitch, L., E.A. McCulloch, and J.E. Till, *The Distribution of Colony-Forming Cells among Spleen Colonies.* J Cell Comp Physiol, 1963. **62**: p. 327-36.
187. Spangrude, G.J., S. Heimfeld, and I.L. Weissman, *Purification and characterization of mouse hematopoietic stem cells.* Science, 1988. **241**(4861): p. 58-62.
188. Till, J.E. and C.E. Mc, *A direct measurement of the radiation sensitivity of normal mouse bone marrow cells.* Radiat Res, 1961. **14**: p. 213-22.
189. Wu, A.M., et al., *Cytological evidence for a relationship between normal hemotopoietic colony-forming cells and cells of the lymphoid system.* J Exp Med, 1968. **127**(3): p. 455-64.
190. Morrison, S.J. and I.L. Weissman, *The long-term repopulating subset of hematopoietic stem cells is deterministic and isolatable by phenotype.* Immunity, 1994. **1**(8): p. 661-73.

191. Akashi, K., et al., *A clonogenic common myeloid progenitor that gives rise to all myeloid lineages.* Nature, 2000. **404**(6774): p. 193-7.
192. Karsunky, H., et al., *Flk2+ common lymphoid progenitors possess equivalent differentiation potential for the B and T lineages.* Blood, 2008. **111**(12): p. 5562-70.
193. Kondo, M., I.L. Weissman, and K. Akashi, *Identification of clonogenic common lymphoid progenitors in mouse bone marrow.* Cell, 1997. **91**(5): p. 661-72.
194. Serwold, T., L.I. Ehrlich, and I.L. Weissman, *Reductive isolation from bone marrow and blood implicates common lymphoid progenitors as the major source of thymopoiesis.* Blood, 2009. **113**(4): p. 807-15.
195. Nakorn, T.N., T. Miyamoto, and I.L. Weissman, *Characterization of mouse clonogenic megakaryocyte progenitors.* Proc Natl Acad Sci U S A, 2003. **100**(1): p. 205-10.
196. Pronk, C.J., et al., *Elucidation of the phenotypic, functional, and molecular topography of a myeloerythroid progenitor cell hierarchy.* Cell Stem Cell, 2007. **1**(4): p. 428-42.
197. Fogg, D.K., et al., *A clonogenic bone marrow progenitor specific for macrophages and dendritic cells.* Science, 2006. **311**(5757): p. 83-7.
198. Hettinger, J., et al., *Origin of monocytes and macrophages in a committed progenitor.* Nat Immunol, 2013. **14**(8): p. 821-30.
199. Laslo, P., et al., *Multilineage transcriptional priming and determination of alternate hematopoietic cell fates.* Cell, 2006. **126**(4): p. 755-66.
200. DeKoter, R.P., J.C. Walsh, and H. Singh, *PU.1 regulates both cytokine-dependent proliferation and differentiation of granulocyte/macrophage progenitors.* EMBO J, 1998. **17**(15): p. 4456-68.
201. Iwasaki, H. and K. Akashi, *Myeloid lineage commitment from the hematopoietic stem cell.* Immunity, 2007. **26**(6): p. 726-40.
202. Nutt, S.L., et al., *Dynamic regulation of PU.1 expression in multipotent hematopoietic progenitors.* J Exp Med, 2005. **201**(2): p. 221-31.
203. Scott, E.W., et al., *Requirement of transcription factor PU.1 in the development of multiple hematopoietic lineages.* Science, 1994. **265**(5178): p. 1573-7.
204. Friedman, A.D., *Transcriptional control of granulocyte and monocyte development.* Oncogene, 2007. **26**(47): p. 6816-28.
205. Friedman, A.D., *Transcriptional regulation of myelopoiesis.* Int J Hematol, 2002. **75**(5): p. 466-72.
206. Ramji, D.P. and P. Foka, *CCAAT/enhancer-binding proteins: structure, function and regulation.* Biochem J, 2002. **365**(Pt 3): p. 561-75.
207. Jones, L.C., et al., *Expression of C/EBPbeta from the C/ebpalpha gene locus is sufficient for normal hematopoiesis in vivo.* Blood, 2002. **99**(6): p. 2032-6.
208. Tamura, A., et al., *Accelerated apoptosis of peripheral blood monocytes in Cebpb-deficient mice.* Biochem Biophys Res Commun, 2015. **464**(2): p. 654-8.
209. Wang, D., et al., *C/EBPalpha directs monocytic commitment of primary myeloid progenitors.* Blood, 2006. **108**(4): p. 1223-9.
210. Zhang, D.E., et al., *Absence of granulocyte colony-stimulating factor signaling and neutrophil development in CCAAT enhancer binding protein alpha-deficient mice.* Proc Natl Acad Sci U S A, 1997. **94**(2): p. 569-74.

211. Laiosa, C.V., et al., *Reprogramming of committed T cell progenitors to macrophages and dendritic cells by C/EBP alpha and PU.1 transcription factors.* Immunity, 2006. **25**(5): p. 731-44.
212. Xie, H., et al., *Stepwise reprogramming of B cells into macrophages.* Cell, 2004. **117**(5): p. 663-76.
213. Wang, H., et al., *IRF8 regulates B-cell lineage specification, commitment, and differentiation.* Blood, 2008. **112**(10): p. 4028-38.
214. Tamura, T., et al., *Identification of target genes and a unique cis element regulated by IRF-8 in developing macrophages.* Blood, 2005. **106**(6): p. 1938-47.
215. Tsujimura, H., et al., *IFN consensus sequence binding protein/IFN regulatory factor-8 guides bone marrow progenitor cells toward the macrophage lineage.* J Immunol, 2002. **169**(3): p. 1261-9.
216. Kurotaki, D., et al., *Essential role of the IRF8-KLF4 transcription factor cascade in murine monocyte differentiation.* Blood, 2013. **121**(10): p. 1839-49.
217. Alder, J.K., et al., *Kruppel-like factor 4 is essential for inflammatory monocyte differentiation in vivo.* J Immunol, 2008. **180**(8): p. 5645-52.
218. Hanna, R.N., et al., *The transcription factor NR4A1 (Nur77) controls bone marrow differentiation and the survival of Ly6C- monocytes.* Nat Immunol, 2011. **12**(8): p. 778-85.
219. Mullican, S.E., et al., *Abrogation of nuclear receptors Nr4a3 and Nr4a1 leads to development of acute myeloid leukemia.* Nat Med, 2007. **13**(6): p. 730-5.
220. Collin, M., R. Dickinson, and V. Bigley, *Haematopoietic and immune defects associated with GATA2 mutation.* Br J Haematol, 2015. **169**(2): p. 173-87.
221. Dickinson, R.E., et al., *Exome sequencing identifies GATA-2 mutation as the cause of dendritic cell, monocyte, B and NK lymphoid deficiency.* Blood, 2011. **118**(10): p. 2656-8.
222. Huang, G., et al., *PU.1 is a major downstream target of AML1 (RUNX1) in adult mouse hematopoiesis.* Nat Genet, 2008. **40**(1): p. 51-60.
223. Ichikawa, M., et al., *Runx1/AML-1 ranks as a master regulator of adult hematopoiesis.* Cell Cycle, 2004. **3**(6): p. 722-4.
224. Nandakumar, S.K., et al., *Low-level GATA2 overexpression promotes myeloid progenitor self-renewal and blocks lymphoid differentiation in mice.* Exp Hematol, 2015. **43**(7): p. 565-77 e1-10.
225. Okuda, T., et al., *AML1, the target of multiple chromosomal translocations in human leukemia, is essential for normal fetal liver hematopoiesis.* Cell, 1996. **84**(2): p. 321-30.
226. Suzuki, E., et al., *The transcription factor Fli-1 regulates monocyte, macrophage and dendritic cell development in mice.* Immunology, 2013. **139**(3): p. 318-27.
227. Cecchini, M.G., et al., *Role of colony stimulating factor-1 in the establishment and regulation of tissue macrophages during postnatal development of the mouse.* Development, 1994. **120**(6): p. 1357-72.
228. Dai, X.M., et al., *Targeted disruption of the mouse colony-stimulating factor 1 receptor gene results in osteopetrosis, mononuclear phagocyte deficiency, increased primitive progenitor cell frequencies, and reproductive defects.* Blood, 2002. **99**(1): p. 111-20.

229. Wiktor-Jedrzejczak, W. and S. Gordon, *Cytokine regulation of the macrophage (M phi) system studied using the colony stimulating factor-1-deficient op/op mouse.* Physiol Rev, 1996. **76**(4): p. 927-47.
230. Shaposhnik, Z., X. Wang, and A.J. Lusis, *Arterial colony stimulating factor-1 influences atherosclerotic lesions by regulating monocyte migration and apoptosis.* J Lipid Res, 2010. **51**(7): p. 1962-70.
231. Tagliani, E., et al., *Coordinate regulation of tissue macrophage and dendritic cell population dynamics by CSF-1.* J Exp Med, 2011. **208**(9): p. 1901-16.
232. Landsman, L., et al., *CX3CR1 is required for monocyte homeostasis and atherogenesis by promoting cell survival.* Blood, 2009. **113**(4): p. 963-72.
233. Nguyen, K.D., et al., *Circadian gene Bmal1 regulates diurnal oscillations of Ly6C(hi) inflammatory monocytes.* Science, 2013. **341**(6153): p. 1483-8.
234. Alibhai, F.J., et al., *Short-term disruption of diurnal rhythms after murine myocardial infarction adversely affects long-term myocardial structure and function.* Circ Res, 2014. **114**(11): p. 1713-22.
235. Ginhoux, F. and S. Jung, *Monocytes and macrophages: developmental pathways and tissue homeostasis.* Nat Rev Immunol, 2014. **14**(6): p. 392-404.
236. Kawamura, S., et al., *Identification of a Human Clonogenic Progenitor with Strict Monocyte Differentiation Potential: A Counterpart of Mouse cMoPs.* Immunity, 2017. **46**(5): p. 835-848 e4.
237. Lee, J., et al., *Restricted dendritic cell and monocyte progenitors in human cord blood and bone marrow.* J Exp Med, 2015. **212**(3): p. 385-99.
238. Merad, M., et al., *The dendritic cell lineage: ontogeny and function of dendritic cells and their subsets in the steady state and the inflamed setting.* Annu Rev Immunol, 2013. **31**: p. 563-604.
239. Seita, J. and I.L. Weissman, *Hematopoietic stem cell: self-renewal versus differentiation.* Wiley Interdiscip Rev Syst Biol Med, 2010. **2**(6): p. 640-53.
240. Savarese, G. and L.H. Lund, *Global Public Health Burden of Heart Failure.* Card Fail Rev, 2017. **3**(1): p. 7-11.
241. Yancy, C.W., et al., *2013 ACCF/AHA guideline for the management of heart failure: a report of the American College of Cardiology Foundation/American Heart Association Task Force on Practice Guidelines.* J Am Coll Cardiol, 2013. **62**(16): p. e147-239.
242. Shahid, F., G.Y.H. Lip, and E. Shantsila, *Role of Monocytes in Heart Failure and Atrial Fibrillation.* J Am Heart Assoc, 2018. **7**(3).
243. Essop, M.R. and V.T. Nkomo, *Rheumatic and nonrheumatic valvular heart disease: epidemiology, management, and prevention in Africa.* Circulation, 2005. **112**(23): p. 3584-91.
244. Dutta, P. and M. Nahrendorf, *Monocytes in myocardial infarction.* Arterioscler Thromb Vasc Biol, 2015. **35**(5): p. 1066-70.
245. Nahrendorf, M., et al., *The healing myocardium sequentially mobilizes two monocyte subsets with divergent and complementary functions.* J Exp Med, 2007. **204**(12): p. 3037-47.
246. Wrigley, B.J., et al., *CD14++CD16+ monocytes in patients with acute ischaemic heart failure.* Eur J Clin Invest, 2013. **43**(2): p. 121-30.

247. Wu, L., et al., *Cardiac fibroblasts mediate IL-17A-driven inflammatory dilated cardiomyopathy.* J Exp Med, 2014. **211**(7): p. 1449-64.
248. Maekawa, Y., et al., *Prognostic significance of peripheral monocytosis after reperfused acute myocardial infarction:a possible role for left ventricular remodeling.* J Am Coll Cardiol, 2002. **39**(2): p. 241-6.
249. Pinto, A.R., et al., *Revisiting Cardiac Cellular Composition.* Circ Res, 2016. **118**(3): p. 400-9.
250. Dewald, O., et al., *CCL2/Monocyte Chemoattractant Protein-1 regulates inflammatory responses critical to healing myocardial infarcts.* Circ Res, 2005. **96**(8): p. 881-9.
251. Reiter, R., et al., *Circadian dependence of infarct size and left ventricular function after ST elevation myocardial infarction.* Circ Res, 2012. **110**(1): p. 105-10.
252. Zouggari, Y., et al., *B lymphocytes trigger monocyte mobilization and impair heart function after acute myocardial infarction.* Nat Med, 2013. **19**(10): p. 1273-80.
253. Horckmans, M., et al., *Neutrophils orchestrate post-myocardial infarction healing by polarizing macrophages towards a reparative phenotype.* Eur Heart J, 2017. **38**(3): p. 187-197.
254. Frangogiannis, N.G., C.W. Smith, and M.L. Entman, *The inflammatory response in myocardial infarction.* Cardiovasc Res, 2002. **53**(1): p. 31-47.
255. Ishibashi, M., et al., *Critical role of monocyte chemoattractant protein-1 receptor CCR2 on monocytes in hypertension-induced vascular inflammation and remodeling.* Circ Res, 2004. **94**(9): p. 1203-10.
256. Swirski, F.K. and M. Nahrendorf, *Leukocyte behavior in atherosclerosis, myocardial infarction, and heart failure.* Science, 2013. **339**(6116): p. 161-6.
257. Frangogiannis, N.G., *Regulation of the inflammatory response in cardiac repair.* Circ Res, 2012. **110**(1): p. 159-73.
258. van Amerongen, M.J., et al., *Macrophage depletion impairs wound healing and increases left ventricular remodeling after myocardial injury in mice.* Am J Pathol, 2007. **170**(3): p. 818-29.
259. Frantz, S., et al., *Monocytes/macrophages prevent healing defects and left ventricular thrombus formation after myocardial infarction.* FASEB J, 2013. **27**(3): p. 871-81.
260. Frangogiannis, N.G., et al., *Critical role of monocyte chemoattractant protein-1/CC chemokine ligand 2 in the pathogenesis of ischemic cardiomyopathy.* Circulation, 2007. **115**(5): p. 584-92.
261. van Loon, R.B., et al., *Left ventricular remodeling after acute myocardial infarction: the influence of viability and revascularization - an echocardiographic substudy of the VIAMI-trial.* Trials, 2014. **15**: p. 329.
262. Sager, H.B., et al., *Proliferation and Recruitment Contribute to Myocardial Macrophage Expansion in Chronic Heart Failure.* Circ Res, 2016. **119**(7): p. 853-64.
263. Chen, B. and N.G. Frangogiannis, *Macrophages in the Remodeling Failing Heart.* Circ Res, 2016. **119**(7): p. 776-8.
264. Benjamin, E.J., et al., *Heart Disease and Stroke Statistics-2018 Update: A Report From the American Heart Association.* Circulation, 2018. **137**(12): p. e67-e492.
265. Owan, T.E., et al., *Trends in prevalence and outcome of heart failure with preserved ejection fraction.* N Engl J Med, 2006. **355**(3): p. 251-9.

266. Ather, S., et al., *Impact of noncardiac comorbidities on morbidity and mortality in a predominantly male population with heart failure and preserved versus reduced ejection fraction.* J Am Coll Cardiol, 2012. **59**(11): p. 998-1005.
267. Vasan, R.S., et al., *Congestive heart failure in subjects with normal versus reduced left ventricular ejection fraction: prevalence and mortality in a population-based cohort.* J Am Coll Cardiol, 1999. **33**(7): p. 1948-55.
268. Cihakova, D., *Interleukin-10 stiffens the heart.* J Exp Med, 2018. **215**(2): p. 379-381.
269. Brubaker, P.H. and D.W. Kitzman, *Chronotropic incompetence: causes, consequences, and management.* Circulation, 2011. **123**(9): p. 1010-20.
270. Hulsmans, M., et al., *Cardiac macrophages promote diastolic dysfunction.* J Exp Med, 2018. **215**(2): p. 423-440.
271. Troidl, C., et al., *Classically and alternatively activated macrophages contribute to tissue remodelling after myocardial infarction.* J Cell Mol Med, 2009. **13**(9B): p. 3485-96.
272. Dutta, P., et al., *Myocardial infarction accelerates atherosclerosis.* Nature, 2012. **487**(7407): p. 325-9.
273. Leuschner, F., et al., *Angiotensin-converting enzyme inhibition prevents the release of monocytes from their splenic reservoir in mice with myocardial infarction.* Circ Res, 2010. **107**(11): p. 1364-73.
274. Swirski, F.K., et al., *Identification of splenic reservoir monocytes and their deployment to inflammatory sites.* Science, 2009. **325**(5940): p. 612-6.
275. Leuschner, F., et al., *Therapeutic siRNA silencing in inflammatory monocytes in mice.* Nat Biotechnol, 2011. **29**(11): p. 1005-10.
276. Majmudar, M.D., et al., *Monocyte-directed RNAi targeting CCR2 improves infarct healing in atherosclerosis-prone mice.* Circulation, 2013. **127**(20): p. 2038-46.
277. Udalova, I.A., A. Mantovani, and M. Feldmann, *Macrophage heterogeneity in the context of rheumatoid arthritis.* Nat Rev Rheumatol, 2016. **12**(8): p. 472-85.
278. Courties, G., et al., *In vivo silencing of the transcription factor IRF5 reprograms the macrophage phenotype and improves infarct healing.* J Am Coll Cardiol, 2014. **63**(15): p. 1556-66.
279. Mouton, A.J., et al., *Mapping macrophage polarization over the myocardial infarction time continuum.* Basic Res Cardiol, 2018. **113**(4): p. 26.
280. Tannahill, G.M., et al., *Succinate is an inflammatory signal that induces IL-1beta through HIF-1alpha.* Nature, 2013. **496**(7444): p. 238-42.
281. Zhang, S., et al., *Efferocytosis Fuels Requirements of Fatty Acid Oxidation and the Electron Transport Chain to Polarize Macrophages for Tissue Repair.* Cell Metab, 2019. **29**(2): p. 443-456 e5.
282. Lloyd-Jones, D., et al., *Executive summary: heart disease and stroke statistics--2010 update: a report from the American Heart Association.* Circulation, 2010. **121**(7): p. 948-54.
283. Moore, K.J. and I. Tabas, *Macrophages in the pathogenesis of atherosclerosis.* Cell, 2011. **145**(3): p. 341-55.
284. Ross, R., *Atherosclerosis--an inflammatory disease.* N Engl J Med, 1999. **340**(2): p. 115-26.

285. Fogelstrand, P. and J. Boren, *Retention of atherogenic lipoproteins in the artery wall and its role in atherogenesis.* Nutr Metab Cardiovasc Dis, 2012. **22**(1): p. 1-7.
286. Williams, K.J. and I. Tabas, *The response-to-retention hypothesis of early atherogenesis.* Arterioscler Thromb Vasc Biol, 1995. **15**(5): p. 551-61.
287. Groh, L., et al., *Monocyte and macrophage immunometabolism in atherosclerosis.* Semin Immunopathol, 2018. **40**(2): p. 203-214.
288. Virmani, R., et al., *Vulnerable plaque: the pathology of unstable coronary lesions.* J Interv Cardiol, 2002. **15**(6): p. 439-46.
289. Tabas, I. and A.H. Lichtman, *Monocyte-Macrophages and T Cells in Atherosclerosis.* Immunity, 2017. **47**(4): p. 621-634.
290. Breslow, J.L., *Mouse models of atherosclerosis.* Science, 1996. **272**(5262): p. 685-8.
291. Rosenfeld, M.E., et al., *Animal models of spontaneous plaque rupture: the holy grail of experimental atherosclerosis research.* Curr Atheroscler Rep, 2002. **4**(3): p. 238-42.
292. Murphy, A.J. and A.R. Tall, *Disordered haematopoiesis and athero-thrombosis.* Eur Heart J, 2016. **37**(14): p. 1113-21.
293. Olivares, R., P. Ducimetiere, and J.R. Claude, *Monocyte count: a risk factor for coronary heart disease?* Am J Epidemiol, 1993. **137**(1): p. 49-53.
294. Glass, C.K. and J.L. Witztum, *Atherosclerosis. the road ahead.* Cell, 2001. **104**(4): p. 503-16.
295. Mestas, J. and K. Ley, *Monocyte-endothelial cell interactions in the development of atherosclerosis.* Trends Cardiovasc Med, 2008. **18**(6): p. 228-32.
296. Rahman, K., et al., *Inflammatory Ly6Chi monocytes and their conversion to M2 macrophages drive atherosclerosis regression.* J Clin Invest, 2017. **127**(8): p. 2904-2915.
297. Jakubzick, C.V., G.J. Randolph, and P.M. Henson, *Monocyte differentiation and antigen-presenting functions.* Nat Rev Immunol, 2017. **17**(6): p. 349-362.
298. Boring, L., et al., *Decreased lesion formation in CCR2-/- mice reveals a role for chemokines in the initiation of atherosclerosis.* Nature, 1998. **394**(6696): p. 894-7.
299. Tacke, F., et al., *Monocyte subsets differentially employ CCR2, CCR5, and CX3CR1 to accumulate within atherosclerotic plaques.* J Clin Invest, 2007. **117**(1): p. 185-94.
300. Moore, K.J., F.J. Sheedy, and E.A. Fisher, *Macrophages in atherosclerosis: a dynamic balance.* Nat Rev Immunol, 2013. **13**(10): p. 709-21.
301. Robbins, C.S., et al., *Local proliferation dominates lesional macrophage accumulation in atherosclerosis.* Nat Med, 2013. **19**(9): p. 1166-72.
302. Tabas, I., *Macrophage death and defective inflammation resolution in atherosclerosis.* Nat Rev Immunol, 2010. **10**(1): p. 36-46.
303. Henson, P.M., D.L. Bratton, and V.A. Fadok, *Apoptotic cell removal.* Curr Biol, 2001. **11**(19): p. R795-805.
304. Sather, S., et al., *A soluble form of the Mer receptor tyrosine kinase inhibits macrophage clearance of apoptotic cells and platelet aggregation.* Blood, 2007. **109**(3): p. 1026-33.
305. Yvan-Charvet, L., et al., *ABCA1 and ABCG1 protect against oxidative stress-induced macrophage apoptosis during efferocytosis.* Circ Res, 2010. **106**(12): p. 1861-9.
306. Galis, Z.S., et al., *Increased expression of matrix metalloproteinases and matrix degrading activity in vulnerable regions of human atherosclerotic plaques.* J Clin Invest, 1994. **94**(6): p. 2493-503.

307. Deguchi, J.O., et al., *Matrix metalloproteinase-13/collagenase-3 deletion promotes collagen accumulation and organization in mouse atherosclerotic plaques.* Circulation, 2005. **112**(17): p. 2708-15.
308. Schneider, F., et al., *Matrix-metalloproteinase-14 deficiency in bone-marrow-derived cells promotes collagen accumulation in mouse atherosclerotic plaques.* Circulation, 2008. **117**(7): p. 931-9.
309. Boyle, J.J., P.L. Weissberg, and M.R. Bennett, *Tumor necrosis factor-alpha promotes macrophage-induced vascular smooth muscle cell apoptosis by direct and autocrine mechanisms.* Arterioscler Thromb Vasc Biol, 2003. **23**(9): p. 1553-8.
310. Peled, M. and E.A. Fisher, *Dynamic Aspects of Macrophage Polarization during Atherosclerosis Progression and Regression.* Front Immunol, 2014. **5**: p. 579.
311. Stoger, J.L., et al., *Distribution of macrophage polarization markers in human atherosclerosis.* Atherosclerosis, 2012. **225**(2): p. 461-8.
312. Ridker, P.M., et al., *Antiinflammatory Therapy with Canakinumab for Atherosclerotic Disease.* N Engl J Med, 2017. **377**(12): p. 1119-1131.
313. Feig, J.E., et al., *LXR promotes the maximal egress of monocyte-derived cells from mouse aortic plaques during atherosclerosis regression.* J Clin Invest, 2010. **120**(12): p. 4415-24.
314. Potteaux, S., et al., *Suppressed monocyte recruitment drives macrophage removal from atherosclerotic plaques of Apoe-/- mice during disease regression.* J Clin Invest, 2011. **121**(5): p. 2025-36.
315. Wang, L., F.S. Wang, and M.E. Gershwin, *Human autoimmune diseases: a comprehensive update.* J Intern Med, 2015. **278**(4): p. 369-95.
316. Lleo, A., et al., *Definition of human autoimmunity--autoantibodies versus autoimmune disease.* Autoimmun Rev, 2010. **9**(5): p. A259-66.
317. Shi, C. and E.G. Pamer, *Monocyte recruitment during infection and inflammation.* Nat Rev Immunol, 2011. **11**(11): p. 762-74.
318. Murray, P.J. and T.A. Wynn, *Protective and pathogenic functions of macrophage subsets.* Nat Rev Immunol, 2011. **11**(11): p. 723-37.
319. Confavreux, C. and S. Vukusic, *Accumulation of irreversible disability in multiple sclerosis: from epidemiology to treatment.* Clin Neurol Neurosurg, 2006. **108**(3): p. 327-32.
320. Herrmann, M.M., et al., *Identification of gene expression patterns crucially involved in experimental autoimmune encephalomyelitis and multiple sclerosis.* Dis Model Mech, 2016. **9**(10): p. 1211-1220.
321. Chu, F., et al., *The roles of macrophages and microglia in multiple sclerosis and experimental autoimmune encephalomyelitis.* J Neuroimmunol, 2018. **318**: p. 1-7.
322. Fan, X., et al., *Follicular Helper CD4+ T Cells in Human Neuroautoimmune Diseases and Their Animal Models.* Mediators Inflamm, 2015. **2015**: p. 638968.
323. Kuhlmann, T., et al., *An updated histological classification system for multiple sclerosis lesions.* Acta Neuropathol, 2017. **133**(1): p. 13-24.
324. Tang, Y. and W. Le, *Differential Roles of M1 and M2 Microglia in Neurodegenerative Diseases.* Mol Neurobiol, 2016. **53**(2): p. 1181-94.
325. Farh, K.K., et al., *Genetic and epigenetic fine mapping of causal autoimmune disease variants.* Nature, 2015. **518**(7539): p. 337-43.

326. International Multiple Sclerosis Genetics, C., et al., *Analysis of immune-related loci identifies 48 new susceptibility variants for multiple sclerosis.* Nat Genet, 2013. **45**(11): p. 1353-60.
327. International Multiple Sclerosis Genetics, C., et al., *Genetic risk and a primary role for cell-mediated immune mechanisms in multiple sclerosis.* Nature, 2011. **476**(7359): p. 214-9.
328. Gjelstrup, M.C., et al., *Subsets of activated monocytes and markers of inflammation in incipient and progressed multiple sclerosis.* Immunol Cell Biol, 2018. **96**(2): p. 160-174.
329. Kawanaka, N., et al., *CD14+,CD16+ blood monocytes and joint inflammation in rheumatoid arthritis.* Arthritis Rheum, 2002. **46**(10): p. 2578-86.
330. Kouris, A., et al., *Proinflammatory cytokine responses in patients with psoriasis.* Eur Cytokine Netw, 2014. **25**(4): p. 63-8.
331. Bjelobaba, I., et al., *Animal models of multiple sclerosis: Focus on experimental autoimmune encephalomyelitis.* J Neurosci Res, 2018. **96**(6): p. 1021-1042.
332. Stromnes, I.M. and J.M. Goverman, *Passive induction of experimental allergic encephalomyelitis.* Nat Protoc, 2006. **1**(4): p. 1952-60.
333. Stromnes, I.M. and J.M. Goverman, *Active induction of experimental allergic encephalomyelitis.* Nat Protoc, 2006. **1**(4): p. 1810-9.
334. Ajami, B., et al., *Infiltrating monocytes trigger EAE progression, but do not contribute to the resident microglia pool.* Nat Neurosci, 2011. **14**(9): p. 1142-9.
335. Ajami, B. and L. Steinman, *Nonclassical monocytes: are they the next therapeutic targets in multiple sclerosis?* Immunol Cell Biol, 2018. **96**(2): p. 125-127.
336. Mildner, A., et al., *CCR2+Ly-6Chi monocytes are crucial for the effector phase of autoimmunity in the central nervous system.* Brain, 2009. **132**(Pt 9): p. 2487-500.
337. Tran, E.H., et al., *Immune invasion of the central nervous system parenchyma and experimental allergic encephalomyelitis, but not leukocyte extravasation from blood, are prevented in macrophage-depleted mice.* J Immunol, 1998. **161**(7): p. 3767-75.
338. Yamasaki, R., et al., *Differential roles of microglia and monocytes in the inflamed central nervous system.* J Exp Med, 2014. **211**(8): p. 1533-49.
339. Gao, H., et al., *Opposing Functions of Microglial and Macrophagic TNFR2 in the Pathogenesis of Experimental Autoimmune Encephalomyelitis.* Cell Rep, 2017. **18**(1): p. 198-212.
340. Hitchon, C.A. and H.S. El-Gabalawy, *The synovium in rheumatoid arthritis.* Open Rheumatol J, 2011. **5**: p. 107-14.
341. Janossy, G., et al., *Rheumatoid arthritis: a disease of T-lymphocyte/macrophage immunoregulation.* Lancet, 1981. **2**(8251): p. 839-42.
342. Barrera, P., et al., *Synovial macrophage depletion with clodronate-containing liposomes in rheumatoid arthritis.* Arthritis Rheum, 2000. **43**(9): p. 1951-9.
343. Smith, M.D., *The normal synovium.* Open Rheumatol J, 2011. **5**: p. 100-6.
344. Bottazzo, G.F., et al., *Role of aberrant HLA-DR expression and antigen presentation in induction of endocrine autoimmunity.* Lancet, 1983. **2**(8359): p. 1115-9.
345. Chu, C.Q., et al., *Localization of tumor necrosis factor alpha in synovial tissues and at the cartilage-pannus junction in patients with rheumatoid arthritis.* Arthritis Rheum, 1991. **34**(9): p. 1125-32.

346. Feldmann, M. and R.N. Maini, *Lasker Clinical Medical Research Award. TNF defined as a therapeutic target for rheumatoid arthritis and other autoimmune diseases.* Nat Med, 2003. **9**(10): p. 1245-50.
347. Salisbury, A.K., O. Duke, and L.W. Poulter, *Macrophage-like cells of the pannus area in rheumatoid arthritic joints.* Scand J Rheumatol, 1987. **16**(4): p. 263-72.
348. Kennedy, A., et al., *Macrophages in synovial inflammation.* Front Immunol, 2011. **2**: p. 52.
349. Asquith, D.L., et al., *Animal models of rheumatoid arthritis.* Eur J Immunol, 2009. **39**(8): p. 2040-4.
350. Misharin, A.V., et al., *Nonclassical Ly6C(-) monocytes drive the development of inflammatory arthritis in mice.* Cell Rep, 2014. **9**(2): p. 591-604.
351. Weiss, M., et al., *IRF5 controls both acute and chronic inflammation.* Proc Natl Acad Sci U S A, 2015. **112**(35): p. 11001-6.
352. Bruhl, H., et al., *Targeting of Gr-1+,CCR2+ monocytes in collagen-induced arthritis.* Arthritis Rheum, 2007. **56**(9): p. 2975-85.
353. Li, J., et al., *Treatment of arthritis by macrophage depletion and immunomodulation: testing an apoptosis-mediated therapy in a humanized death receptor mouse model.* Arthritis Rheum, 2012. **64**(4): p. 1098-109.
354. Quinones, M.P., et al., *Experimental arthritis in CC chemokine receptor 2-null mice closely mimics severe human rheumatoid arthritis.* J Clin Invest, 2004. **113**(6): p. 856-66.
355. Rossol, M., et al., *The CD14(bright) CD16+ monocyte subset is expanded in rheumatoid arthritis and promotes expansion of the Th17 cell population.* Arthritis Rheum, 2012. **64**(3): p. 671-7.
356. Akiyama, Y., et al., *Characterization of a human blood monocyte subset with low peroxidase activity.* J Clin Invest, 1983. **72**(3): p. 1093-105.
357. Hamilton, J.A., *Colony stimulating factors, cytokines and monocyte-macrophages--some controversies.* Immunol Today, 1993. **14**(1): p. 18-24.
358. Grainger, J.R., et al., *Macrophages in gastrointestinal homeostasis and inflammation.* Pflugers Arch, 2017. **469**(3-4): p. 527-539.
359. Jostins, L., et al., *Host-microbe interactions have shaped the genetic architecture of inflammatory bowel disease.* Nature, 2012. **491**(7422): p. 119-24.
360. Hume, D.A., V.H. Perry, and S. Gordon, *The mononuclear phagocyte system of the mouse defined by immunohistochemical localisation of antigen F4/80: macrophages associated with epithelia.* Anat Rec, 1984. **210**(3): p. 503-12.
361. Lee, S.H., P.M. Starkey, and S. Gordon, *Quantitative analysis of total macrophage content in adult mouse tissues. Immunochemical studies with monoclonal antibody F4/80.* J Exp Med, 1985. **161**(3): p. 475-89.
362. Jaensson, E., et al., *Small intestinal CD103+ dendritic cells display unique functional properties that are conserved between mice and humans.* J Exp Med, 2008. **205**(9): p. 2139-49.
363. Hadis, U., et al., *Intestinal tolerance requires gut homing and expansion of FoxP3+ regulatory T cells in the lamina propria.* Immunity, 2011. **34**(2): p. 237-46.
364. Panea, C., et al., *Intestinal Monocyte-Derived Macrophages Control Commensal-Specific Th17 Responses.* Cell Rep, 2015. **12**(8): p. 1314-24.

365. Weaver, C.T., et al., *The Th17 pathway and inflammatory diseases of the intestines, lungs, and skin.* Annu Rev Pathol, 2013. **8**: p. 477-512.
366. Grainger, J.R., et al., *Inflammatory monocytes regulate pathologic responses to commensals during acute gastrointestinal infection.* Nat Med, 2013. **19**(6): p. 713-21.
367. Smith, P.D., et al., *Intestinal macrophages and response to microbial encroachment.* Mucosal Immunol, 2011. **4**(1): p. 31-42.
368. Smythies, L.E., et al., *Human intestinal macrophages display profound inflammatory anergy despite avid phagocytic and bacteriocidal activity.* J Clin Invest, 2005. **115**(1): p. 66-75.
369. Muller, P.A., et al., *Crosstalk between Muscularis Macrophages and Enteric Neurons Regulates Gastrointestinal Motility.* Cell, 2014. **158**(5): p. 1210.
370. Bain, C.C., et al., *Resident and pro-inflammatory macrophages in the colon represent alternative context-dependent fates of the same Ly6Chi monocyte precursors.* Mucosal Immunol, 2013. **6**(3): p. 498-510.
371. Hedl, M., et al., *Chronic stimulation of Nod2 mediates tolerance to bacterial products.* Proc Natl Acad Sci U S A, 2007. **104**(49): p. 19440-5.
372. Zigmond, E. and S. Jung, *Intestinal macrophages: well educated exceptions from the rule.* Trends Immunol, 2013. **34**(4): p. 162-8.
373. Kuhn, R., et al., *Interleukin-10-deficient mice develop chronic enterocolitis.* Cell, 1993. **75**(2): p. 263-74.
374. Shouval, D.S., et al., *Interleukin-10 receptor signaling in innate immune cells regulates mucosal immune tolerance and anti-inflammatory macrophage function.* Immunity, 2014. **40**(5): p. 706-19.
375. Zigmond, E., et al., *Macrophage-restricted interleukin-10 receptor deficiency, but not IL-10 deficiency, causes severe spontaneous colitis.* Immunity, 2014. **40**(5): p. 720-33.
376. Serbina, N.V. and E.G. Pamer, *Monocyte emigration from bone marrow during bacterial infection requires signals mediated by chemokine receptor CCR2.* Nat Immunol, 2006. **7**(3): p. 311-7.
377. Gautier, E.L., et al., *Local apoptosis mediates clearance of macrophages from resolving inflammation in mice.* Blood, 2013. **122**(15): p. 2714-22.
378. Cook, M.G. and M.F. Dixon, *An analysis of the reliability of detection and diagnostic value of various pathological features in Crohn's disease and ulcerative colitis.* Gut, 1973. **14**(4): p. 255-62.
379. Rotterdam, H., B.I. Korelitz, and S.C. Sommers, *Microgranulomas in grossly normal rectal mucosa in Crohn's disease.* Am J Clin Pathol, 1977. **67**(6): p. 550-4.
380. Kamada, N., et al., *Unique CD14 intestinal macrophages contribute to the pathogenesis of Crohn disease via IL-23/IFN-gamma axis.* J Clin Invest, 2008. **118**(6): p. 2269-80.
381. Grimm, M.C., et al., *Evidence for a CD14+ population of monocytes in inflammatory bowel disease mucosa--implications for pathogenesis.* Clin Exp Immunol, 1995. **100**(2): p. 291-7.
382. Rugtveit, J., et al., *Cytokine profiles differ in newly recruited and resident subsets of mucosal macrophages from inflammatory bowel disease.* Gastroenterology, 1997. **112**(5): p. 1493-505.

383. Smythies, L.E., et al., *Mucosal IL-8 and TGF-beta recruit blood monocytes: evidence for cross-talk between the lamina propria stroma and myeloid cells.* J Leukoc Biol, 2006. **80**(3): p. 492-9.
384. Kuhl, A.A., et al., *Diversity of Intestinal Macrophages in Inflammatory Bowel Diseases.* Front Immunol, 2015. **6**: p. 613.
385. Louis, E., et al., *Behaviour of Crohn's disease according to the Vienna classification: changing pattern over the course of the disease.* Gut, 2001. **49**(6): p. 777-82.
386. Van Assche, G., K. Geboes, and P. Rutgeerts, *Medical therapy for Crohn's disease strictures.* Inflamm Bowel Dis, 2004. **10**(1): p. 55-60.
387. Yamagata, M., et al., *Submucosal fibrosis and basic-fibroblast growth factor-positive neutrophils correlate with colonic stenosis in cases of ulcerative colitis.* Digestion, 2011. **84**(1): p. 12-21.
388. Bailey, J.R., et al., *IL-13 promotes collagen accumulation in Crohn's disease fibrosis by down-regulation of fibroblast MMP synthesis: a role for innate lymphoid cells?* PLoS One, 2012. **7**(12): p. e52332.
389. Kirkegaard, T., et al., *Expression and localisation of matrix metalloproteinases and their natural inhibitors in fistulae of patients with Crohn's disease.* Gut, 2004. **53**(5): p. 701-9.
390. Reeves, G.E., *Update on the immunology, diagnosis and management of systemic lupus erythematosus.* Intern Med J, 2004. **34**(6): p. 338-47.
391. Li, Y., P.Y. Lee, and W.H. Reeves, *Monocyte and macrophage abnormalities in systemic lupus erythematosus.* Arch Immunol Ther Exp (Warsz), 2010. **58**(5): p. 355-64.
392. Katsiari, C.G., S.N. Liossis, and P.P. Sfikakis, *The pathophysiologic role of monocytes and macrophages in systemic lupus erythematosus: a reappraisal.* Semin Arthritis Rheum, 2010. **39**(6): p. 491-503.
393. Herrmann, M., et al., *Impaired phagocytosis of apoptotic cell material by monocyte-derived macrophages from patients with systemic lupus erythematosus.* Arthritis Rheum, 1998. **41**(7): p. 1241-50.
394. Tas, S.W., et al., *Macrophages from patients with SLE and rheumatoid arthritis have defective adhesion in vitro, while only SLE macrophages have impaired uptake of apoptotic cells.* Ann Rheum Dis, 2006. **65**(2): p. 216-21.
395. Baumann, I., et al., *Impaired uptake of apoptotic cells into tingible body macrophages in germinal centers of patients with systemic lupus erythematosus.* Arthritis Rheum, 2002. **46**(1): p. 191-201.
396. Bengtsson, A.A., et al., *Induction of apoptosis in monocytes and lymphocytes by serum from patients with systemic lupus erythematosus - an additional mechanism to increased autoantigen load?* Clin Exp Immunol, 2004. **135**(3): p. 535-43.
397. Ren, Y., et al., *Increased apoptotic neutrophils and macrophages and impaired macrophage phagocytic clearance of apoptotic neutrophils in systemic lupus erythematosus.* Arthritis Rheum, 2003. **48**(10): p. 2888-97.
398. Mestas, J. and C.C. Hughes, *Of mice and not men: differences between mouse and human immunology.* J Immunol, 2004. **172**(5): p. 2731-8.
399. Nadeau, J.H., *Maps of linkage and synteny homologies between mouse and man.* Trends Genet, 1989. **5**(3): p. 82-6.

400. Perry, D., et al., *Murine models of systemic lupus erythematosus.* J Biomed Biotechnol, 2011. **2011**: p. 271694.
401. Richard, M.L. and G. Gilkeson, *Mouse models of lupus: what they tell us and what they don't.* Lupus Sci Med, 2018. **5**(1): p. e000199.
402. Freedman, B.S., *Modeling Kidney Disease with iPS Cells.* Biomark Insights, 2015. **10**(Suppl 1): p. 153-69.
403. Andrade, D., et al., *Engraftment of peripheral blood mononuclear cells from systemic lupus erythematosus and antiphospholipid syndrome patient donors into BALB-RAG-2-/- IL-2Rgamma-/- mice: a promising model for studying human disease.* Arthritis Rheum, 2011. **63**(9): p. 2764-73.
404. Kerekov, N., et al., *Humanized SCID mice models of SLE.* Curr Pharm Des, 2011. **17**(13): p. 1261-6.
405. Andrews, B.S., et al., *Spontaneous murine lupus-like syndromes. Clinical and immunopathological manifestations in several strains.* J Exp Med, 1978. **148**(5): p. 1198-215.
406. Dixon, F.J., et al., *Etiology and pathogenesis of a spontaneous lupus-like syndrome in mice.* Arthritis Rheum, 1978. **21**(5 Suppl): p. S64-7.
407. Morel, L., et al., *Genetic reconstitution of systemic lupus erythematosus immunopathology with polycongenic murine strains.* Proc Natl Acad Sci U S A, 2000. **97**(12): p. 6670-5.
408. Mohan, C., et al., *Genetic dissection of lupus pathogenesis: a recipe for nephrophilic autoantibodies.* J Clin Invest, 1999. **103**(12): p. 1685-95.
409. Rudofsky, U.H. and D.A. Lawrence, *New Zealand mixed mice: a genetic systemic lupus erythematosus model for assessing environmental effects.* Environ Health Perspect, 1999. **107 Suppl 5**: p. 713-21.
410. Bagavant, H., et al., *Role for nephritogenic T cells in lupus glomerulonephritis: progression to renal failure is accompanied by T cell activation and expansion in regional lymph nodes.* J Immunol, 2006. **177**(11): p. 8258-65.
411. Ge, Y., et al., *Genetic approach to study lupus glomerulonephritis.* Methods Mol Biol, 2012. **900**: p. 271-90.
412. Rauch, J., et al., *A high frequency idiotypic marker of anti-DNA autoantibodies in MRL-lpr/lpr mice.* J Immunol, 1982. **129**(1): p. 236-41.
413. Alexander, E.L., et al., *Congenic autoimmune murine models of central nervous system disease in connective tissue disorders.* Ann Neurol, 1983. **14**(2): p. 242-8.
414. Eisenberg, R.A., E.M. Tan, and F.J. Dixon, *Presence of anti-Sm reactivity in autoimmune mouse strains.* J Exp Med, 1978. **147**(2): p. 582-7.
415. Izui, S., et al., *The Y chromosome from autoimmune BXSB/MpJ mice induces a lupus-like syndrome in (NZW x C57BL/6)F1 male mice, but not in C57BL/6 male mice.* Eur J Immunol, 1988. **18**(6): p. 911-5.
416. Merino, R., L. Fossati, and S. Izui, *The lupus-prone BXSB strain: the Yaa gene model of systemic lupus erythematosus.* Springer Semin Immunopathol, 1992. **14**(2): p. 141-57.
417. Johnson, B.M., et al., *Impact of dietary deviation on disease progression and gut microbiome composition in lupus-prone SNF1 mice.* Clin Exp Immunol, 2015. **181**(2): p. 323-37.

418. Satoh, M. and W.H. Reeves, *Induction of lupus-associated autoantibodies in BALB/c mice by intraperitoneal injection of pristane.* J Exp Med, 1994. **180**(6): p. 2341-6.
419. Lee, P.Y., et al., *A novel type I IFN-producing cell subset in murine lupus.* J Immunol, 2008. **180**(7): p. 5101-8.
420. Satoh, M., et al., *Anti-nuclear antibody production and immune-complex glomerulonephritis in BALB/c mice treated with pristane.* Proc Natl Acad Sci U S A, 1995. **92**(24): p. 10934-8.
421. Yokogawa, M., et al., *Epicutaneous application of toll-like receptor 7 agonists leads to systemic autoimmunity in wild-type mice: a new model of systemic Lupus erythematosus.* Arthritis Rheumatol, 2014. **66**(3): p. 694-706.
422. Yoshida, H., et al., *Effect of an exogenous trigger on the pathogenesis of lupus in (NZB x NZW)F1 mice.* Arthritis Rheum, 2002. **46**(8): p. 2235-44.
423. Eisenberg, R.A. and C.S. Via, *T cells, murine chronic graft-versus-host disease and autoimmunity.* J Autoimmun, 2012. **39**(3): p. 240-7.
424. Lefkowith, J.B., et al., *Murine glomerulotropic monoclonal antibodies are highly oligoclonal and exhibit distinctive molecular features.* J Immunol, 1996. **157**(3): p. 1297-305.
425. Lefkowith, J.B. and G.S. Gilkeson, *Nephritogenic autoantibodies in lupus: current concepts and continuing controversies.* Arthritis Rheum, 1996. **39**(6): p. 894-903.
426. Caforio, A.L., et al., *Immune-mediated and autoimmune myocarditis: clinical presentation, diagnosis and management.* Heart Fail Rev, 2013. **18**(6): p. 715-32.
427. Dimas, V.V., et al., *Frequency of cardiac death in children with idiopathic dilated cardiomyopathy.* Am J Cardiol, 2009. **104**(11): p. 1574-7.
428. Kang, M. and J. An, *Myocarditis, Viral*, in *StatPearls*. 2018: Treasure Island (FL).
429. Fung, G., et al., *Myocarditis.* Circ Res, 2016. **118**(3): p. 496-514.
430. Fairweather, D., T.R. Guilarte, and L.T. Cooper, Jr., *Biomarker and more: can translocator protein 18 kDa predict recovery from brain injury and myocarditis?* Biomark Med, 2014. **8**(5): p. 605-7.
431. Hochholzer, W., D.A. Morrow, and R.P. Giugliano, *Novel biomarkers in cardiovascular disease: update 2010.* Am Heart J, 2010. **160**(4): p. 583-94.
432. Barin, J.G., N.R. Rose, and D. Cihakova, *Macrophage diversity in cardiac inflammation: a review.* Immunobiology, 2012. **217**(5): p. 468-75.
433. Theaker, J.M., et al., *Giant cell myocarditis: evidence for the macrophage origin of the giant cells.* J Clin Pathol, 1985. **38**(2): p. 160-4.
434. Guilliams, M., et al., *Dendritic cells, monocytes and macrophages: a unified nomenclature based on ontogeny.* Nat Rev Immunol, 2014. **14**(8): p. 571-8.
435. Gordon, S. and P.R. Taylor, *Monocyte and macrophage heterogeneity.* Nat Rev Immunol, 2005. **5**(12): p. 953-64.
436. Ingersoll, M.A., et al., *Comparison of gene expression profiles between human and mouse monocyte subsets.* Blood, 2010. **115**(3): p. e10-9.
437. Jakubzick, C., et al., *Minimal differentiation of classical monocytes as they survey steady-state tissues and transport antigen to lymph nodes.* Immunity, 2013. **39**(3): p. 599-610.
438. Ziegler-Heitbrock, L., *The CD14+ CD16+ blood monocytes: their role in infection and inflammation.* J Leukoc Biol, 2007. **81**(3): p. 584-92.

439. Bronte, V. and M.J. Pittet, *The spleen in local and systemic regulation of immunity.* Immunity, 2013. **39**(5): p. 806-18.
440. Leuschner, F., et al., *Rapid monocyte kinetics in acute myocardial infarction are sustained by extramedullary monocytopoiesis.* J Exp Med, 2012. **209**(1): p. 123-37.
441. Heidt, T., et al., *Differential contribution of monocytes to heart macrophages in steady-state and after myocardial infarction.* Circ Res, 2014. **115**(2): p. 284-95.
442. Baldeviano, G.C., et al., *Interleukin-17A is dispensable for myocarditis but essential for the progression to dilated cardiomyopathy.* Circ Res, 2010. **106**(10): p. 1646-55.
443. Amoah, B.P., et al., *Immunopathogenesis of Myocarditis: The Interplay Between Cardiac Fibroblast Cells, Dendritic Cells, Macrophages and CD4+ T Cells.* Scand J Immunol, 2015. **82**(1): p. 1-9.
444. Chen, G., et al., *Sca-1(+) cardiac fibroblasts promote development of heart failure.* Eur J Immunol, 2018.
445. Amir el, A.D., et al., *viSNE enables visualization of high dimensional single-cell data and reveals phenotypic heterogeneity of leukemia.* Nat Biotechnol, 2013. **31**(6): p. 545-52.
446. Becher, B., et al., *High-dimensional analysis of the murine myeloid cell system.* Nat Immunol, 2014. **15**(12): p. 1181-9.
447. Martinez, F.O. and S. Gordon, *The M1 and M2 paradigm of macrophage activation: time for reassessment.* F1000Prime Rep, 2014. **6**: p. 13.
448. Nahrendorf, M. and F.K. Swirski, *Abandoning M1/M2 for a Network Model of Macrophage Function.* Circ Res, 2016. **119**(3): p. 414-7.
449. Scott, R.S., et al., *Phagocytosis and clearance of apoptotic cells is mediated by MER.* Nature, 2001. **411**(6834): p. 207-11.
450. Zizzo, G., et al., *Efficient clearance of early apoptotic cells by human macrophages requires M2c polarization and MerTK induction.* J Immunol, 2012. **189**(7): p. 3508-20.
451. Bosurgi, L., et al., *Macrophage function in tissue repair and remodeling requires IL-4 or IL-13 with apoptotic cells.* Science, 2017. **356**(6342): p. 1072-1076.
452. Camenisch, T.D., et al., *A novel receptor tyrosine kinase, Mer, inhibits TNF-alpha production and lipopolysaccharide-induced endotoxic shock.* J Immunol, 1999. **162**(6): p. 3498-503.
453. Healy, L.M., et al., *MerTK Is a Functional Regulator of Myelin Phagocytosis by Human Myeloid Cells.* J Immunol, 2016. **196**(8): p. 3375-84.
454. Myers, J.M., et al., *Cardiac myosin-Th17 responses promote heart failure in human myocarditis.* JCI Insight, 2016. **1**(9).
455. Lavine, K.J., et al., *Distinct macrophage lineages contribute to disparate patterns of cardiac recovery and remodeling in the neonatal and adult heart.* Proc Natl Acad Sci U S A, 2014. **111**(45): p. 16029-34.
456. Aurora, A.B., et al., *Macrophages are required for neonatal heart regeneration.* J Clin Invest, 2014. **124**(3): p. 1382-92.
457. Bajpai, G., et al., *The human heart contains distinct macrophage subsets with divergent origins and functions.* Nat Med, 2018.
458. Li, W., et al., *Heart-resident CCR2(+) macrophages promote neutrophil extravasation through TLR9/MyD88/CXCL5 signaling.* JCI Insight, 2016. **1**(12).

459. Anzai, A., et al., *The infarcted myocardium solicits GM-CSF for the detrimental oversupply of inflammatory leukocytes.* J Exp Med, 2017.
460. Stock, A.T., et al., *GM-CSF primes cardiac inflammation in a mouse model of Kawasaki disease.* J Exp Med, 2016. **213**(10): p. 1983-98.
461. Croxford, A.L., et al., *The Cytokine GM-CSF Drives the Inflammatory Signature of CCR2+ Monocytes and Licenses Autoimmunity.* Immunity, 2015. **43**(3): p. 502-14.
462. Menezes, S., et al., *The Heterogeneity of Ly6C(hi) Monocytes Controls Their Differentiation into iNOS(+) Macrophages or Monocyte-Derived Dendritic Cells.* Immunity, 2016. **45**(6): p. 1205-1218.
463. Yanez, A., et al., *Granulocyte-Monocyte Progenitors and Monocyte-Dendritic Cell Progenitors Independently Produce Functionally Distinct Monocytes.* Immunity, 2017. **47**(5): p. 890-902 e4.
464. Ikeda, N., et al., *Emergence of immunoregulatory Ym1(+)Ly6C(hi) monocytes during recovery phase of tissue injury.* Sci Immunol, 2018. **3**(28).
465. Satoh, T., et al., *Identification of an atypical monocyte and committed progenitor involved in fibrosis.* Nature, 2017. **541**(7635): p. 96-101.
466. Mildner, A., et al., *Genomic Characterization of Murine Monocytes Reveals C/EBPbeta Transcription Factor Dependence of Ly6C(-) Cells.* Immunity, 2017. **46**(5): p. 849-862 e7.
467. Hansson, J., et al., *Biomarkers of extracellular matrix metabolism (MMP-9 and TIMP-1) and risk of stroke, myocardial infarction, and cause-specific mortality: cohort study.* PLoS One, 2011. **6**(1): p. e16185.
468. Heymans, S., et al., *Increased cardiac expression of tissue inhibitor of metalloproteinase-1 and tissue inhibitor of metalloproteinase-2 is related to cardiac fibrosis and dysfunction in the chronic pressure-overloaded human heart.* Circulation, 2005. **112**(8): p. 1136-44.
469. Hirota, H., et al., *Circulating interleukin-6 family cytokines and their receptors in patients with congestive heart failure.* Heart Vessels, 2004. **19**(5): p. 237-41.
470. Kubin, T., et al., *Oncostatin M is a major mediator of cardiomyocyte dedifferentiation and remodeling.* Cell Stem Cell, 2011. **9**(5): p. 420-32.
471. Kubota, T., et al., *Expression of proinflammatory cytokines in the failing human heart: comparison of recent-onset and end-stage congestive heart failure.* J Heart Lung Transplant, 2000. **19**(9): p. 819-24.
472. Morishita, T., et al., *Association between matrix metalloproteinase-9 and worsening heart failure events in patients with chronic heart failure.* ESC Heart Fail, 2017. **4**(3): p. 321-330.
473. Anzai, A., et al., *Self-reactive CD4(+) IL-3(+) T cells amplify autoimmune inflammation in myocarditis by inciting monocyte chemotaxis.* J Exp Med, 2019. **216**(2): p. 369-383.
474. Panduro, M., C. Benoist, and D. Mathis, *Treg cells limit IFN-gamma production to control macrophage accrual and phenotype during skeletal muscle regeneration.* Proc Natl Acad Sci U S A, 2018. **115**(11): p. E2585-E2593.
475. Proto, J.D., et al., *Regulatory T Cells Promote Macrophage Efferocytosis during Inflammation Resolution.* Immunity, 2018. **49**(4): p. 666-677 e6.
476. Debien, E., et al., *S1PR5 is pivotal for the homeostasis of patrolling monocytes.* Eur J Immunol, 2013. **43**(6): p. 1667-75.

477. Foo, R.S., K. Mani, and R.N. Kitsis, *Death begets failure in the heart.* J Clin Invest, 2005. **115**(3): p. 565-71.
478. Whelan, R.S., V. Kaplinskiy, and R.N. Kitsis, *Cell death in the pathogenesis of heart disease: mechanisms and significance.* Annu Rev Physiol, 2010. **72**: p. 19-44.
479. Howangyin, K.Y., et al., *Myeloid-Epithelial-Reproductive Receptor Tyrosine Kinase and Milk Fat Globule Epidermal Growth Factor 8 Coordinately Improve Remodeling After Myocardial Infarction via Local Delivery of Vascular Endothelial Growth Factor.* Circulation, 2016. **133**(9): p. 826-39.
480. Wan, E., et al., *Enhanced efferocytosis of apoptotic cardiomyocytes through myeloid-epithelial-reproductive tyrosine kinase links acute inflammation resolution to cardiac repair after infarction.* Circ Res, 2013. **113**(8): p. 1004-12.
481. Wermeling, F., M.C. Karlsson, and T.L. McGaha, *An anatomical view on macrophages in tolerance.* Autoimmun Rev, 2009. **9**(1): p. 49-52.
482. Chen, J., K. Carey, and P.J. Godowski, *Identification of Gas6 as a ligand for Mer, a neural cell adhesion molecule related receptor tyrosine kinase implicated in cellular transformation.* Oncogene, 1997. **14**(17): p. 2033-9.
483. Hilliard, B.A., et al., *Increased expression of Mer tyrosine kinase in circulating dendritic cells and monocytes of lupus patients: correlations with plasma interferon activity and steroid therapy.* Arthritis Res Ther, 2014. **16**(2): p. R76.
484. Seitz, H.M., et al., *Macrophages and dendritic cells use different Axl/Mertk/Tyro3 receptors in clearance of apoptotic cells.* J Immunol, 2007. **178**(9): p. 5635-42.
485. Fadok, V.A., et al., *Macrophages that have ingested apoptotic cells in vitro inhibit proinflammatory cytokine production through autocrine/paracrine mechanisms involving TGF-beta, PGE2, and PAF.* J Clin Invest, 1998. **101**(4): p. 890-8.
486. Zhang, S., et al., *Cardiomyocytes induce macrophage receptor shedding to suppress phagocytosis.* J Mol Cell Cardiol, 2015. **87**: p. 171-9.
487. Misharin, A.V., et al., *Monocyte-derived alveolar macrophages drive lung fibrosis and persist in the lung over the life span.* J Exp Med, 2017. **214**(8): p. 2387-2404.
488. Mishra, M.K., et al., *Kinetics of proinflammatory monocytes in a model of multiple sclerosis and its perturbation by laquinimod.* Am J Pathol, 2012. **181**(2): p. 642-51.
489. Razeghi, P., et al., *Metabolic gene expression in fetal and failing human heart.* Circulation, 2001. **104**(24): p. 2923-31.
490. Zuern, C.S., et al., *Cyclophilin A predicts clinical outcome in patients with congestive heart failure undergoing endomyocardial biopsy.* Eur J Heart Fail, 2013. **15**(2): p. 176-84.
491. Yu, J.J., et al., *The interleukin-17 receptor plays a gender-dependent role in host protection against Porphyromonas gingivalis-induced periodontal bone loss.* Infect Immun, 2008. **76**(9): p. 4206-13.
492. Pummerer, C.L., et al., *Identification of cardiac myosin peptides capable of inducing autoimmune myocarditis in BALB/c mice.* J Clin Invest, 1996. **97**(9): p. 2057-62.
493. Diny, N.L., et al., *Eosinophil-derived IL-4 drives progression of myocarditis to inflammatory dilated cardiomyopathy.* J Exp Med, 2017. **214**(4): p. 943-957.
494. Livak, K.J. and T.D. Schmittgen, *Analysis of relative gene expression data using real-time quantitative PCR and the 2(-Delta Delta C(T)) Method.* Methods, 2001. **25**(4): p. 402-8.

495. Swirski, F.K. and M. Nahrendorf, *Cardioimmunology: the immune system in cardiac homeostasis and disease.* Nat Rev Immunol, 2018.
496. Geissmann, F., et al., *Development of monocytes, macrophages, and dendritic cells.* Science, 2010. **327**(5966): p. 656-61.
497. Hulsmans, M., et al., *Macrophages Facilitate Electrical Conduction in the Heart.* Cell, 2017. **169**(3): p. 510-522 e20.
498. Ma, Y., A.J. Mouton, and M.L. Lindsey, *Cardiac macrophage biology in the steady-state heart, the aging heart, and following myocardial infarction.* Transl Res, 2018. **191**: p. 15-28.
499. Tacke, F., et al., *Immature monocytes acquire antigens from other cells in the bone marrow and present them to T cells after maturing in the periphery.* J Exp Med, 2006. **203**(3): p. 583-97.
500. Cihakova, D., et al., *Interleukin-13 protects against experimental autoimmune myocarditis by regulating macrophage differentiation.* Am J Pathol, 2008. **172**(5): p. 1195-208.
501. Widyantoro, B., et al., *Endothelial cell-derived endothelin-1 promotes cardiac fibrosis in diabetic hearts through stimulation of endothelial-to-mesenchymal transition.* Circulation, 2010. **121**(22): p. 2407-18.
502. Zeisberg, E.M., et al., *Endothelial-to-mesenchymal transition contributes to cardiac fibrosis.* Nat Med, 2007. **13**(8): p. 952-61.
503. Haudek, S.B., et al., *Bone marrow-derived fibroblast precursors mediate ischemic cardiomyopathy in mice.* Proc Natl Acad Sci U S A, 2006. **103**(48): p. 18284-9.
504. Mollmann, H., et al., *Bone marrow-derived cells contribute to infarct remodelling.* Cardiovasc Res, 2006. **71**(4): p. 661-71.
505. van Amerongen, M.J., et al., *Bone marrow-derived myofibroblasts contribute functionally to scar formation after myocardial infarction.* J Pathol, 2008. **214**(3): p. 377-86.
506. Zeisberg, E.M. and R. Kalluri, *Origins of cardiac fibroblasts.* Circ Res, 2010. **107**(11): p. 1304-12.
507. Kanisicak, O., et al., *Genetic lineage tracing defines myofibroblast origin and function in the injured heart.* Nat Commun, 2016. **7**: p. 12260.
508. Chen, G., et al., *Sca-1(+) cardiac fibroblasts promote development of heart failure.* Eur J Immunol, 2018. **48**(9): p. 1522-1538.
509. Anzai, A., et al., *The infarcted myocardium solicits GM-CSF for the detrimental oversupply of inflammatory leukocytes.* J Exp Med, 2017. **214**(11): p. 3293-3310.
510. Kaur, H., et al., *Targeted Ablation of Periostin-Expressing Activated Fibroblasts Prevents Adverse Cardiac Remodeling in Mice.* Circ Res, 2016. **118**(12): p. 1906-17.
511. Benhaiem-Sigaux, N., et al., *Characterization of human pericardial macrophages.* J Leukoc Biol, 1985. **38**(6): p. 709-21.
512. Wang, J. and P. Kubes, *A Reservoir of Mature Cavity Macrophages that Can Rapidly Invade Visceral Organs to Affect Tissue Repair.* Cell, 2016. **165**(3): p. 668-78.
513. Ziegler-Heitbrock, L. and T.P. Hofer, *Toward a refined definition of monocyte subsets.* Front Immunol, 2013. **4**: p. 23.

Curriculum vitae

Xuezhou (Snow) Hou

General information

Home Address: 6517 37th AVE NE, Seattle, WA 98115
Business Address: Johns Hopkins University, Ross 648c, 720 Rutland Ave. Baltimore, MD 21205
Phone: 484-393-5888
E-mail: xhou3@jhu.edu
Linkedin.com/in/snow-hou/

Education and Training

Johns Hopkins University, Bloomberg School of Public Health, Ph.D., Molecular Microbiology and Immunology department, Baltimore, MD
Rochester Institute of Technology, Bachelor of Science, Biological Science, graduated August 2011, Rochester, NY

Professional Activities

YEAR	OCCUPATION	INSTITUTION/COMPANY
Sept. 2013 ~ Jan. 2019	Ph.D.	Johns Hopkins University, MD
2012 ~ 2013	Research Technician I	Fred Hutchinson Cancer Research Center, WA
2011 ~ 2012	Intern, Research Associate II	QIAGEN Inc., MD
Summer 2010	Summer research scholar	Princeton University, NJ
Summer 2009	Summer research scholar	Rochester Institute of Technology, NY
Summer 2009	Summer Lab Tech	Rochester Institute of Technology, NY

Honors and Awards

2017 - 2018: Katherine E. Welsh Fellowship in Immunology and Infectious Disease
2017 - 2018: Outstanding abstract awards for poster presented on 19th and 20th annual department of Pathology Young Investigators' Day
2016 - 2018: The Richard J. and Margaret Conn Himelfarb Student Support Fund
2015 - 2017: O'Leary Wilson pre-doctoral fellowship in autoimmune disease
2016: The American Heart Association Predoctoral Fellowship Award (unable to accept due to funding conflict)

2015 -2016: SA Travel awards from Johns Hopkins University, Bloomberg School of Public Health
2014 - 2015: Eleanor Bliss Honorary Fellowship for academic excellence and research potential in molecular microbiology and immunology
2013 - 2014: Dr. J. Harold Drudge Scholarship recognize outstanding academic and research achievements
2011 RIT Outstanding Undergraduate Scholar: recognizing high academic attainment
2011 RIT Distinguish Research Scholar
2009 - 2011: M. Richard Rose Nathaniel Rochester Society Scholarship
2008 - 2011: RIT Outstanding International Student Scholarship (Al & Margaret Davis Scholarship, Alfred L. and Ruby C. Davis Scholarship, William F. and Mildred Feinbloom Scholarship)
2008 Wahls-Olsen Leadership Scholarship
2007 - 2011: Dean's List

Publications

1. **Xuezhou Hou**, Guobao Chen, William Bracamonte-Baran, Hee Sun Choi, Monica V. Talor, Nicola L. Diny, Jungeun Sung, David Joel Hackam, Karin Klingel, Giovanni E. Davogustto, Heinrich Taegtmeyer, Isabelle Coppens, Jobert G. Barin, Daniela Čiháková. "Cardiac fibroblasts regulate macrophage development and function during cardiac injury" (Submitted).
2. **Xuezhou Hou**, Hee Sun Choi, Nicola L. Diny, Wu Lei, Monica V. Talor, Daniela Čiháková. "The interplay between cardiac fibroblasts and lymphocytes during myocarditis development" (In preparation).
3. William Bracamonte-Baran, Guobao Chen, **Xuezhou Hou**, Monica V. Talor, Hee Sun Choi, Giovanni E. Davogustto, Heinrich Taegtmeyer, Jungeun Sung, David Joel Hackam, David Nauen, Daniela Čiháková. "Cardiac Innate Lymphoid Cells are a Resident Quiescent Type 2-commited Population" (Submitted).
4. Jungeun Sung, Chhinder Sodhi, Lysandra Voltaggio, **Xuezhou Hou**, Hongpeng Jia, Qinjie Zhou, Daniela Čiháková and David Joel Hackam. "The recruitment of extra-intestinal cells to the injured mucosa promotes healing in radiation enteritis and chemical colitis in a mouse parabiosis model" *Mucosal Immunology* (2018).
5. Guobao Chen, William Bracamonte-Baran, Nicola L Diny, **Xuezhou Hou**, Monica V Talor, Kai Fu, Giovanni E. Davogustto, Heinrich Taegtmeyer, Ari Waisman, Fengyi Wan, Daniela Čiháková. "Sca-1^{+} Cardiac Fibroblasts modulate Development of Heart Failure" *The European Journal of Immunology* (2018).

6. Jobert Barin, Monica V Talor, Nicola L Diny, SuFey Ong, Julie A Schaub, Elizabeth Gebremariam, DjahidaBedja, Guobao Chen, Hee Sun Choi, **Xuezhou Hou**, Lei Wu, Ashley Bcardamone, Daniel A Peterson, Noel R Rose, Daniela Čiháková. "Regulation of autoimmune myocarditis by host responses to the microbiome" *Experimental and Molecular Pathology* (2017).
7. Nicola L. Diny, **Xuezhou Hou**, Jobert Barin, Guobao Chen, Monica V Talor, Julie Schaub, Stuart D. Russell, Karin Klingel, Noel R Rose, and Daniela Cihakova. "Macrophage and cardiac fibroblasts are the main producers of eotaxins and regulate eosinophil trafficking to the heart" *The European Journal of Immunology* (2016).
8. Jobert Barin, Monica Talor, Julie Schaub, Nicola Diny, **Xuezhou Hou**, Matthew Hoyer, Nathan Archer, Elizabeth Gebremariam, Megan Davis, Lloyd MillerNoel R Rose, and Daniela Cihakova. "Collaborative IFNγ and IL17 signaling protects the oral mucosa from Staphylococcus aureus" *The American Journal of Pathology* (2016).
9. Wu Lei, Nicola Diny, SuFey Ong, Jobert Barin, **Xuezhou Hou**, Noel Rose, Monica Talor and Daniela Cihakova. "Pathogenic IL-23 signaling is required to initiate GM-CSF-driven autoimmune myocarditis in mice" *The European Journal of Immunology* (2015).

Acknowledged contributions:

1. Mitchell CM, Haick A, Nkwopara E, Garcia R, Rendi M, Agnew K, Fredricks DN, Eschenbach D. "Colonization of the upper genital tract by vaginal bacterial species in non-pregnant women" *Am J Obstet Gynecol* (2016).
2. Srinivasan S, Morgan MT, Fiedler TL, Djukovic D, Hoffman NG, Raftery D, Marrazzo JM, Fredricks DN. "Metabolic Signatures of Bacterial Vaginosis" *mBio* (2015).

Teaching and Mentoring

Johns Hopkins University:

Training Megan Wood, 1st year PhD student, to identify infiltrating immune cells in the hearts using flow cytometry. Spring, 2018.

Training Vivian Sun, Intern from Peddie School, to optimize magnetic cell sorting. Summer, 2017

Clinical and Epidemiological Aspects of Tropical Disease, 4th term, 2015

Training Mankaah Acho, Intern from the Diversity Summer Internship program, molecular biology techniques to look at gene expressions by cardiac fibroblasts. Summer, 2015

Intro to Biomedical Science, summer course, 2014 and 2015

Rochester Institute of Technology:

College Physics III, 2011

Intro to Biological Science, 1st through 3rd term, 2009 ~ 2010

Posters and Oral Presentations

1. **Xuezhou Hou**, Hee Sun Choi, Nicola Diny, William Bracamonte Baran, Guobao Chen, Jobert Barin, Monica V. Talor and Daniela Čiháková. Cardiac fibroblasts regulate macrophage development and function during cardiac injury. Poster presentation at the 20th annual department of pathology young investigators' day at Johns Hopkins University, Baltimore MD. 2018, March. **The poster was selected as one of the outstanding abstracts in the Basic research category.**
2. **Xuezhou Hou** as Invited speaker: The Immunobiology Affinity Group meeting at Brigham and Women's Hospital, Departmenet of Pathology at Harvard Univerity: The intricacies of cardiac networks: cardiac fibroblasts facilitate changes in monocytes during heart failure. Boston, MA. 2018, Jan.
3. **Xuezhou Hou**, Hee Sun Choi, Nicola Diny, William Bracamonte Baran, Guobao Chen, Jobert Barin, Monica V. Talor and Daniela Čiháková. Monocyte and Macrophage Subsets Fate Mapping in Myocarditis and Dilated Cardiomyopathy. Poster presentation at the 19th annual department of pathology young investigators' day at Johns Hopkins University, Baltimore MD. 2017, March. **The poster was selected as one of the outstanding abstracts in the Basic research category.**
4. **Xuezhou Hou**, Hee Sun Choi, Jobert Barin, Monica V. Talor and Daniela Čiháková. Cardiac Fibroblasts Facilitate Monocyte Survival and Differentiation during DCMi. Poster presentation at the Unraveling Vascular Inflammation: From Immunology to Imaging Symposium, hosted by National Heart, Lung, and Blood Institute (NHLBI), NIH, DHHS, Bethesda, MD. 2016, October.
5. **Xuezhou Hou**, Jobert Barin, Hee Sun Choi, Monica V. Talor and Daniela Čiháková. Characterizing monocyte and macrophage subpopulations during the course of EAM development. Poster presentation at the 7th Annual Cardiovascular Research Retreat at Johns Hopkins University, School of Medicine, Baltimore MD. 2016, June.
6. **Xuezhou Hou**, Jobert Barin, Hee Sun Choi, Nicola Diny, Julie Schaub, Monica V. Talor, Noel R. Rose, Daniela Čiháková. Characterizing the heterogeneity of monocytes and macrophages during the development of experimental autoimmune myocarditis. Poster presentation at the 18th annual department of pathology young investigators' day at Johns Hopkins University, Baltimore MD. 2016, March.
7. **Xuezhou Hou**, Jobert Barin, Hee Sun Choi, Monica V. Talor, Noel R. Rose and Daniela Čiháková. Characterizing monocyte and macrophage subpopulations during the course of EAM development. Oral presentation at the Immunopathology Research Seminar at Johns Hopkins University, School of Medicine, Baltimore MD. 2015, April.

8. **Xuezhou Hou**, Monica V. Talor, Lei Wu, Noel R. Rose, Daniela Čiháková. Cardiac fibroblasts in concert with CD4+ T cells determine infiltrating immune cells profile and the subtype of myocarditis. Poster presentation at the 17th annual department of pathology young investigators' day at Johns Hopkins University, Baltimore MD. 2015, March.
9. **Xuezhou Hou**, John Wolff and Victoria Doseeva. Multiplex Isothermal Helicase-Dependent Amplification Assay for the Detection of Chlamydia trachomatis---Optimizing tHDA assay for point-of-care testing. Oral presentation at QIAGEN Inc., summer internship program. 2011.
10. **Xuezhou Hou**, Qingfu Xu, Dina Newman, and Michael Pichichero. Correlation of viral load of respiratory syncytial virus with bacterial colonization in nasopharynx of children with or without acute otitis media. Oral presentation of Research Scholar Program at Rochester Institute of Technology, Rochester, NY. 2011, May.
11. **Xuezhou Hou**, Gunnar Kleemann, Leonid Kruglyak, and Coleen T. Murphy. Natural Variation in Aging---Studying longevity genes in Caenorhabditis elegans. Princeton University, Department of Molecular Biology and Lewis-Sigler Institute for Integrative Genomics, Princeton, NJ. Poster Presentation at the Rochester Academy of Science 37th Annual Fall Scientific Paper Session, Rochester, NY. 2010, September.
12. **Xuezhou Hou** and F. Harvey Pough. Do you believe what the package label says? --- A closer look at lactose intolerance therapies. Oral presentation at the 18th Undergraduate Research Symposium at Rochester Institute of Technology, Rochester, NY. 2009, August.

Professional Memberships

Trainee Member, American Association of Immunologists	2017 – 2018
Student/Trainee Member, American Heart Association	2015 – 2017